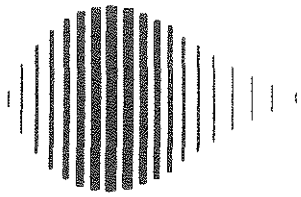

NATIONAL CENTER FOR EARTHQUAKE
ENGINEERING RESEARCH
State University of New York at Buffalo

SOIL EFFECTS ON EARTHQUAKE GROUND MOTIONS IN THE MEMPHIS AREA

by

H. Hwang, C. S. Lee and K. W. Ng
Center for Earthquake Research and Information
Memphis State University
Memphis, Tennessee 38152

Technical Report NCEER-90-0029

August 2, 1990

This research was conducted at Memphis State University and was partially supported by the National Science Foundation under Grant No. ECE 86-07591.

NOTICE

This report was prepared by Memphis State University as a result of research sponsored by the National Center for Earthquake Engineering Research (NCEER). Neither NCEER, associates of NCEER, its sponsors, Memphis State University, nor any person acting on their behalf:

a. makes any warranty, express or implied, with respect to the use of any information, apparatus, method, or process disclosed in this report or that such use may not infringe upon privately owned rights; or

b. assumes any liabilities of whatsoever kind with respect to the use of, or the damage resulting from the use of, any information, apparatus, method or process disclosed in this report.

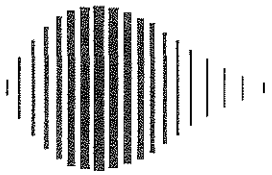

SOIL EFFECTS ON EARTHQUAKE GROUND MOTIONS IN THE MEMPHIS AREA

by

H. Hwang[1], C.S. Lee[2] and K.W. Ng[2]

August 2, 1990

Technical Report NCEER-90-0029

NCEER Contract Number 88-3016 and 89-3009

NSF Master Contract Number ECE 86-07591

1 Associate Research Professor, Center for Earthquake Research and Information, Memphis State University

2 Research Associate, Center for Earthquake Research and Information, Memphis State University

NATIONAL CENTER FOR EARTHQUAKE ENGINEERING RESEARCH
State University of New York at Buffalo
Red Jacket Quadrangle, Buffalo, NY 14261

PREFACE

The National Center for Earthquake Engineering Research (NCEER) is devoted to the expansion and dissemination of knowledge about earthquakes, the improvement of earthquake-resistant design, and the implementation of seismic hazard mitigation procedures to minimize loss of lives and property. The emphasis is on structures and lifelines that are found in zones of moderate to high seismicity throughout the United States.

NCEER's research is being carried out in an integrated and coordinated manner following a structured program. The current research program comprises four main areas:

- Existing and New Structures
- Secondary and Protective Systems
- Lifeline Systems
- Disaster Research and Planning

This technical report pertains to Program 3, Lifeline Systems, and more specifically to the study of dams, bridges and infrastructures.

The safe and serviceable operation of lifeline systems such as gas, electricity, oil, water, communication and transportation networks, immediately after a severe earthquake, is of crucial importance to the welfare of the general public, and to the mitigation of seismic hazards upon society at large. The long-term goals of the lifeline study are to evaluate the seismic performance of lifeline systems in general, and to recommend measures for mitigating the societal risk arising from their failures.

In addition to the study of specific lifeline systems, such as water delivery and crude oil transmission systems, effort is directed toward the study of the behavior of dams, bridges and infrastructures under seismic conditions. Seismological and geotechnical issues, such as variation in seismic intensity from attenuation effects, faulting, liquefaction and spatial variability of soil properties are topics under investigation. These topics are shown in the figure below.

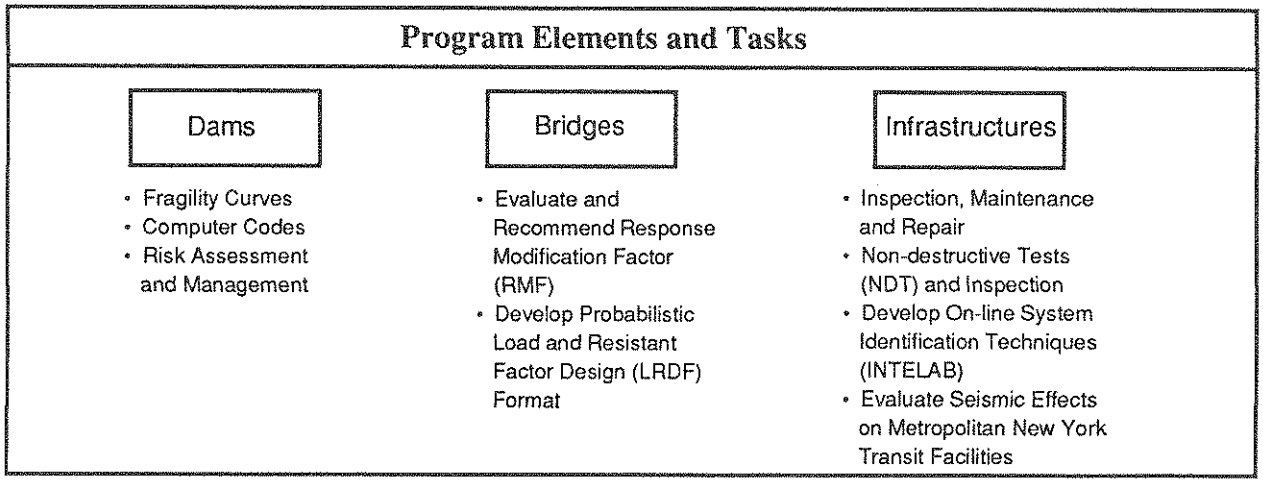

This report presents a thorough microzonation study of the Memphis area using state-of-practice methods. The authors have processed 424 soil logs out of 8,500 existing boring logs using the MASH computer program. A dynamic soil model is established for each soil log and then excited by an acceleration time history at the bedrock level resulting from a moment magnitude 7.5 New Madrid earthquake. The low-strain site period estimated from average shear wave velocity of a soil profile and the dynamic site period, at which the maximum spectral accelerations ratio occurs, are determined and shown in contour maps. The results of the site response analysis indicate that the soils have significant effects on ground motions in Memphis and Shelby County. The soil deposit acts as a filter when the bedrock earthquake motions are transmitted through it. The soil deposit filters out a significant portion of high frequency contents of the bedrock accelerations. On the other hand, it strongly amplifies the bedrock spectral accelerations between 0.15 and 1.4 seconds. This amplification is important in engineering applications since most structures have fundamental periods in this range.

ABSTRACT

The site response study for Memphis and Shelby County, Tennessee, has been carried out using the MASH computer program with the hysteretic curves for sands and clays proposed by Hwang and Lee. A total of 424 soil logs (boring logs) compiled by Ng et al. are used. A dynamic soil model is established for each soil log and then excited by an acceleration time history at the bedrock level resulting from a moment magnitude 7.5 New Madrid earthquake. The low-strain site period estimated from average shear wave velocity of a soil profile and the dynamic site period, at which the maximum spectral acceleration ratio occurs, are determined and shown in contour maps. The average shear wave velocity of the upper 200 ft soil profile in the study area is also shown in contour map. In addition, the mean ground response spectra for soil profile categories as specified in the 1988 Uniform Building Code are also established. Furthermore, maps showing the largest spectral accelerations in three period intervals are presented, from which an approximate response spectrum at any location in the study area can be readily constructed.

The results of the site response analysis indicate that the soils have significant effects on ground motions in Memphis and Shelby County. The soil deposit acts as a filter when the bedrock earthquake motions are transmitted through it. The soil deposit filters out a significant portion of high frequency contents of the bedrock accelerations. On the other hand, it strongly amplifies the bedrock spectral accelerations between 0.15 and 1.4 seconds. This amplification is important in engineering applications since most structures have fundamental periods in this range.

TABLE OF CONTENTS

LIST OF ILLUSTRATIONS

LIST OF TABLES

SECTION 1

INTRODUCTION

The soil conditions at a site have significant effects on the characteristics of earthquake ground motions and corresponding response spectra [1-4]. Earthquake motions at the base of a soil column (bedrock level) can be drastically modified in frequency contents and amplitude as seismic waves are transmitted through a soil deposit. Historical events such as the 1967 Caracas earthquake [3], the 1985 Mexico City earthquake [1,4], and the 1989 Loma Prieta earthquake [5] have demonstrated the effect of soils on earthquake ground motions. Thus, it is important to include the soil effects in the evaluation of earthquake ground motions.

Analytical methods for site response analysis incorporating nonlinear soil behavior have been shown to yield results in reasonably close agreements with field observations [6]. Hence, analytical site response analysis, in particular, one-dimensional site response analysis is increasingly being used for engineering applications to evaluate the characteristics of earthquake ground motions. In this study, the computer program MASH [7] is used to evaluate the soil effects on earthquake ground motions in the Memphis area. In this report, Section 2 describes the bedrock earthquake motions and Section 3 discusses the static and dynamic soil properties in the Memphis area. The results obtained from the site response analysis are described in Section 4 and Section 5 presents the conclusions of this study.

SECTION 2

BEDROCK EARTHQUAKE MOTIONS

Memphis and Shelby County, Tennessee, are geographically close to the southern segment of the New Madrid seismic zone (NMSZ) (figure 2-1). The NMSZ is being regarded by seismologists and earthquake engineers as the most hazardous zone in the eastern United States. Estimating the characteristics of ground motions induced by large New Madrid earthquakes is quite challenging, since the strong motion data in the region are scarce. Thus, a seismologically based model has been used to establish the horizontal bedrock motions that are primarily caused by shear waves generated from a seismic source [8]. This model is centered on a power spectrum that in turn is developed from a seismologically based Fourier amplitude spectrum. From the power spectrum, earthquake time histories and probability-based response spectra can be generated directly. The power spectrum can also be used to estimate the peak value of earthquake accelerations based on the extreme value distribution of a random process.

The peak bedrock accelerations for Memphis and Shelby County were estimated resulting from two New Madrid earthquakes of moment magnitude **M** 7.5 and 6.5, respectively [8]. Two cases of seismic sources were considered: (1) a single source at Marked Tree, Arkansas, and (2) the southern segment of the NMSZ. The results were presented in contour maps. The contour map of the peak bedrock acceleration corresponding to the mean plus one standard deviation (SD) value resulting from an **M** 7.5 earthquake occurring anywhere in the southern segment of NMSZ is shown in figure 2-2.

In this study, using the same seismologically based model described above, 16 synthetic horizontal bedrock acceleration time histories are generated from an **M** 7.5 earthquake for a site at epicentral distance R of 50 km (31 miles). The average response spectrum is derived from the 16 individual response spectra. The earthquake time history with

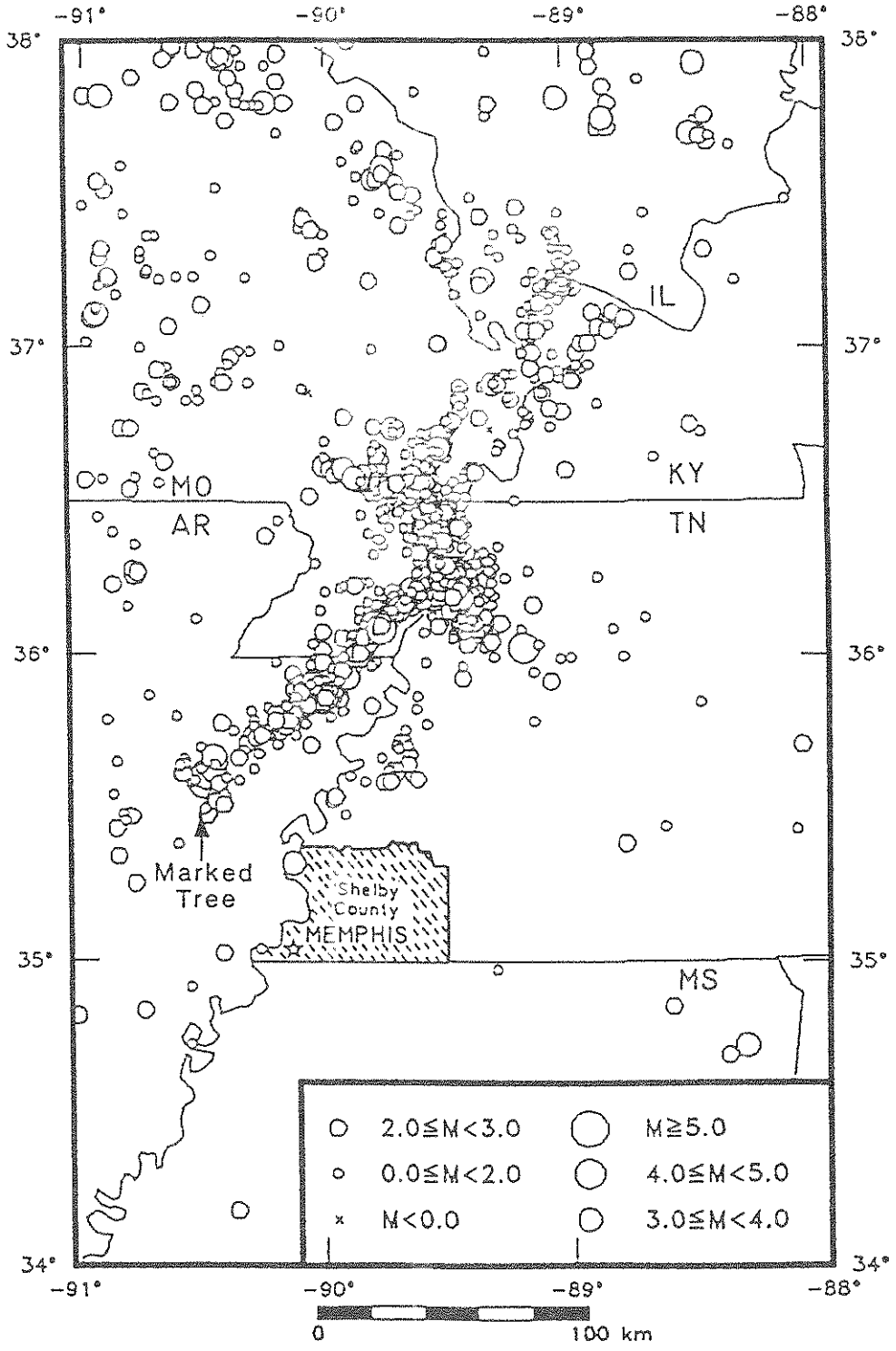

FIGURE 2-1 Epicenters of New Madrid Earthquakes

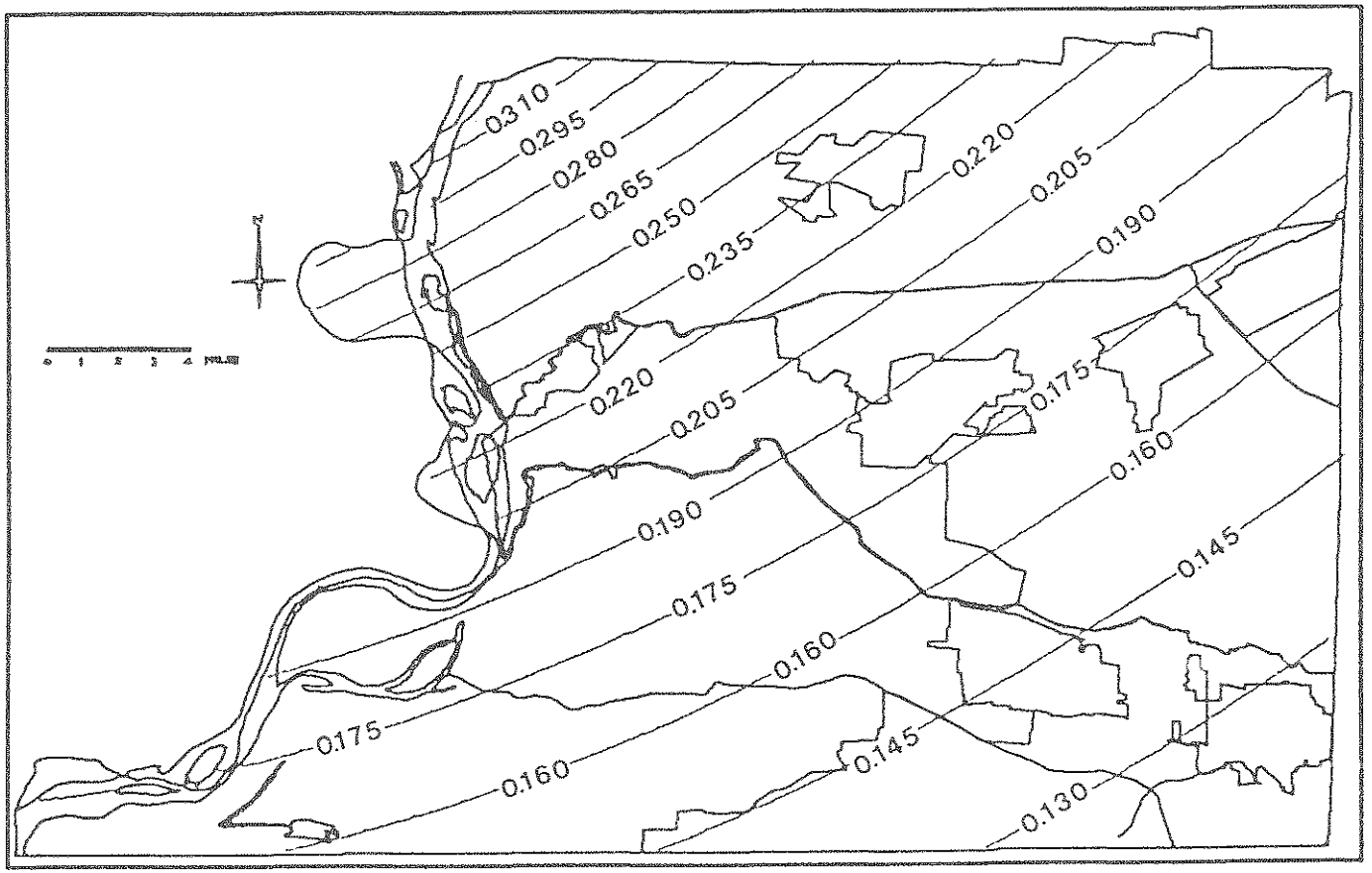

FIGURE 2-2 Contour Map of Mean + SD Peak Bedrock Acceleration (M = 7.5, Southern NMSZ)

the response spectrum closest to the average response spectrum is selected. The selected synthetic acceleration time history has a duration of 32 seconds and a peak value of about 0.25g. The time history is normalized by its peak value (0.25g) to produce a normalized acceleration time history as shown in figure 2-3. The bedrock acceleration time history for any site in Memphis and Shelby County is established by multiplying the normalized time history with the peak bedrock acceleration taken from the mean + SD contour map (figure 2-2).

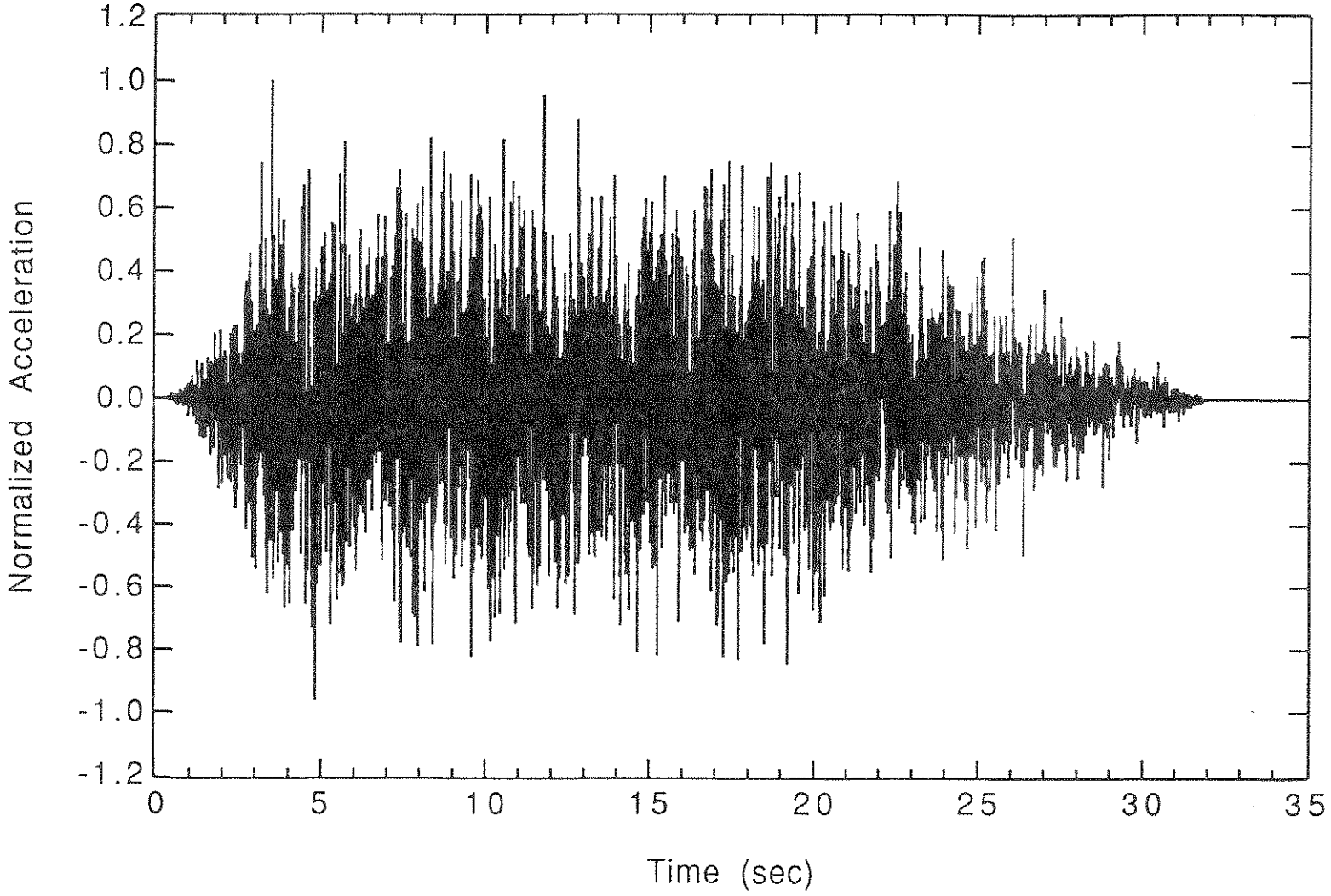

FIGURE 2-3 Normalized Bedrock Acceleration Time History (M = 7.5, R = 50 km)

SECTION 3

DYNAMIC SOIL MODELS

The dynamic soil model in the MASH program basically consists of a horizontally multilayered soil profile that extends to an actual or assumed horizontal bedrock (figure 3-1). To establish dynamic soil models for site response analysis in the Memphis area, the following geotechnical data are required:

(1) Subsurface conditions
(2) Engineering (static and dynamic) properties of soil layers
(3) Bedrock depth

In addition, the locations of water table and saturation line are also needed. The location of water table is usually documented in a boring log and the saturation line is determined from the depth of water table minus the estimated capillary rise of water. In this study, the estimated capillary rise of water for various types of soils are taken from Hunt [9].

3.1 Subsurface Conditions

Ng et al. [10] have collected about 8500 existing boring logs in Memphis and Shelby County. These boring logs were supplemented by available data from water-well logs, soil surveys, and technical publications. The data were compiled and analyzed using a grid system that consists of rectangular cells with equal size of 30 seconds in both latitude and longitude as shown in figure 3-2. The number indicated in each cell (figure 3-2) represents the total number of original boring logs available at that location. These boring logs were utilized to create a representative soil log (boring log) for each cell. A total of 424 boring logs with good geotechnical data are used in this study for performing site response analysis.

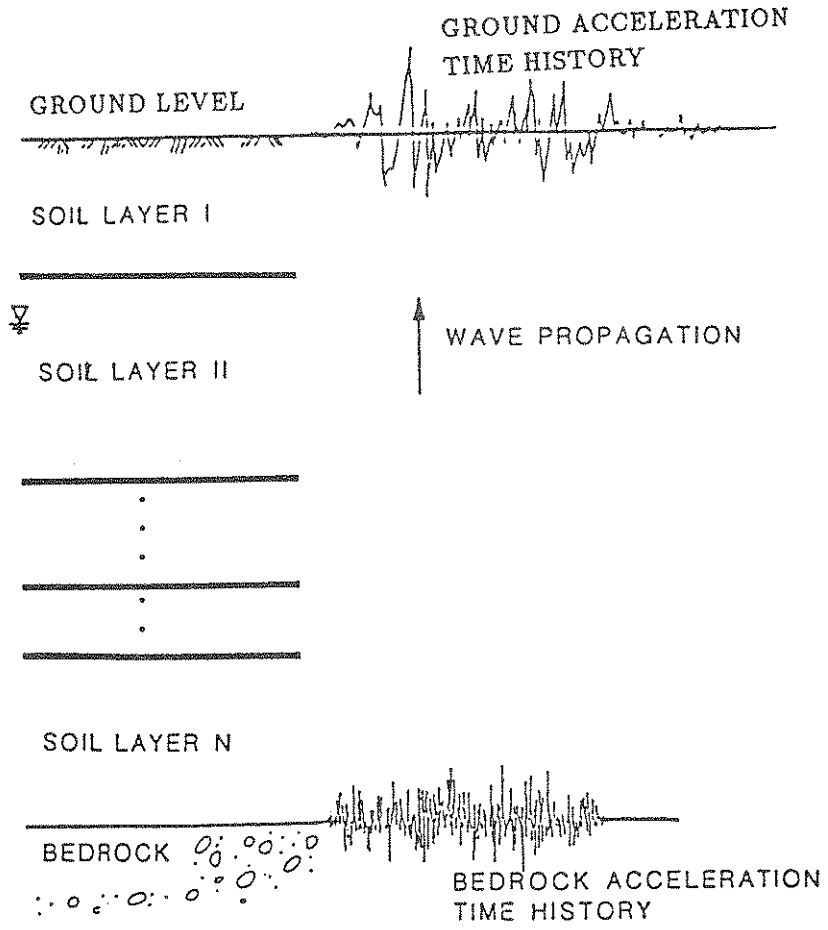

FIGURE 3-1 Illustration of Site Response Analysis

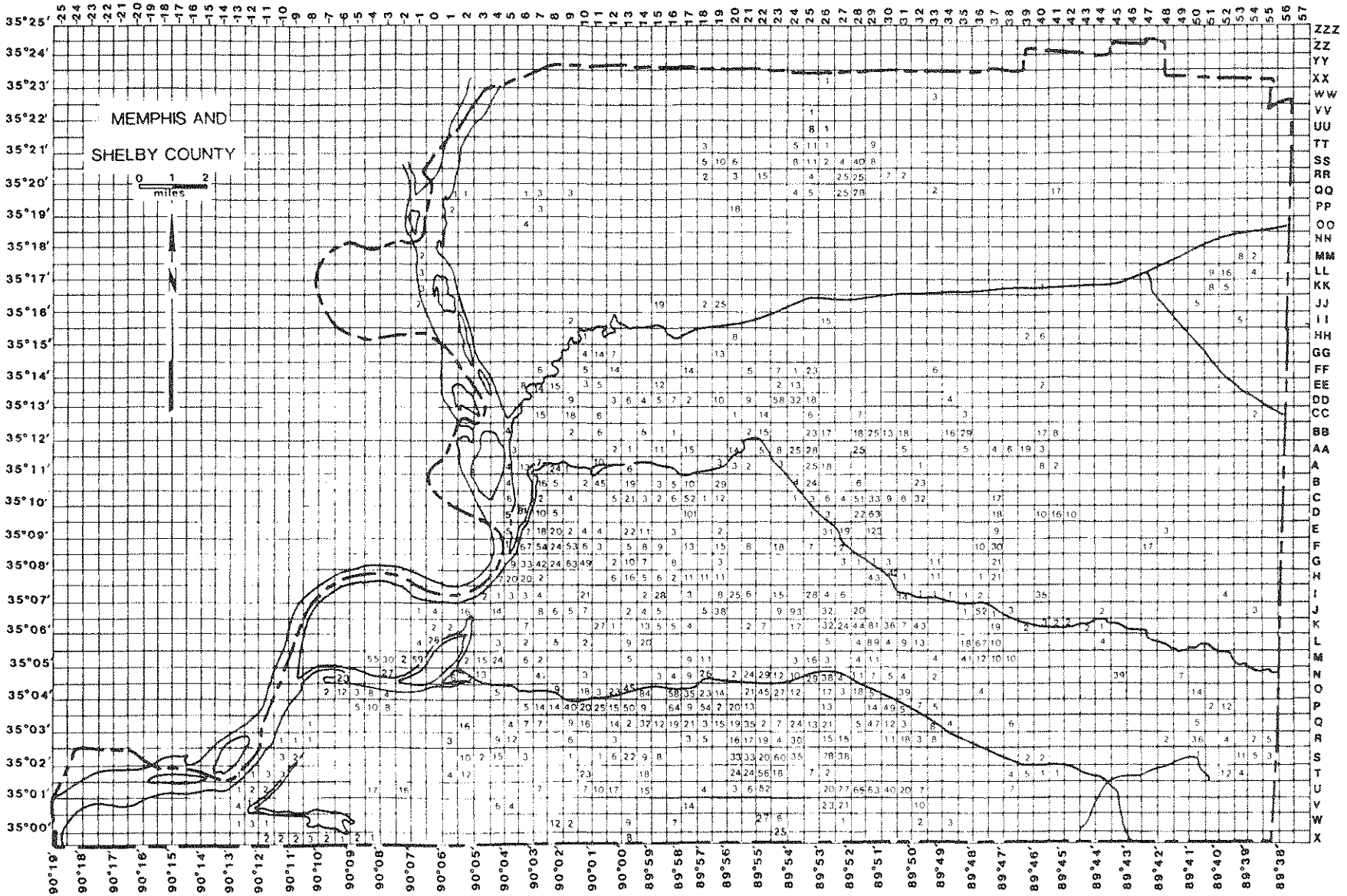

FIGURE 3-2 Boring Data Distribution Map

3.2 Static Soil Properties

The static and dynamic properties of soils can be established from an extensive laboratory test program. However, such a test program is not within the scope of this study. Thus, geotechnical data from the existing boring logs and the empirical correlations between engineering properties and soil index available in the literature are used as the primary sources for establishing the static and dynamic properties of soils in the Memphis area. Two dynamic tests of soil samples in the Memphis area are carried out. The results are close to those established in this study. The detail of the comparison is discussed in Section 3.4.

3.2.1 Cohesionless Soils

The static soil properties for sand and gravel required in the MASH computer program are the unit weight γ_s, relative density D_r, effective angle of internal friction ϕ', and coefficient of earth pressure at rest K_o.

The unit weight of cohesionless soils used in this study is taken from existing boring logs. The values of unit weight γ_s for SC, SM, SP-SW, and GP-GW soils classified according to the Unified Soil Classification System [11] are shown in table 3-I. The value assigned to each soil classification represents the average value inferred from the review of original boring logs.

The correlations between the relative density D_r for cohesionless soils and the blow counts from the Standard Penetration Test N_{SPT} as suggested by Hunt [9] are shown in table 3-II and converted to a smooth curve in figure 3-3. This curve is used to determine the value of relative density D_r of a soil layer based on the N_{SPT} value documented in the boring logs.

The effective angle of internal friction ϕ' for cohesionless soils classified as GW, GP, SW, SP, and SM are given in table 3-III based on the degrees of compactness ranging from loose to dense [9]. For very dense sand and

Table 3-I Unit Weight for Cohesionless Soils

Soil Classifications	Description	γ_s (pcf)
SC	Loose Medium Dense Dense	125 130 135
SM	Loose Medium Dense Dense	115 120 125
SP-SW	Loose Medium Dense Dense	115 125 135
GP-GW	Loose Medium Dense Dense	125 135 145

Table 3-II Relative Density for Cohesionless Soils

Description	N_{SPT}	D_r
Very Loose	< 4	< 0.15
Loose	4 - 10	0.15 - 0.35
Medium Dense	10 - 30	0.35 - 0.65
Dense	30 - 50	0.65 - 0.85
Very Dense	> 50	0.85 - 1.0

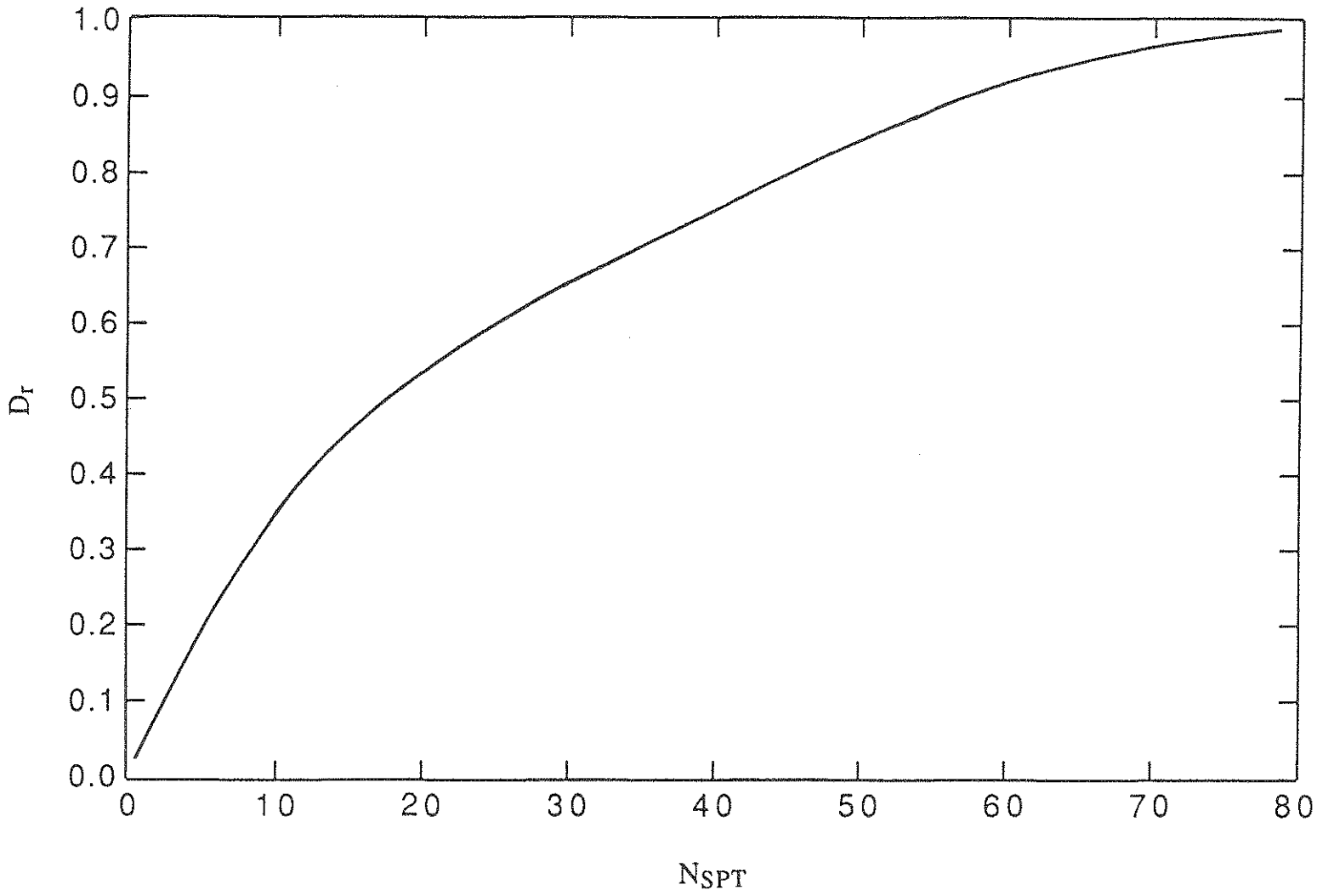

FIGURE 3-3 Correlations Between D_r and N_{SPT} for Cohesionless Soil

Table 3-III Effective Angle of Internal Friction for Cohesionless Soils

Soil Classifications	Description	ϕ'
GW	Dense Medium Dense Loose	40° 36° 32°
GP	Dense Medium Dense Loose	38° 35° 32°
SW	Dense Medium Dense Loose	37° 34° 30°
SP	Dense Medium Dense Loose	36° 33° 29°
SM	Dense Medium Dense Loose	35° 32° 29°

gravel, the angle of internal friction is taken as the ϕ' value for dense sand/gravel plus 3°. The coefficient of earth pressure at rest K_o for sand and gravel is then estimated from the following empirical equation [11].

$$K_o = 1 - \sin \phi' \qquad (3.1)$$

3.2.2 Cohesive Soils

The static soil properties for cohesive soils required in the MASH program are the unit weight γ_s, undrained shear strength S_u, and plasticity index PI. The values of unit weight γ_s for CL, ML, and CH soils in the Memphis area are shown in table 3-IV. The values assigned to these classifications represent the average value inferred from review of original boring logs.

The undrained shear strength S_u for clay is obtained from the review of available boring logs. The correlations between S_u and N_{SPT} for clay classified as CH and CL-ML are shown in table 3-V. Linear interpolation is used to obtain the undrained shear strength S_u for value of N_{spt} that are not listed in table 3-V. The plasticity index PI for clay classified as CL, ML, CH, and OH as shown in table 3-VI is also taken from the review of available boring logs.

3.3 Dynamic Soil Properties

The dynamic soil properties needed in the MASH program are the low-strain damping ratio β_o and the secant shear modulus G. The low-strain damping ratio β_o reflects the viscosity of soils. The damping ratio at small strain levels may be chosen between 1% to 5%, depending on soil types [12]. In this study, an average value of 3% is used.

Soil exhibits pronounced nonlinear behavior under cyclic loadings. For a level ground condition, a symmetric cyclic shear stress in the absence of static driving components produces, in approximation, a closed

Table 3-IV Unit Weight for Cohesive Soils

Soil Classifications	Description	γ_s (pcf)
CL	Soft Medium Stiff Stiff to Hard	120 125 130
ML	Soft Medium Stiff Stiff to Hard	100 110 120
CH	Soft Medium Stiff Stiff to Hard	113 122 126

Table 3-V Undrained Shear Strength for Cohesive Soils

N_{SPT}	S_u (psf)	
	CL-ML	CH
0	0	0
5	625	1000
10	1250	2000
15	1875	3000
20	2500	4000
25	3125	5000
30	3750	6000
35	4375	6000
40	5000	6000
45	5625	6000
50	6250	6000

Table 3-VI Plasticity Index for Cohesive Soils

Classifications	Depth	PI
CL	< 50 ft 50-200 ft	10-20 20-40
ML	All	< 10
CH	All	40-80
OH	All	40-80

hysteresis loop as shown in figure 3-4 [1]. The secant shear modulus G is the slope of the line OD in figure 3-4.

$$G = \frac{\tau_a}{\gamma_a} \tag{3.2}$$

where τ_a and γ_a are the shear stress and shear strain respectively, at the tip of the loop. The secant shear modulus is strain-dependent and decreases with increasing shear strain levels γ. In the MASH program, the secant shear modulus is expressed as

$$\frac{G}{G_o} = 1 - \left[\frac{[\gamma/\gamma_o]^{2B}}{1 + [\gamma/\gamma_o]^{2B}}\right]^A \tag{3.3}$$

where G_o, γ_o, A, and B are four parameters to be determined. G_o is the low-strain shear modulus and is usually taken as the shear modulus corresponding to shear strain of 10^{-6} or less. γ_o is the reference strain and is defined as

$$\gamma_o = \frac{\tau_{max}}{G_o} \tag{3.4}$$

where τ_{max} is the maximum shear stress of soils under dynamic loadings. A and B are two parameters that define the reduction of shear modulus with increasing shear strain levels. In this study, the four parameters G_o, γ_o, A, and B for sand and clay suggested by Hwang and Lee [13] are used.

3.3.1 Secant Shear Modulus for Cohesionless Soils

The secant shear modulus for sand is affected primarily by the confining pressure and relative density (or void ratio) [14-17]. In general, the shear modulus reduction curve shifts to the right with

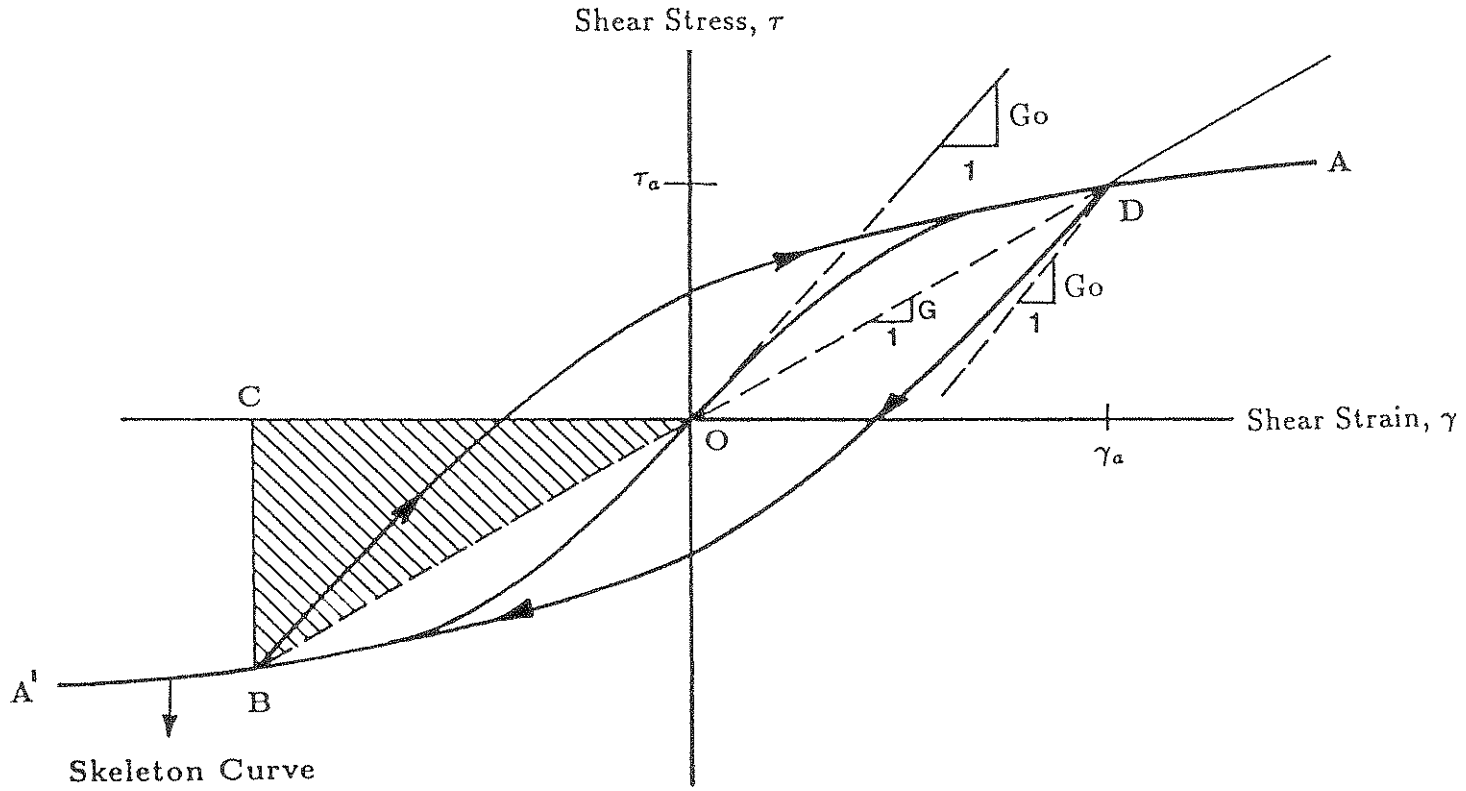

FIGURE 3-4 Hysteresis Loop for Soil

increasing confining pressure (figure 3-5), indicating a smaller reduction of shear modulus with increasing confining pressure at the same strain level [16].

The shear modulus reduction curve for sand in this study is taken from Hwang and Lee [13] and shown in figure 3-6. The A and B parameters of the mean curve in figure 3-6 are 0.941 and 0.441, respectively. The low-strain shear modulus G_o in psf is estimated from the following empirical equation.

$$G_o = 61000\,[1 + (D_r - 75)\,0.01]\,(\bar{\sigma})^{1/2} \qquad (3.5)$$

where $\bar{\sigma}$ is the average effective confining pressure in psf and D_r is the relative density in percentage. The reference strain γ_o is equal to τ_{max}/G_o (equation 3.4). Hardin and Drnevich [18] suggested that τ_{max} can be computed using the following equation.

$$\tau_{max} = \left\{ \left[\left(\frac{1 + K_o}{2}\right) \sigma_v' \sin\phi' + c' \cos\phi' \right]^2 - \left[\left(\frac{1 - K_o}{2}\right) \sigma_v' \right]^2 \right\}^{1/2} \qquad (3.6)$$

in which c' is the apparent cohesion and is negligible for sand; σ_v' is the effective vertical stress. From equations (3.5) and (3.6), it is obvious that G_o and γ_o are a function of the confining pressure and usually increases with depth of a soil profile [19]. In addition, G_o is also affected by the relative density (equation 3.5). Thus, the shear modulus model used in this study accounts for the effect of confining pressure and relative density.

3.3.2 Secant Shear Modulus for Cohesive Soils

Various studies [1, 20-21] have demonstrated that the plasticity index is the most dominant factor affecting the shape of the shear modulus

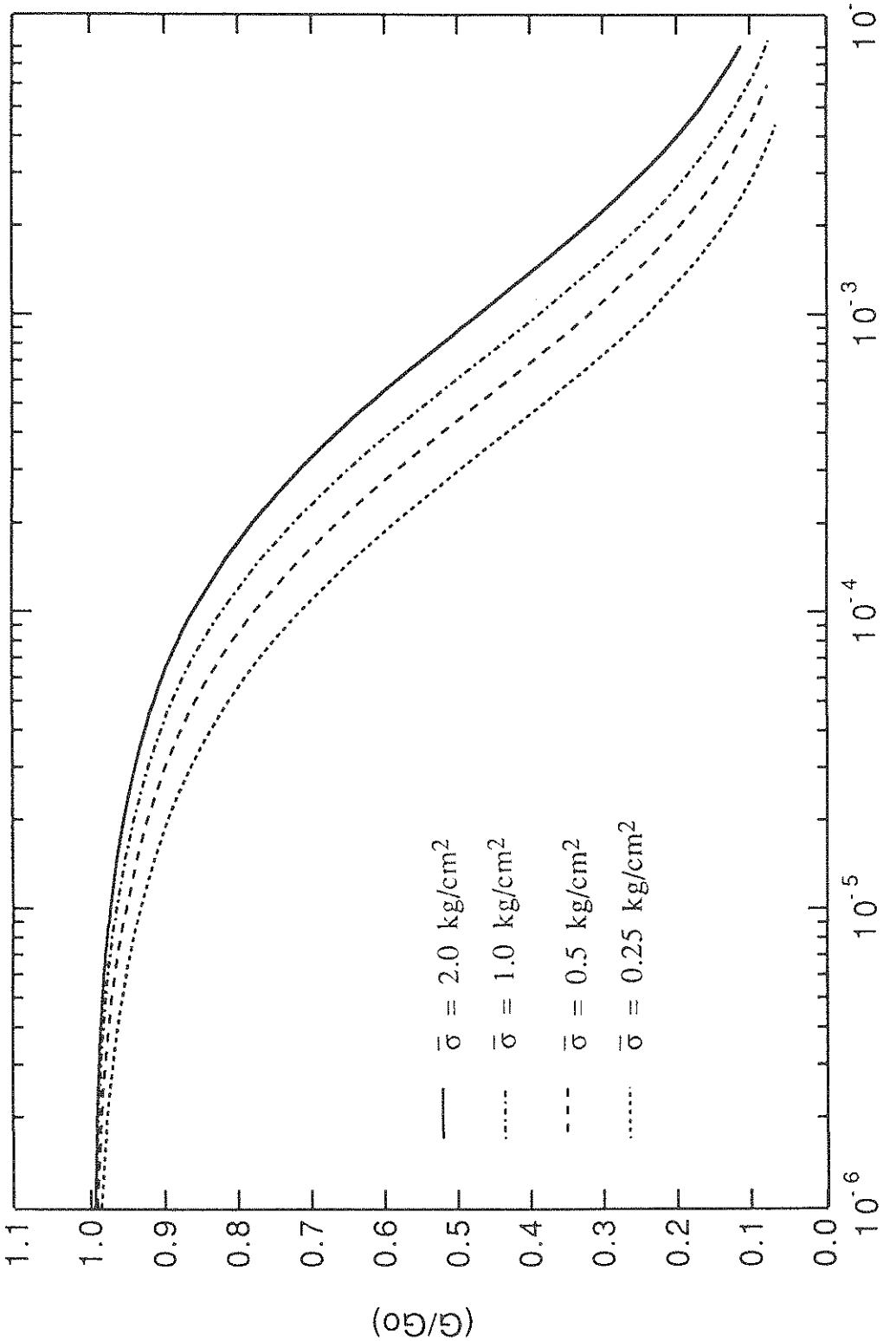

FIGURE 3-5 Influence of Confining Pressure on Shear Modulus for Sand (after Iwasaki et al.)

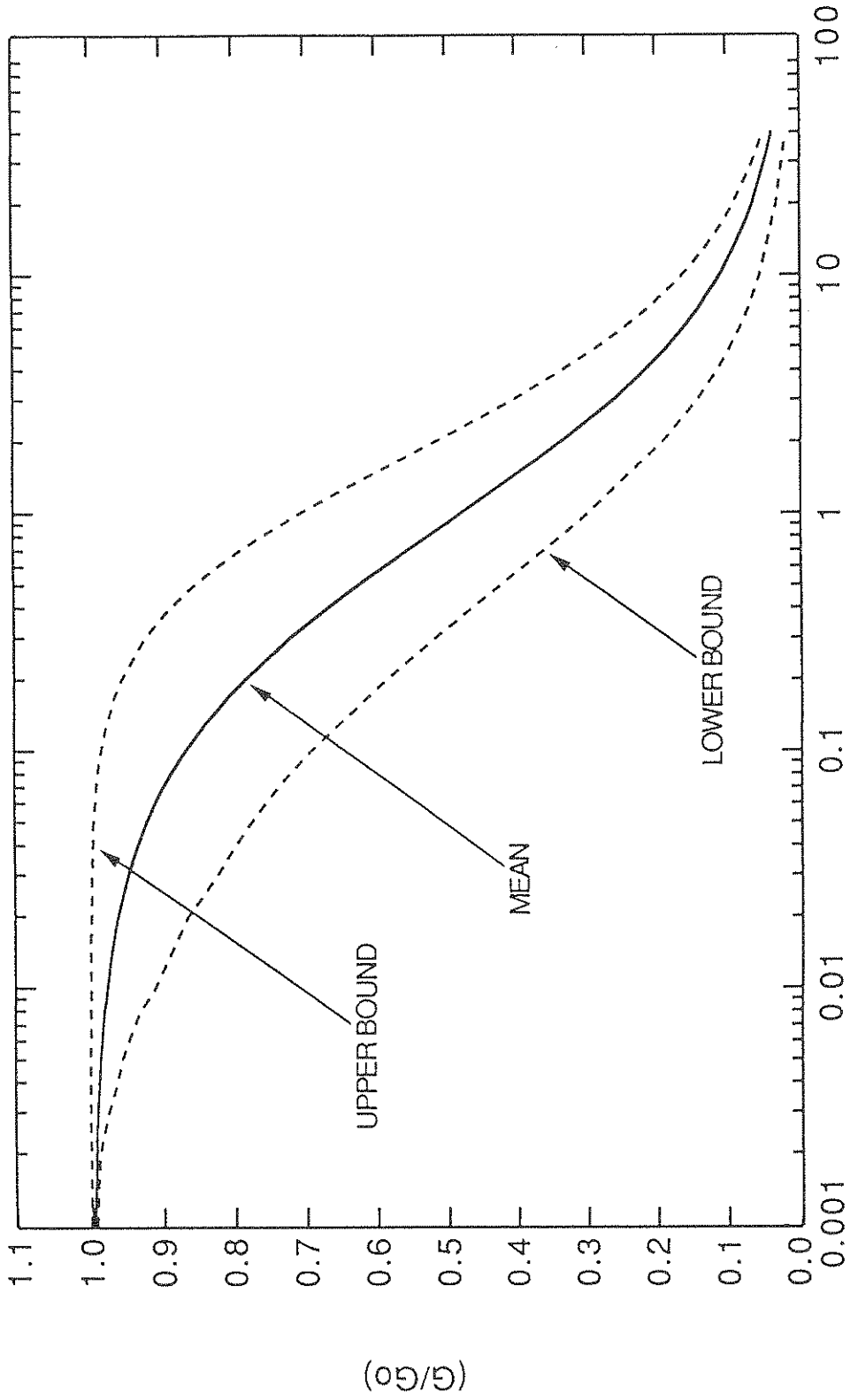

FIGURE 3-6 Shear Modulus Reduction Curves for Sand

reduction curve for clay. Figure 3-7 shows the shear modulus reduction curves corresponding to various ranges of plasticity indices suggested by Sun et al. [21]. The curves gradually shift to the right as the plasticity index increases, which indicates a smaller reduction in shear modulus at a specified level of shear strain as the plasticity index of clay increases. These shear modulus reduction curves are adopted for this study. The parameters A and B for these curves determined by Hwang and Lee [13] are shown in table 3-VII. The low-strain shear modulus G_o of clay is computed as

$$G_o = 2500\ S_u \qquad (3.7)$$

where S_u is the undrained shear strength of clay. In this study, τ_{max} is taken as S_u and G_o is taken as 2500 S_u; thus, the reference strain γ_o is equal to 0.0004. Using these parameter values, the shear modulus reduction curves are generated and also shown in figure 3-7. The two sets of curves are almost identical.

3.4 Results of Two Dynamic Soil Tests

A series of dynamic tests were performed in the laboratory on two soil samples: (1) Collierville sand and (2) Peabody clayey silt (loess). The resonant column test (low-strain amplitude) and cyclic torsional test (high-strain amplitude) are used to determine the shear modulus for the range of shear strain from about 10^{-6} to 10^{-2}.

3.4.1 Collierville Sand

The relative density D_r of the Collierville sand is determined to be 0.7. The low-strain shear moduli G_o at confining pressures of 5, 10, 20, and 40 psi are determined and shown in figure 3-8. The values of G_o used in the MASH program (equation 3.5) are also shown in figure 3-8. For confining pressures of 5, 10, and 20 psi, G_o computed using equation (3.5) is about 12 to 26% larger than those from test results. For

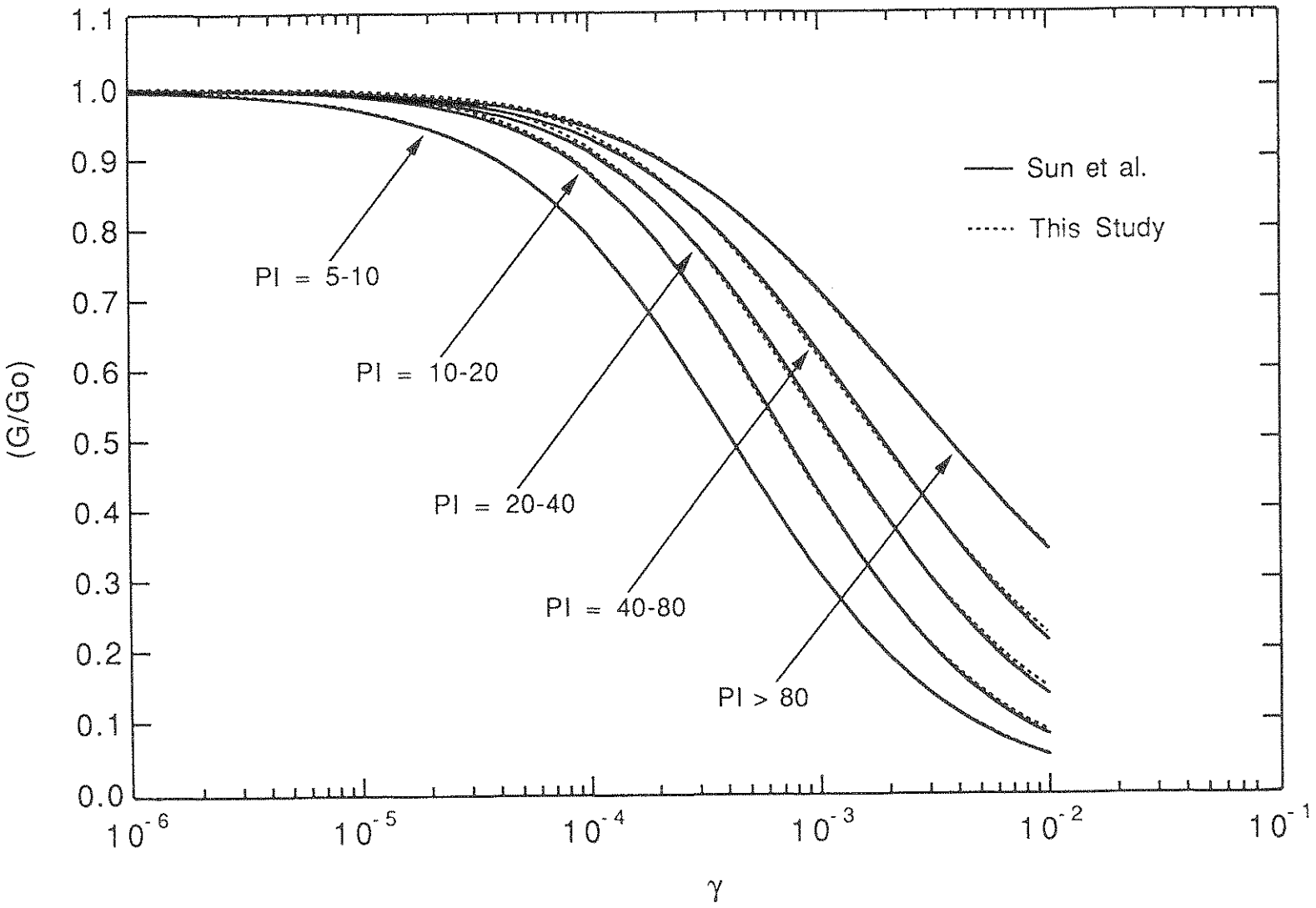

FIGURE 3-7 Shear Modulus Reduction Curves for Clay

Table 3-VII Parameter Values of A and B for Cohesive Soils

PI	A	B
5-10	1.026	0.458
10-20	1.464	0.433
20-40	1.837	0.376
40-80	2.197	0.328
> 80	2.591	0.268

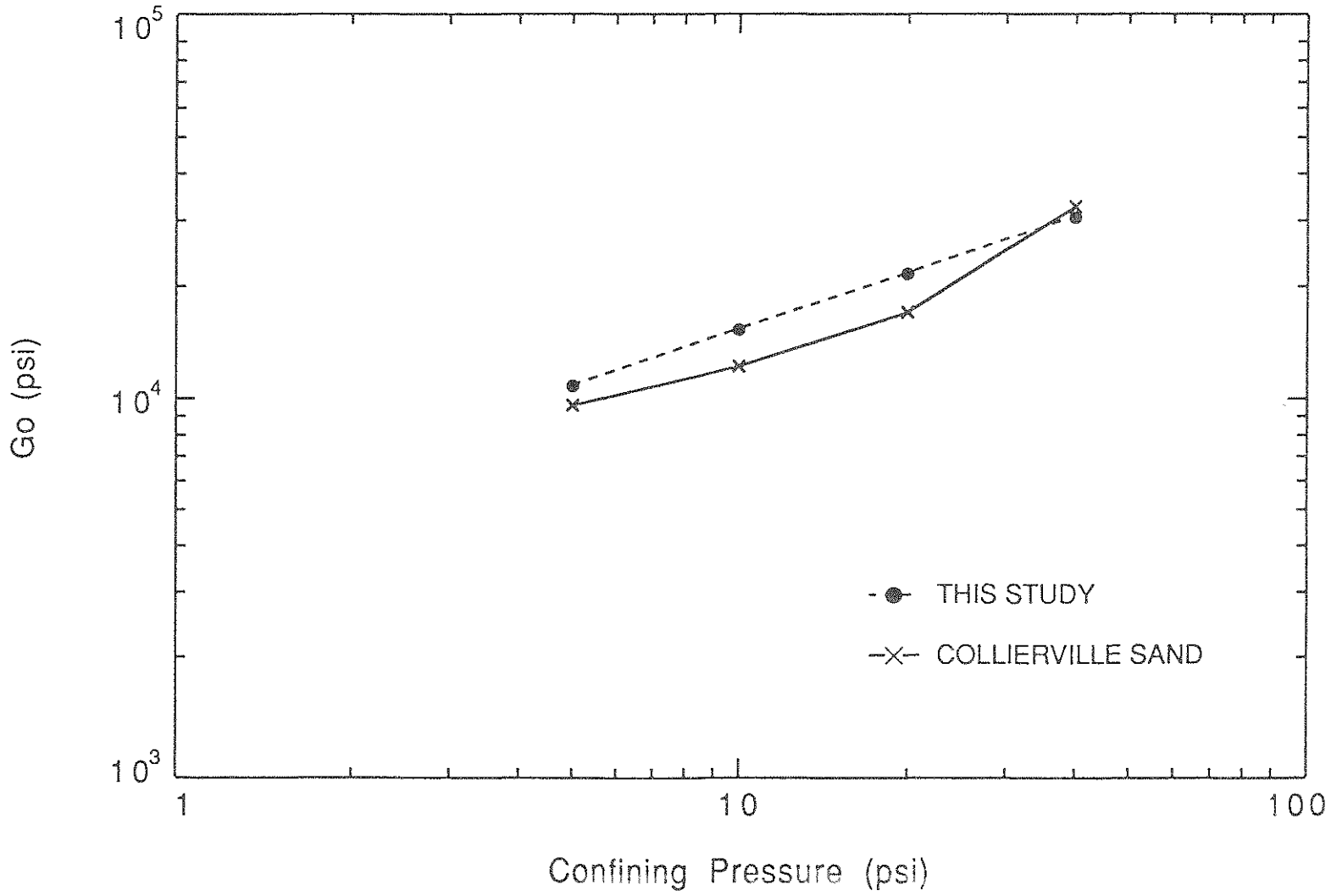

FIGURE 3-8 Low-Strain Shear Modulus for Collierville Sand

confining pressure of 40 psi, the two values appear to be in good agreement. A series of tests are also performed at a confining pressure of 40 psi and the shear strain level ranging from 10^{-6} to 10^{-2}. The shear modulus reduction curve established from the tests and the curve used in this study, with A = 0.941, B = 0.441, and γ_0 = 0.00034 are shown in figure 3-9. The value of γ_0 is determined based on the same testing conditions. It is noted that the curve used in this study is close to the curve established from dynamic testing.

3.4.2 Peabody Clayey Silt

The plasticity index PI of the Peabody clayey silt is estimated to be between 5 and 10. A series of dynamic tests are carried out to determine the shear modulus for the clayey silt at a confining pressure of 40 psi and with shear strain level ranging from about 10^{-6} to 10^{-2}. Figure 3-10 shows the comparison of the shear modulus reduction curve established from the dynamic tests and the curve used in this study with PI range of 5 to 10. These two curves are in close agreement.

3.5 Bedrock Depth

The basement rock in the Memphis area is located approximately 3,000 ft below the ground level, which is beyond the depth commonly found in engineering boring logs. Various studies have demonstrated that site response during earthquakes is primarily affected by the soil layers near the ground surface [22-24]. Sharma and Kovacs [2] suggested that reasonably reliable site-response results for Memphis and Shelby County can be achieved if a soil profile has a depth of 150 ft or greater. In this study, the bedrock is assumed to be located at 200 ft below the ground surface.

Three soil logs T38, T39, and U21 in Memphis and Shelby County reported by Ng et al. [10] have depths of more than 200 ft. The soil logs T38 and T39 are next to each other and almost identical. Thus, the soil log T39 is used in this study. The locations of soil logs U21 and T39 are

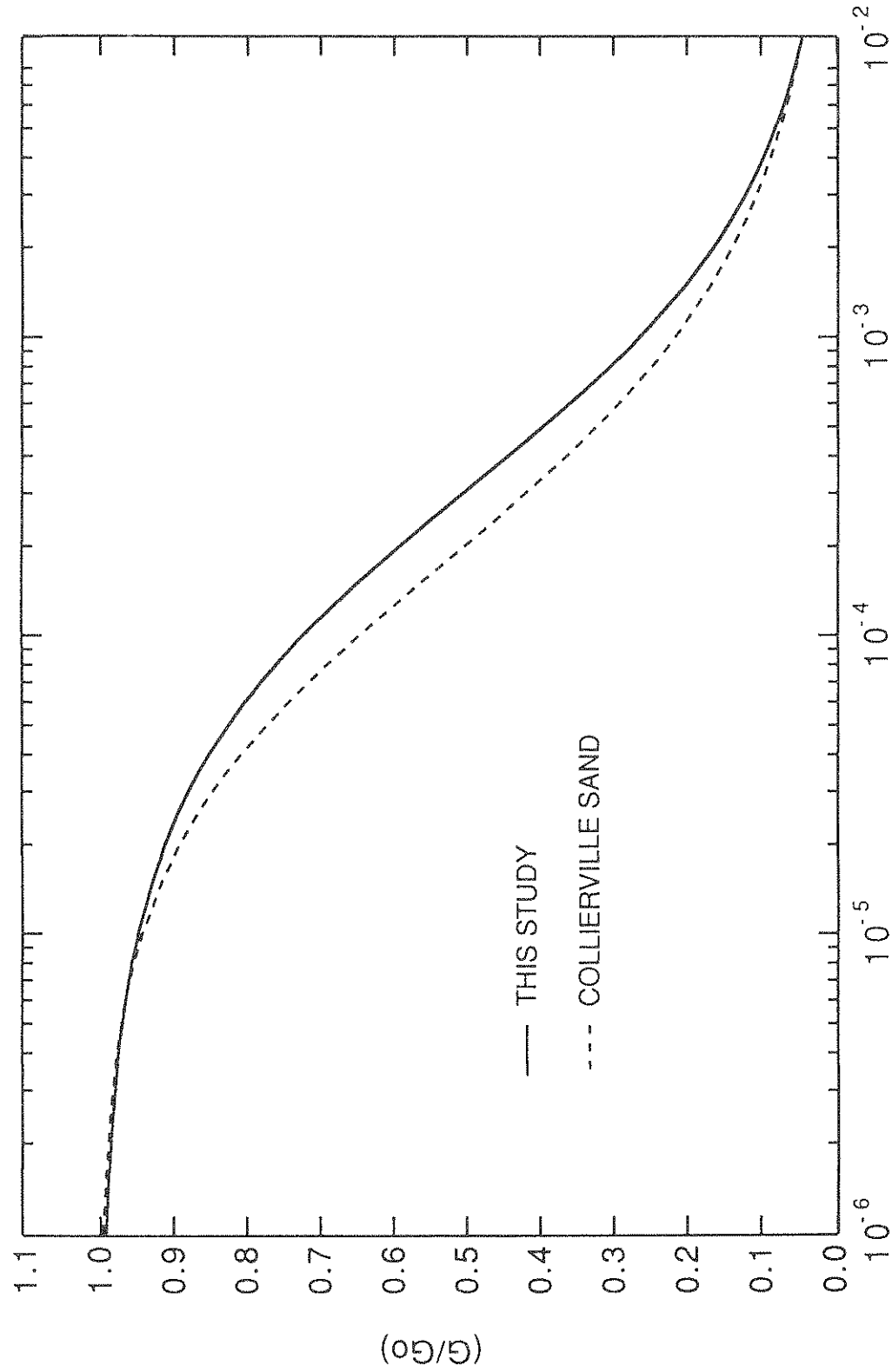

FIGURE 3-9 Shear Modulus Reduction Curve for Collierville Sand

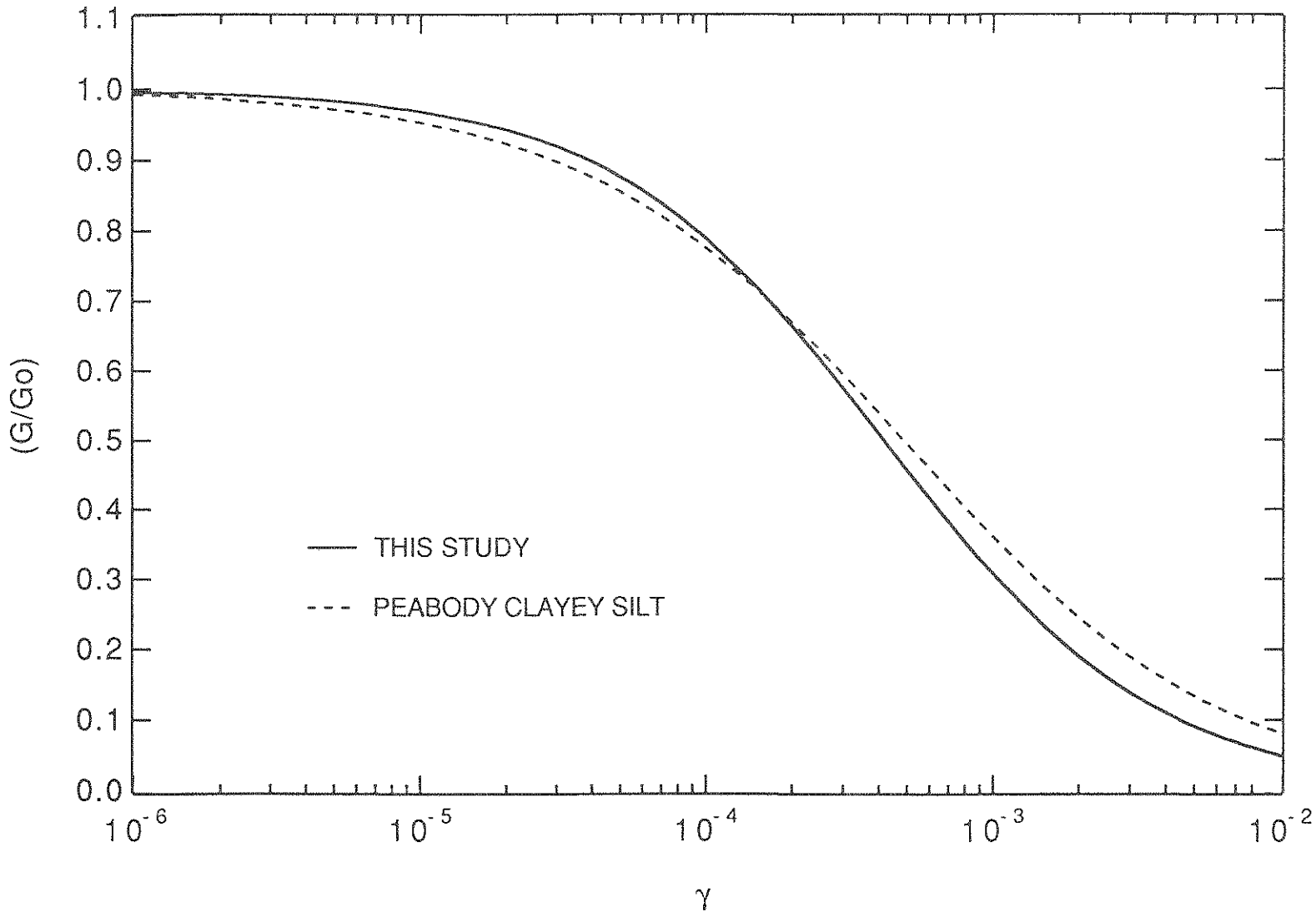

FIGURE 3-10 Shear Modulus Reduction Curve for Peabody Clayey Silt

shown in figure 3-11 as indicated by triangles. These two soil profiles as shown in figures 3-12 and 3-13 are used to extend soil logs with depths less than 200 ft for sites located in the vicinity area. In order to extend soil logs in other areas, 9 general soil profiles are established from water well logs. The locations of these 9 soil profiles are also shown in figure 3-11 by solid circles. The soil types and strata of each general soil profile are obtained from several water well logs in the vicinity of the area. However, the water well logs only have simple descriptions of soil layers. Thus, the engineering properties of the soil layers are estimated from the existing boring logs with the same descriptions. The general soil profiles for Central Memphis, Northwest Memphis, President Island, Mississippi Alluvial Plain, Germantown, Bartlett, Millington, Arlington, and Collierville are shown in figures 3-14 to 3-22. The soil logs available in the Memphis area are usually less than 200 ft. Thus, the soil layers between the depth where soil logs terminated and 200 ft are taken from these 11 soil profiles.

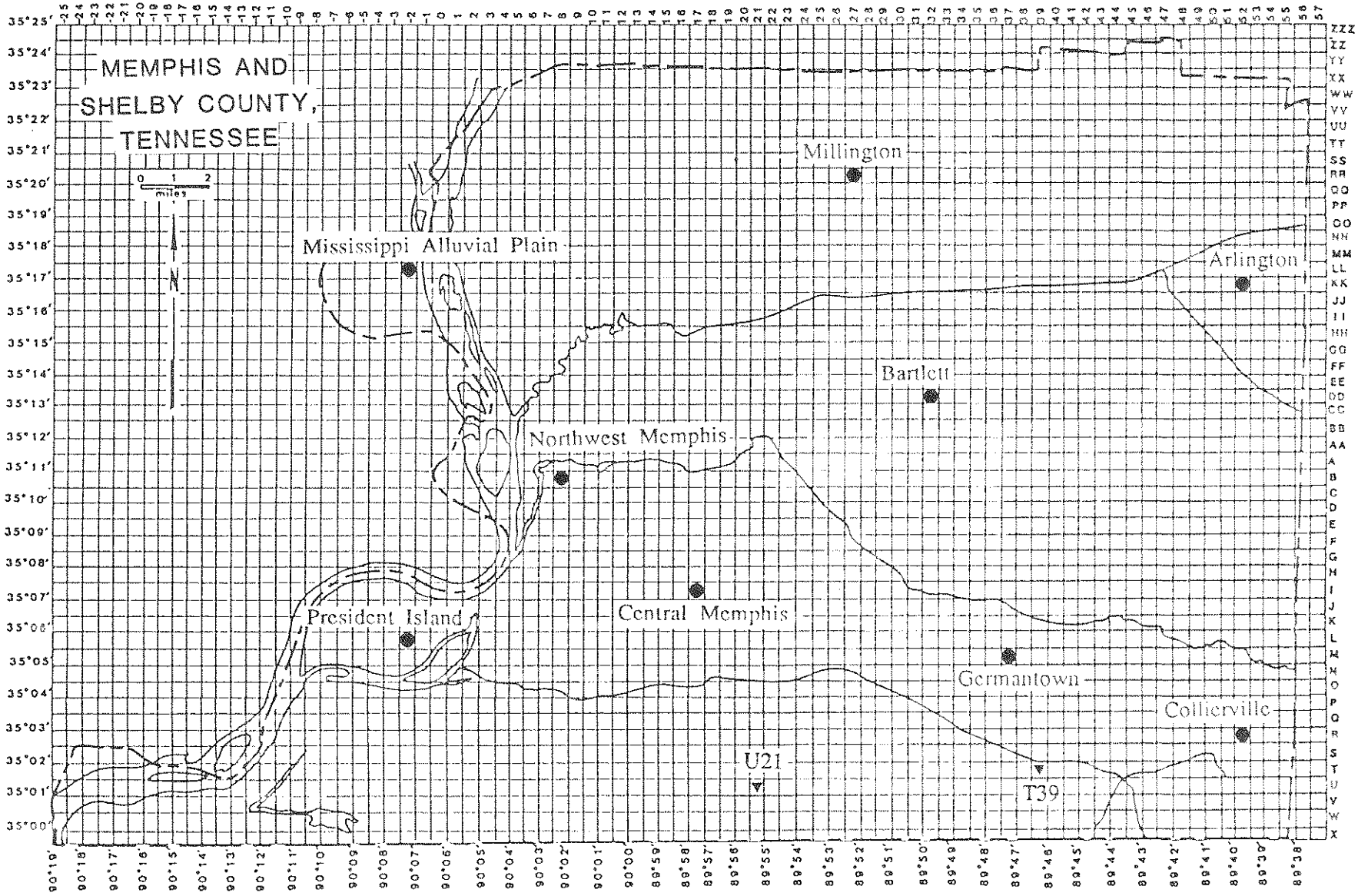

FIGURE 3-11 Locations of General Soil Profiles

Depth (ft)

0

STIFF CLAYEY SILT AND SILTY CLAY (ML-CL)

γ_s = 120 pcf PI = 5-10 S_u = 1500 psf

12

VERY STIFF SILTY CLAY (CL)

γ_s = 125 pcf PI = 10-20 S_u = 2500 psf

21

DENSE SAND AND CLAYEY SAND (SP-SC)

γ_s = 135 pcf K_o = 0.41 D_r = 0.80 ϕ' = 36°

42

MEDIUM DENSE SAND AND CLAYEY SAND (SP-SC)

γ_s = 130 pcf K_o = 0.46 D_r = 0.55 ϕ' = 33°

51

DENSE TO VERY DENSE SAND AND SILTY SAND (SP-SM)

γ_s = 130 pcf K_o = 0.40 D_r = 0.85 ϕ' = 37°

91

HARD CLAY AND SANDY CLAY (CL)

γ_s = 125 pcf PI = 10-20 S_u = 4000 psf

115

DENSE TO VERY DENSE SILTY AND CLAYEY SAND (SM-SC)

γ_s = 130 pcf K_o = 0.38 D_r = 0.90 ϕ' = 38°

145

VERY DENSE SAND (SP)

γ_s = 140 pcf K_o = 0.37 D_r = 1.0 ϕ' = 39°

181

HARD SILTY CLAY (CL)

γ_s = 135 pcf PI = 20-40 S_u = 4500 psf

200

FIGURE 3-12 Soil Profile for Site U21

Depth (ft)

0

VERY STIFF CLAYEY SILT AND SILTY CLAY (ML-CL)

γ_s = 125 pcf PI = 10-20 S_u = 3000 psf

23

VERY DENSE SANDY GRAVEL (GP)

γ_s = 140 pcf K_o = 0.35 D_r = 1.0 ϕ' = 41°

53

VERY DENSE SILTY SAND (SM)

γ_s = 130 pcf K_o = 0.38 D_r = 1.0 ϕ' = 38°

65

VERY DENSE SAND (SP)

γ_s = 140 pcf K_o = 0.37 D_r = 1.0 ϕ' = 39°

72

VERY DENSE SILTY SAND (SM)

γ_s = 135 pcf K_o = 0.37 D_r = 1.0 ϕ' = 39°

161

VERY DENSE GRAVELLY SAND (SP)

γ_s = 140 pcf K_o = 0.36 D_r = 1.0 ϕ' = 40°

200

FIGURE 3-13 Soil Profile for Site T39

Depth (ft)				
0				
	CLAY			
	γ_s = 120 pcf	PI = 5-10	S_u = 1000 psf	
18				
	CLAY			
	γ_s = 122 pcf	PI = 10-20	S_u = 1500 psf	
30				
	SAND AND GRAVEL			
	γ_s = 125 pcf	K_o = 0.47	D_r = 0.7	ϕ' = 33°
50				
	SAND AND GRAVEL			
	γ_s = 130 pcf	K_o = 0.42	D_r = 0.8	ϕ' = 36°
70				
	SAND AND GRAVEL			
	γ_s = 135 pcf	K_o = 0.40	D_r = 1.0	ϕ' = 37°
100				
	CLAY			
	γ_s = 125 pcf	PI = 40-80	S_u = 4000 psf	
150				
	CLAY			
	γ_s = 130 pcf	PI = 20-40	S_u = 4500 psf	
200				

FIGURE 3-14 General Soil Profile for Central Memphis

Depth (ft)				
0				
	CLAY			
	γ_s = 122 pcf	PI = 10-20	S_u = 2500 psf	
30				
	SAND AND GRAVEL			
	γ_s = 130 pcf	K_o = 0.45	D_r = 0.6	ϕ' = 35°
50				
	CLAY			
	γ_s = 125 pcf	PI = 20-40	S_u = 3500 psf	
60				
	SAND AND GRAVEL			
	γ_s = 135 pcf	K_o = 0.40	D_r = 0.75	ϕ' = 38°
80				
	CLAY			
	γ_s = 125 pcf	PI = 40-80	S_u = 4500 psf	
110				
	CLAY			
	γ_s = 130 pcf	PI = 20-40	S_u = 5000 psf	
150				
	CLAY			
	γ_s = 135 pcf	PI = 20-40	S_u = 5500 psf	
200				

FIGURE 3-15 General Soil Profile for Northwest Memphis

Depth (ft)				
0				
	TOP SOIL			
20				
	SAND			
	γ_s = 120 pcf	K_o = 0.5	D_r = 0.65	ϕ' = 30°
40				
	CLAY			
	γ_s = 120 pcf	K_o = 0.48	D_r = 0.70	ϕ' = 33°
60				
	SAND			
	γ_s = 125 pcf	K_o = 0.44	D_r = 0.75	ϕ' = 35°
80				
	SAND			
	γ_s = 130 pcf	K_o = 0.40	D_r = 0.80	ϕ' = 37°
110				
	SAND AND GRAVEL			
	γ_s = 135 pcf	K_o = 0.38	D_r = 0.90	ϕ' = 38°
130				
	SAND AND GRAVEL			
	γ_s = 140 pcf	K_o = 0.36	D_r = 0.95	ϕ' = 40°
150				
	CLAY			
	γ_s = 130 pcf	PI = 20-40	S_u = 4000 psf	
175				
	CLAY			
	γ_s = 135 pcf	PI = 20-40	S_u = 4500 psf	
200				

FIGURE 3-16 General Soil Profile for President Island

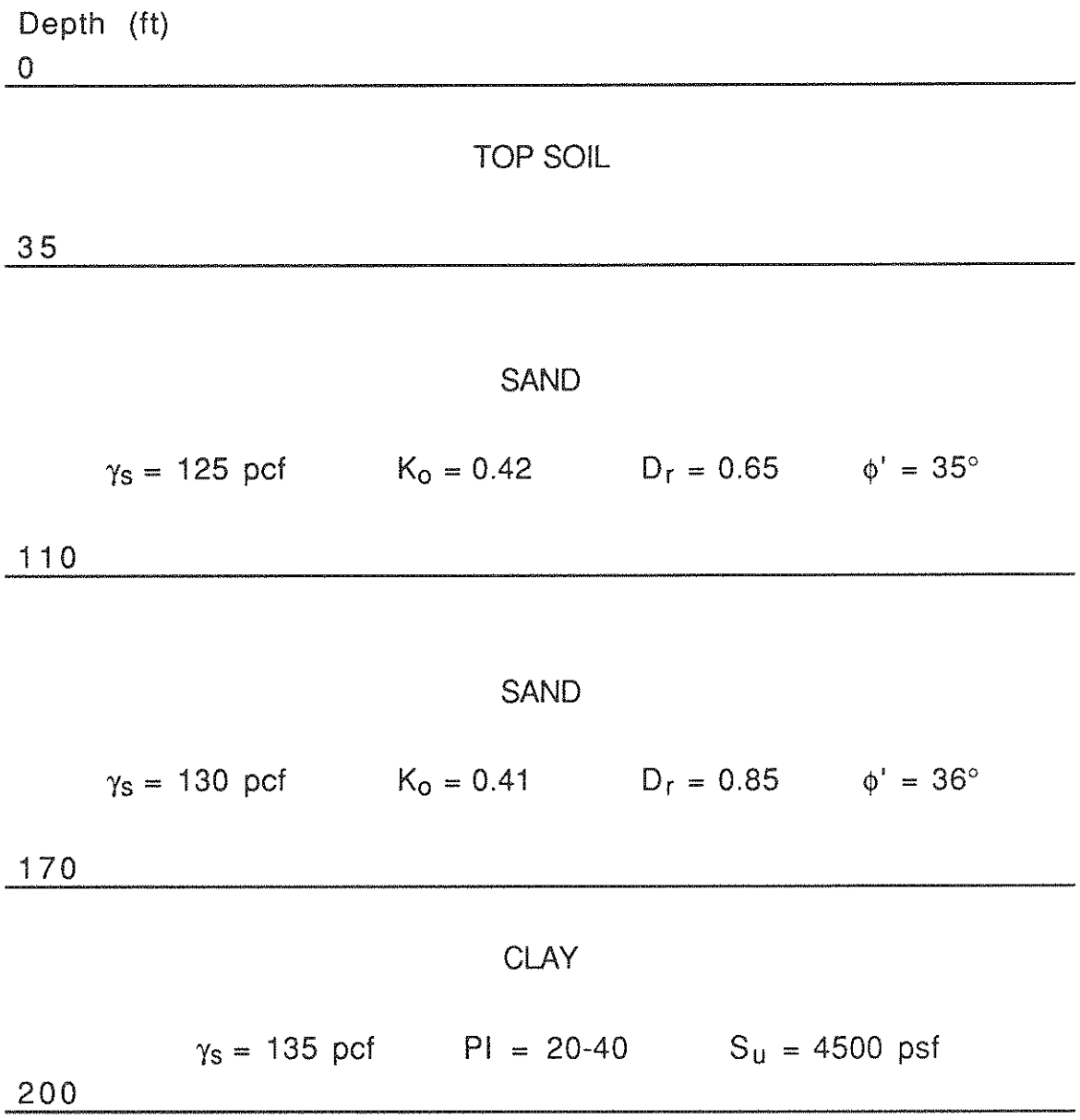

FIGURE 3-17 General Soil Profile for Mississippi Alluvial Plain

Depth (ft)				
0				
	TOP SOIL			
20				
	SAND AND GRAVEL			
	γ_s = 130 pcf	K_o = 0.42	D_r = 0.70	ϕ' = 38°
38				
	SAND AND GRAVEL			
	γ_s = 135 pcf	K_o = 0.4	D_r = 0.80	ϕ' = 40°
50				
	CLAY			
	γ_s = 120 pcf	PI = 10-20	S_u = 2500 psf	
60				
	SANDY CLAY			
	γ_s = 122 pcf	PI = 10-20	S_u = 3000 psf	
78				
	SANDY CLAY			
	γ_s = 125 pcf	PI = 10-20	S_u = 3500 psf	
90				
	HARD CLAY			
	γ_s = 130 pcf	PI = 20-40	S_u = 4000 psf	
110				
	HARD CLAY			
	γ_s = 130 pcf	PI = 20-40	S_u = 4500 psf	
130				
	HARD CLAY			
	γ_s = 130 pcf	PI = 40-80	S_u = 5000 psf	
160				
	SANDY CLAY AND LIGNITE			
	γ_s = 130 pcf	PI = 10-20	S_u = 4000 psf	
180				
	SANDY CLAY AND LIGNITE			
	γ_s = 135 pcf	PI = 20-40	S_u = 5000 psf	
200				

FIGURE 3-18 General Soil Profile for Germantown

Depth (ft)				
0				
	CLAY			
	γ_s = 120 pcf	PI = 10-20	S_u = 1000 psf	
20				
	SAND			
	γ_s = 125 pcf	K_o = 0.45	D_r = 0.7	ϕ' = 33°
35				
	GRAVEL			
	γ_s = 135 pcf	K_o = 0.40	D_r = 0.9	ϕ' = 39°
50				
	CLAY			
	γ_s = 125 pcf	PI = 20-40	S_u = 2500 psf	
70				
	CLAY			
	γ_s = 125 pcf	PI = 20-40	S_u = 3000 psf	
90				
	CLAY			
	γ_s = 128 pcf	PI = 20-40	S_u = 3500 psf	
110				
	SAND			
	γ_s = 130 pcf	K_o = 0.4	D_r = 0.95	ϕ' = 37°
125				
	SAND			
	γ_s = 135 pcf	K_o = 0.4	D_r = 1.00	ϕ' = 39°
140				
	CLAY			
	γ_s = 125 pcf	PI = 20-40	S_u = 3500 psf	
160				
	CLAY			
	γ_s = 130 pcf	PI = 20-40	S_u = 4000 psf	
180				
	CLAY			
	γ_s = 130 pcf	PI = 20-40	S_u = 4500 psf	
200				

FIGURE 3-19 General Soil Profile for Bartlett

Depth (ft)				
0				
	CLAY			
	γ_s = 115 pcf	PI = 10-20	S_u = 1000 psf	
20				
	CLAY			
	γ_s = 120 pcf	PI = 10-20	S_u = 1500 psf	
40				
	SAND AND GRAVEL			
	γ_s = 130 pcf	K_o = 0.4	D_r = 0.85	ϕ' = 38°
65				
	SAND AND GRAVEL			
	γ_s = 140 pcf	K_o = 0.4	D_r = 0.95	ϕ' = 40°
90				
	CLAY			
	γ_s = 125 pcf	PI = 20-40	S_u = 3500 psf	
105				
	SAND			
	γ_s = 135 pcf	K_o = 0.4	D_r = 0.95	ϕ' = 39°
120				
	CLAY			
	γ_s = 125 pcf	PI = 40-80	S_u = 4000 psf	
140				
	CLAY			
	γ_s = 125 pcf	PI = 40-80	S_u = 4000 psf	
160				
	CLAY			
	γ_s = 130 pcf	PI = 20-40	S_u = 4500 psf	
180				
	CLAY			
	γ_s = 130 pcf	PI = 20-40	S_u = 4500 psf	
200				

FIGURE 3-20 General Soil Profile for Millington

Depth (ft)				
0				
	TOP SOIL			
20				
	SAND			
	γ_s = 125 pcf	K_o = 0.4	D_r = 0.75	ϕ' = 38°
35				
	SAND			
	γ_s = 130 pcf	K_o = 0.4	D_r = 0.85	ϕ' = 38°
50				
	CLAY			
	γ_s = 120 pcf	PI = 40-80	S_u = 5000 psf	
70				
	CLAY			
	γ_s = 125 pcf	PI = 20-40	S_u = 4500 psf	
95				
	CLAY			
	γ_s = 125 pcf	PI = 20-40	S_u = 5000 psf	
120				
	SAND			
	γ_s = 135 pcf	K_o = 0.4	D_r = 0.95	ϕ' = 40°
140				
	SAND			
	γ_s = 140 pcf	K_o = 0.4	D_r = 0.95	ϕ' = 40°
160				
	SAND			
	γ_s = 140 pcf	K_o = 0.4	D_r = 1.00	ϕ' = 40°
180				
	SAND			
	γ_s = 145 pcf	K_o = 0.4	D_r = 1.00	ϕ' = 40°
200				

FIGURE 3-21 General Soil Profile for Arlington

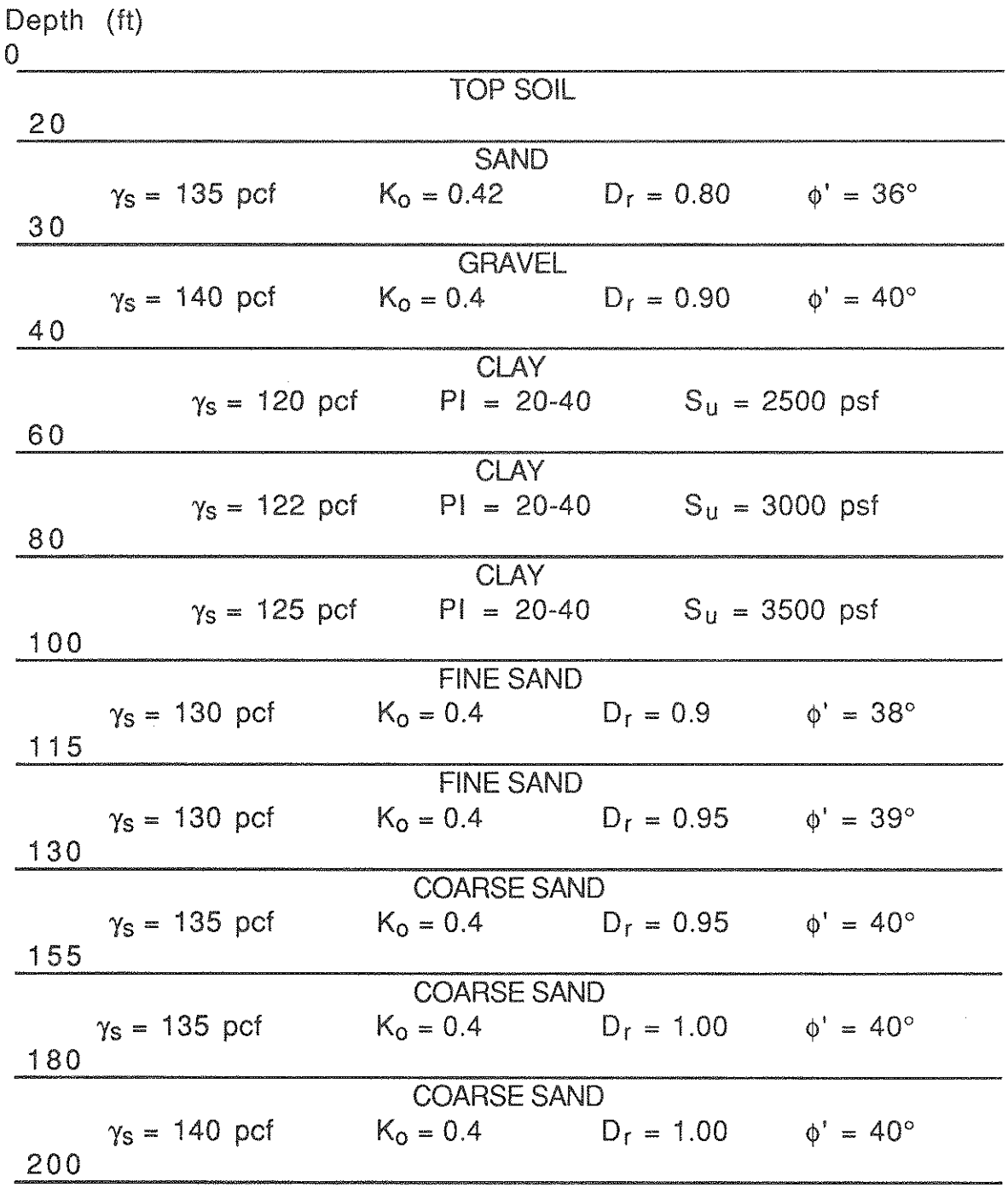

FIGURE 3-22 General Soil Profile for Collierville

SECTION 4

RESULTS OF SITE RESPONSE ANALYSES

The site response analyses are performed for the boring logs with good geotechnical data in the Memphis area. A total of 424 boring logs reported by Ng et al. [10] is used as indicated in figure 4-1. The area lacking data are usually agricultural lands, forests, state parks, and sparsely populated rural areas. The site J2 is selected to illustrate the site response analysis using the MASH program. Then, the results of all site response analyses are presented in this section.

4.1 Soil Profile Classification

The 424 sites used in this study are first classified according to the soil profile categories specified in the 1988 Uniform Building Code (UBC) [25]. The soil profile categories S_1, S_2, S_3, and S_4 are described in table 4-I. The soft clay mentioned in table 4-I is interpreted as soft clay and loose sand. In addition, medium dense sand and medium stiff clay are treated as the same material for the purpose of classifications. Under these interpretations, the 424 soil profiles in Memphis and Shelby County are classified into S_2, S_3, and S_4 categories. The soil category S_1 does not exist in the study area. Additional 171 existing boring logs are also classified and used to establish a generalized map of soil profile classification for Memphis and Shelby County. The distributions of the soil profile categories in Memphis and Shelby County are shown in figure 4-2. The generalized map of soil profile classification is shown in figure 4-3.

4.2 Site Response Analysis of Site J2

The site J2 is located at President Island and the soil profile consists predominantly of sand deposits. The boring log terminates at 152 ft (figure 4-4). To extend the soil profile, the soil layers between 152 and 200 ft are taken from the general soil profile for the President Island

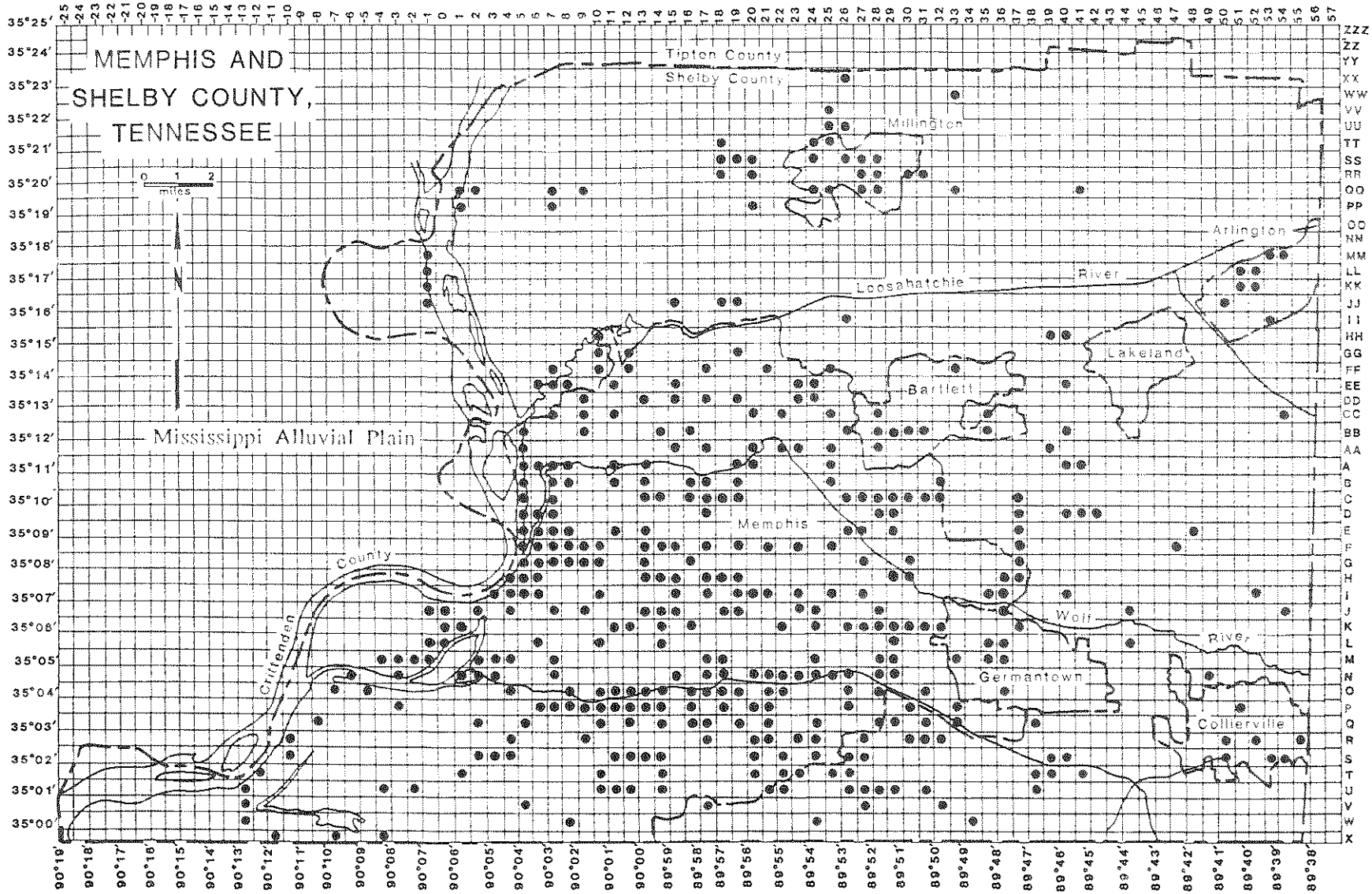

FIGURE 4-1 Distribution of Selected Sites

Table 4-I Soil Profile Classifications

Type	Description
S_1	A soil profile with either: (a) A rock-like material characterized by a shear-wave velocity greater than 2,500 ft per second or by other suitable means of classification, or (b) Stiff or dense soil condition where the soil depth is less than 200 ft.
S_2	A soil profile with dense or stiff soil conditions, where the soil depth exceeds 200 ft.
S_3	A soil profile 40 ft or more in depth and containing more than 20 ft of soft to medium stiff clay but not more than 40 ft of soft clay.
S_4	A soil profile containing more than 40 ft of soft clay.

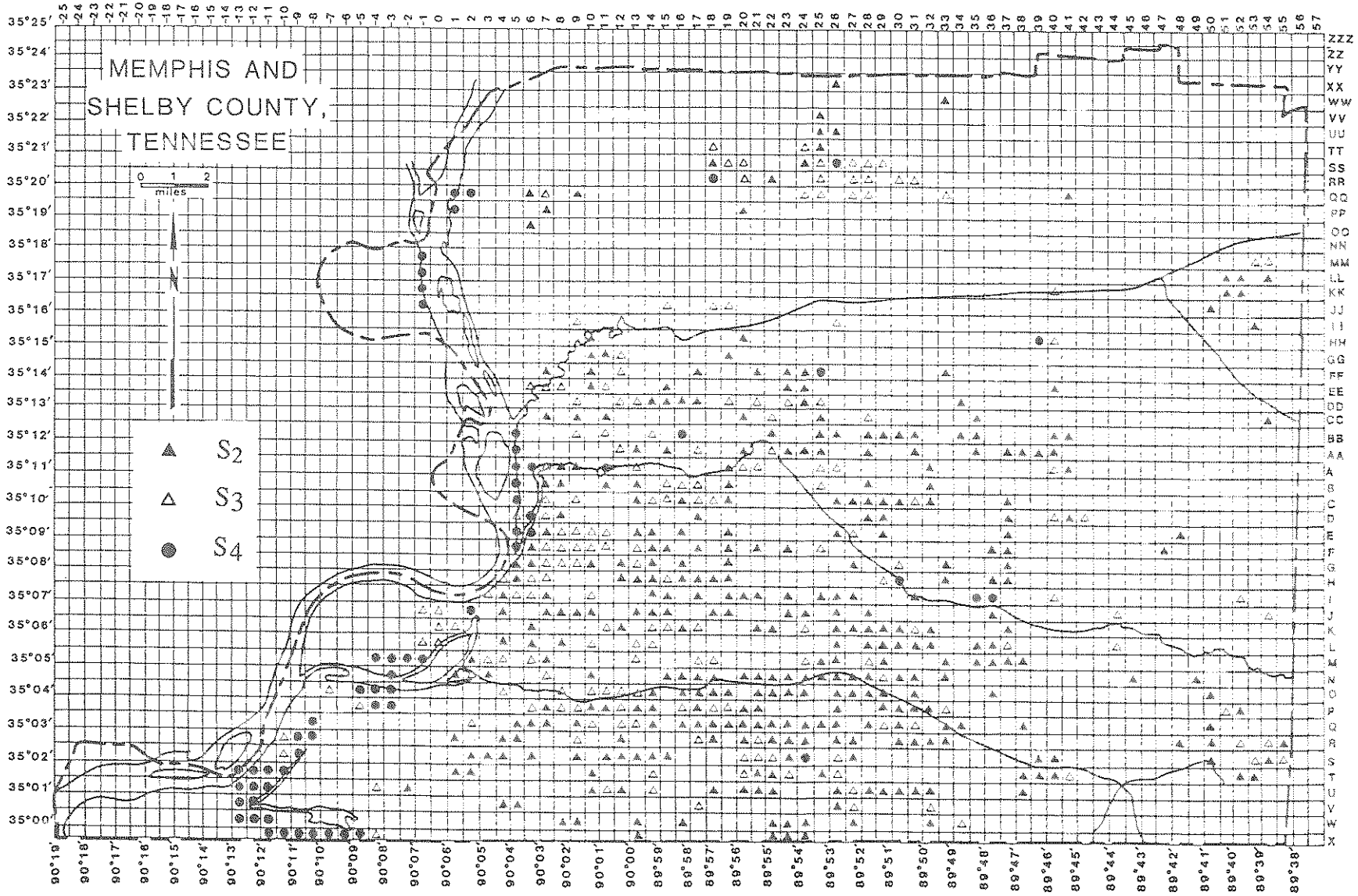

FIGURE 4-2 Distribution of Soil Profile Categories

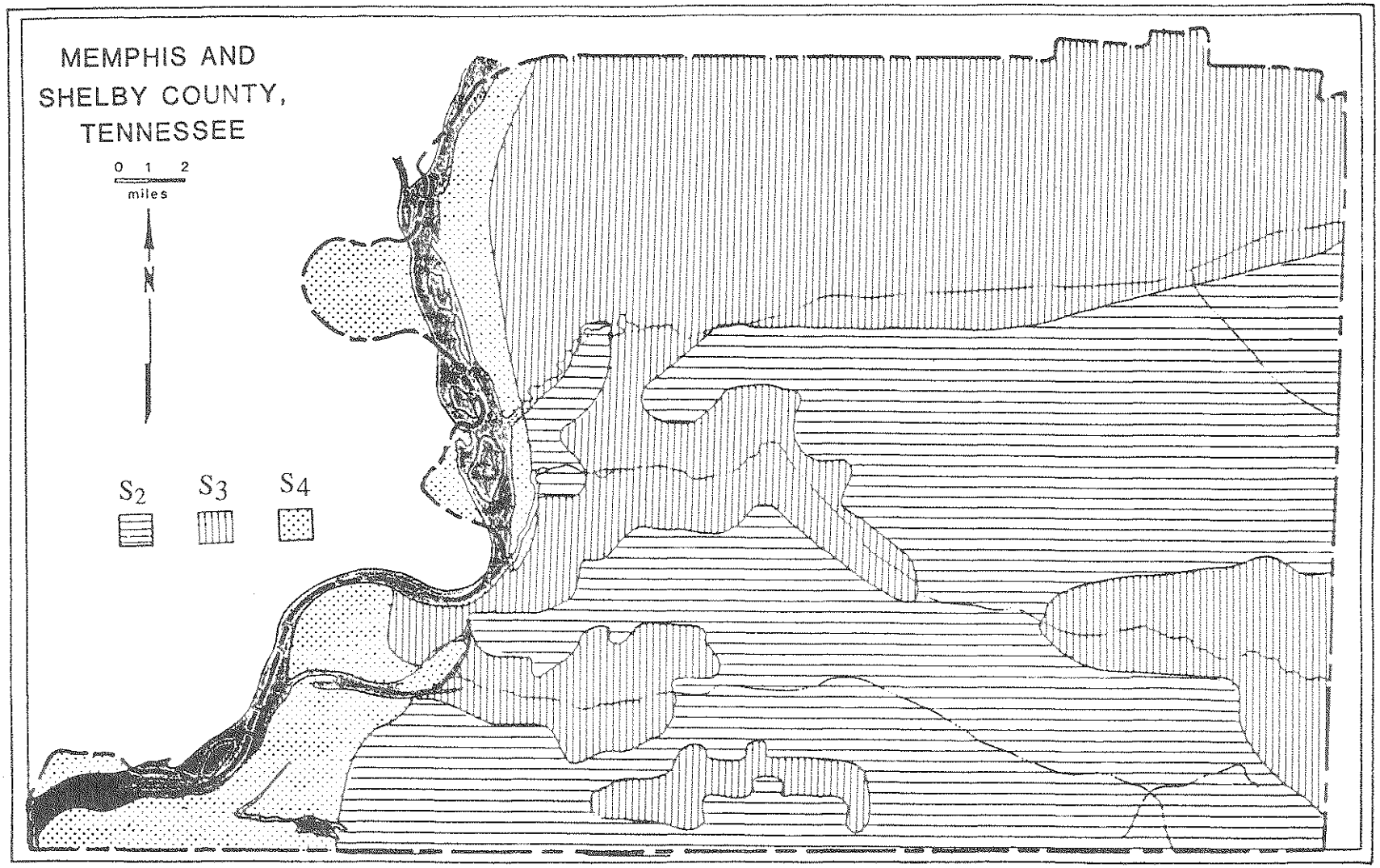

FIGURE 4-3 Generalized Map of Soil Profile Classifications

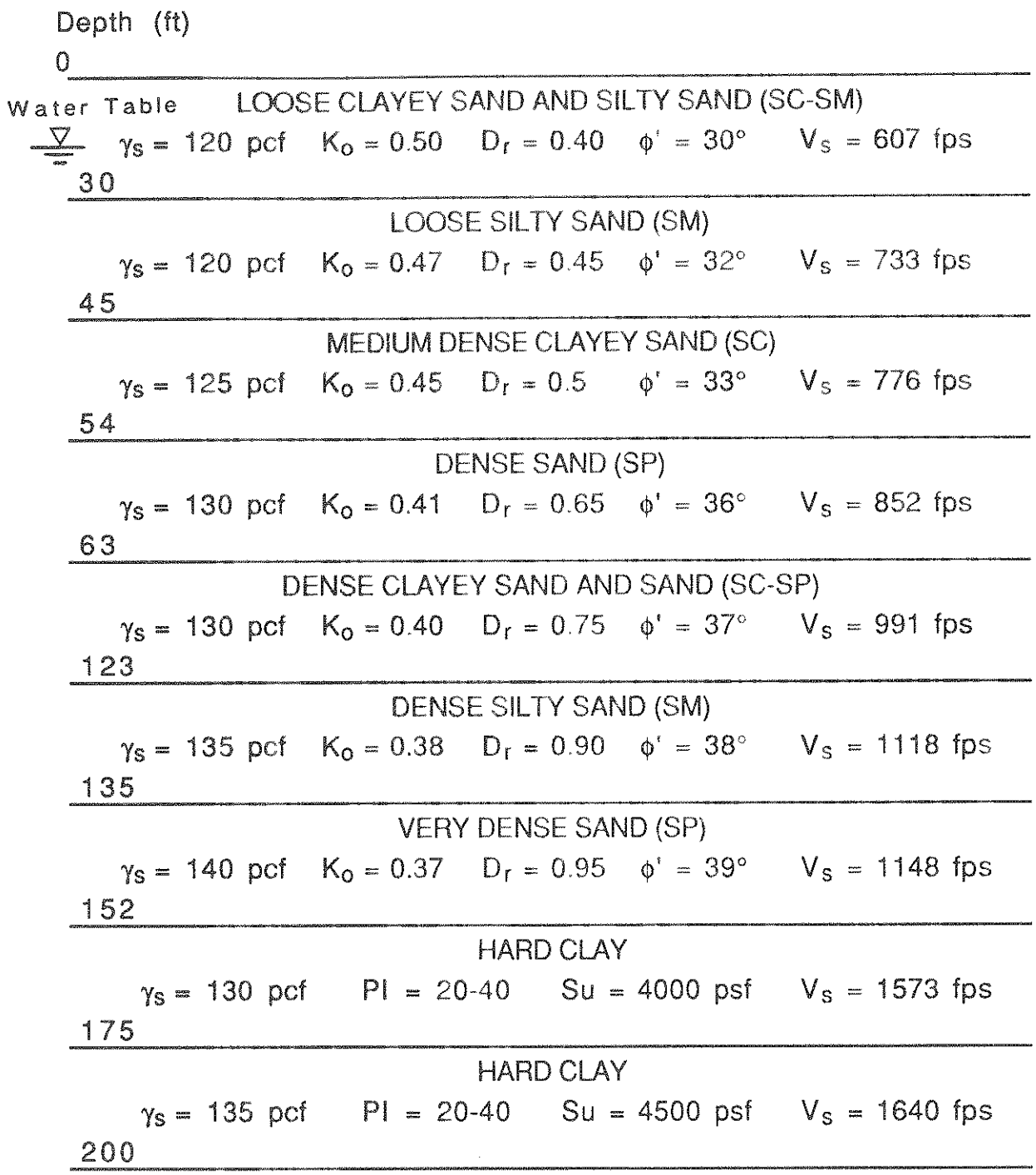

FIGURE 4-4 Soil Profile for Site J2

area (figure 3-16). The profile is divided into 9 layers as shown in figure 4-4. Division of soil layers is made at boundaries of different soil types (clay, sand, gravel, and silt, etc.) and at boundary where an abrupt change of soil properties occurs, e.g., sudden change of N_{SPT} values. The soil properties of each layer are shown in figure 4-4. The shear wave velocity of a soil layer V_s is determined as

$$V_s = \sqrt{G_o/\rho} \qquad (4.1)$$

where ρ is the mass density. Each layer is further discretized into several equal-size elements. The boring log indicates that the water table is located at 20 ft below the ground level, and the depth of full saturation line is estimated to be 16 ft below the ground level. The soil properties required to run the MASH program are discussed in Section 3.

The dynamic soil model is excited by an earthquake acceleration time history at the bedrock level. This bedrock acceleration as shown in figure 4-5 is established by multiplying the normalized time history with a peak value of 0.19g as discussed in Section 2. From the site response analysis, the acceleration time history at the ground surface is obtained and shown in figure 4-6. The peak ground acceleration (PGA) is 0.14g. Thus, the peak value of the bedrock accelerations is reduced as the shear waves propagate through the soil deposit.

The ground and bedrock response spectra with 5% damping ratio are shown in figure 4-7. The frequency contents of the ground and bedrock accelerations have a tremendous difference. The spectral accelerations of the ground acceleration are considerably higher than those of the bedrock accelerations between the period of 0.15 and 1.4 seconds. The spectral acceleration ratio is defined as the ratio of the ground spectral acceleration to the bedrock spectral acceleration at the same period. The spectral acceleration ratio spectrum for periods up to 3.0 seconds is shown in figure 4-8. The F_{PSA} factor is the peak value of the spectral

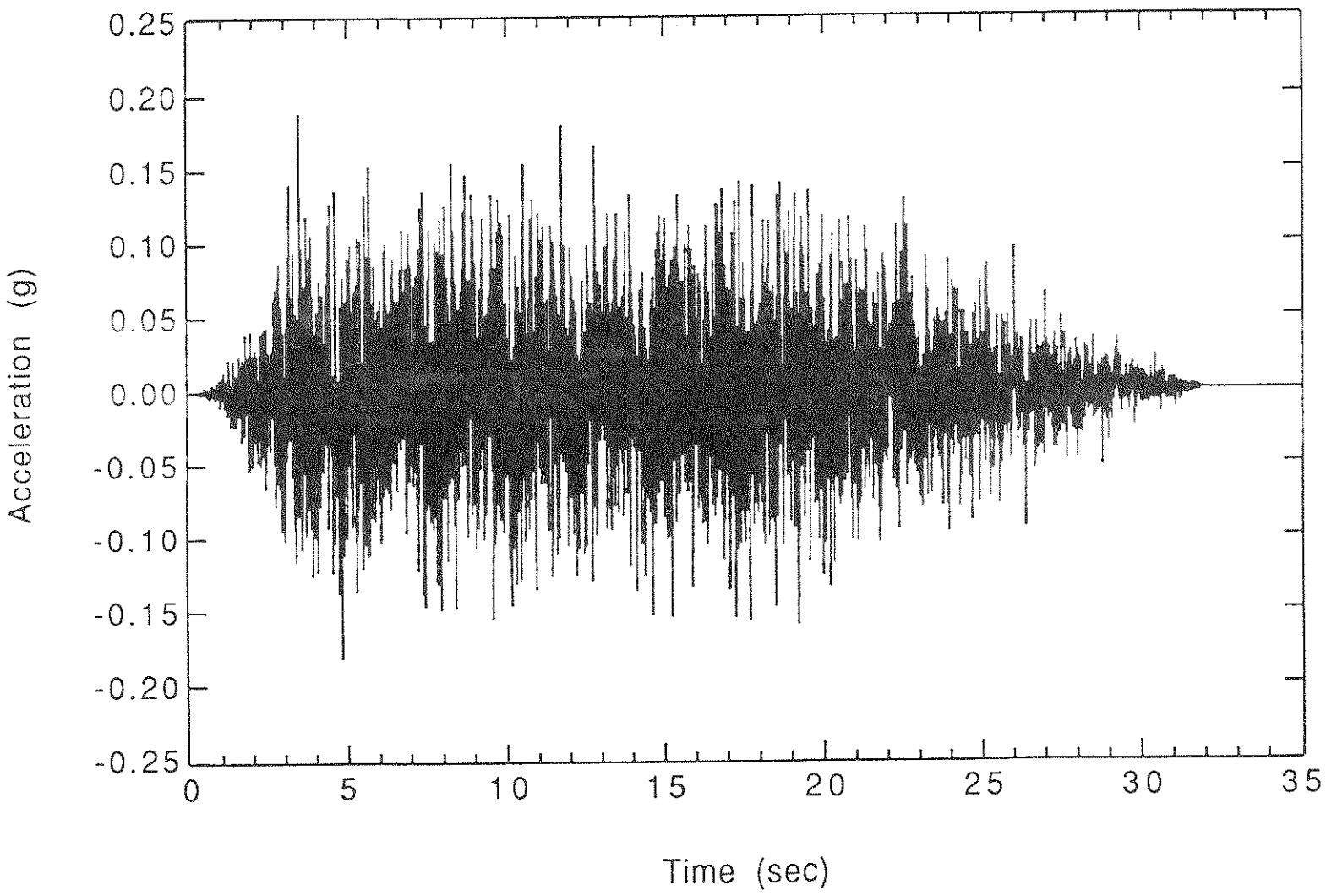

FIGURE 4-5 Bedrock Acceleration Time History for Site J2

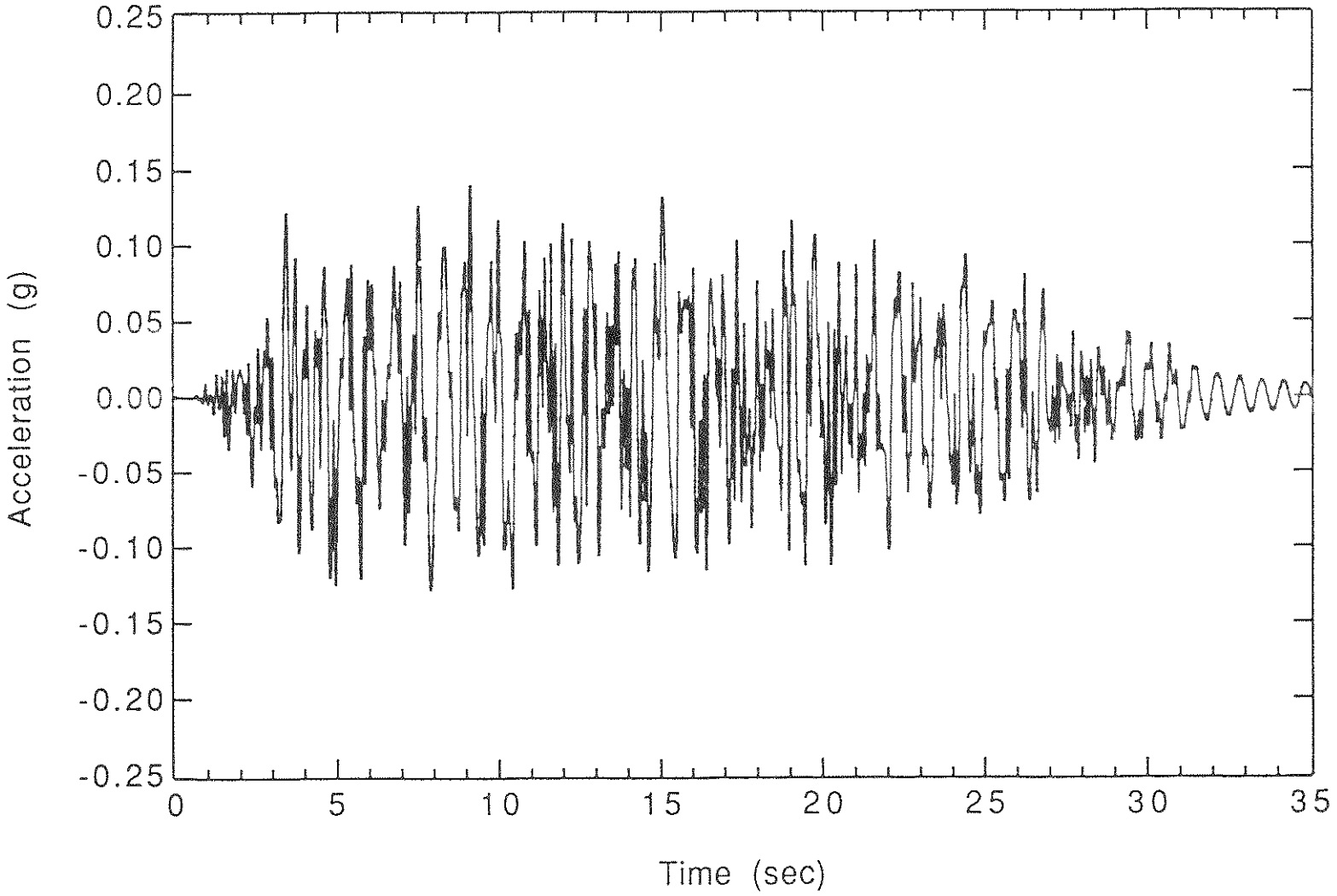

FIGURE 4-6 Ground Acceleration Time History for Site J2

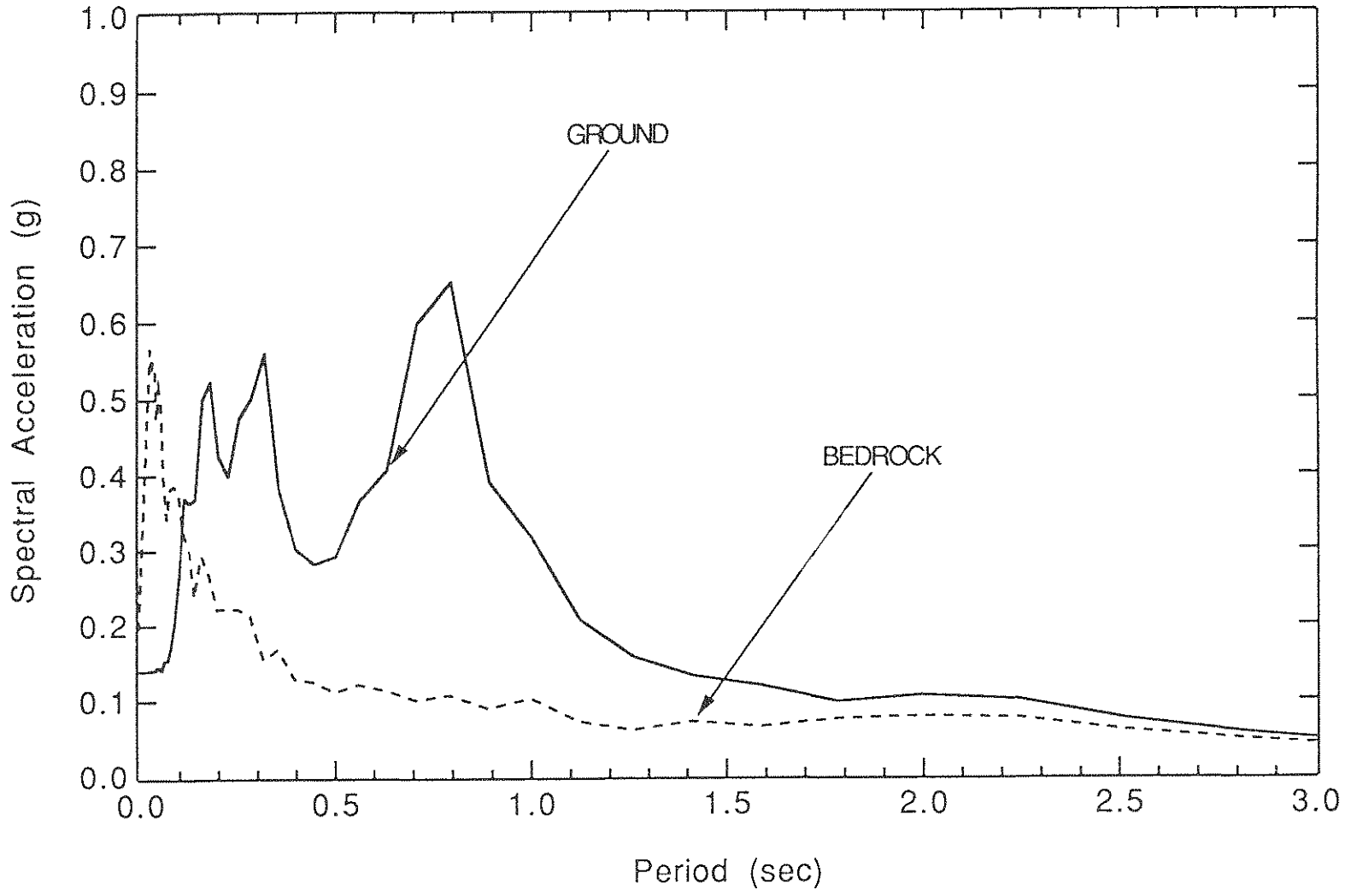

FIGURE 4-7 Ground and Bedrock Response Spectra for Site J2

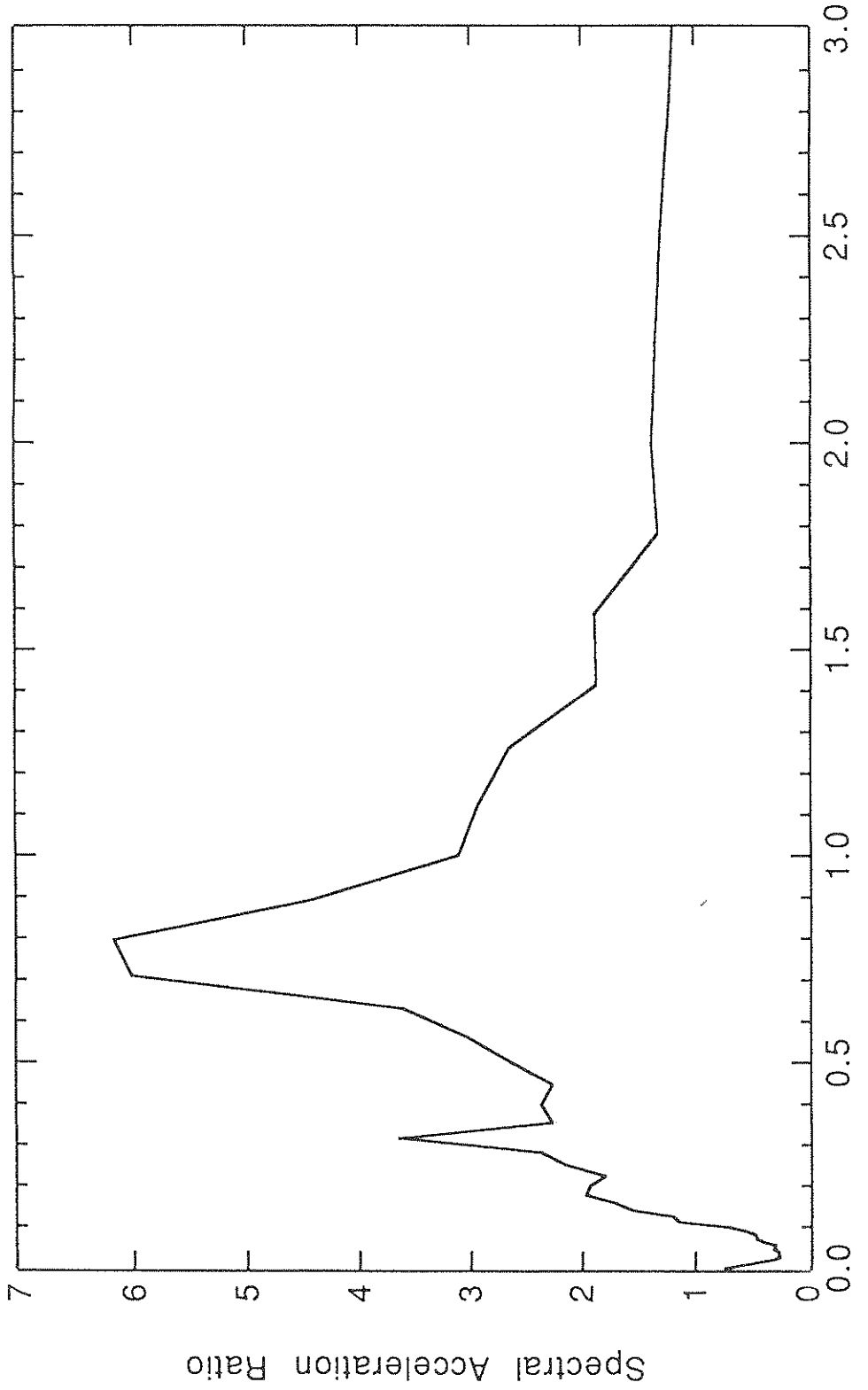

FIGURE 4-8 Spectral Acceleration Ratio Spectrum for Site J2

acceleration ratio. As shown in figure 4-8, the F_{PSA} value for site J2 is 6.18 at the period of 0.80 second. The period at which the largest spectral acceleration ratio occurs corresponds to the dynamic site period of a site. On the other hand, the so-called low-strain site period T_S is estimated as

$$T_S = \frac{4H}{V_{S,ave}} \qquad (4.2)$$

where H is the total depth of the soil profile and $V_{S,ave}$ is the average shear wave velocity of the soil profile, which can be estimated from the shear wave velocity of individual layers. For the site J2, the low-strain site period is 0.75 second. The dynamic site period is usually larger than the low-strain site period because the shear modulus is reduced when the soil behavior is in the nonlinear range. The results of the site response analysis indicate that the soil deposit acts as a filter when the bedrock earthquake motions are transmitted through it. The soil deposit filters out a significant portion of the high frequency contents of the bedrock accelerations. On the other hand, it strongly amplifies the bedrock spectral accelerations between 0.15 and 1.4 seconds.

4.3 Peak Ground Acceleration

The peak ground acceleration (PGA) in unit of gravity "g" is summarized in figure 4-9. The PGA ranges from 0.09 to 0.23g. In general, the PGA does not vary significantly from one site to the surrounding sites; thus the PGA for any site, which is not shown in figure 4-9, may be estimated by taking the average of PGA values from the surrounding sites. The results from the analyses indicate that the peak bedrock acceleration (PBA) is reduced for most of the sites. The bedrock accelerations generated from the analytical model contains significant portion of high frequency contents which are filtered out by the soil deposits, especially when soil behavior is in substantial nonlinear range. Thus, the peak ground acceleration is usually less than the corresponding peak bedrock acceleration.

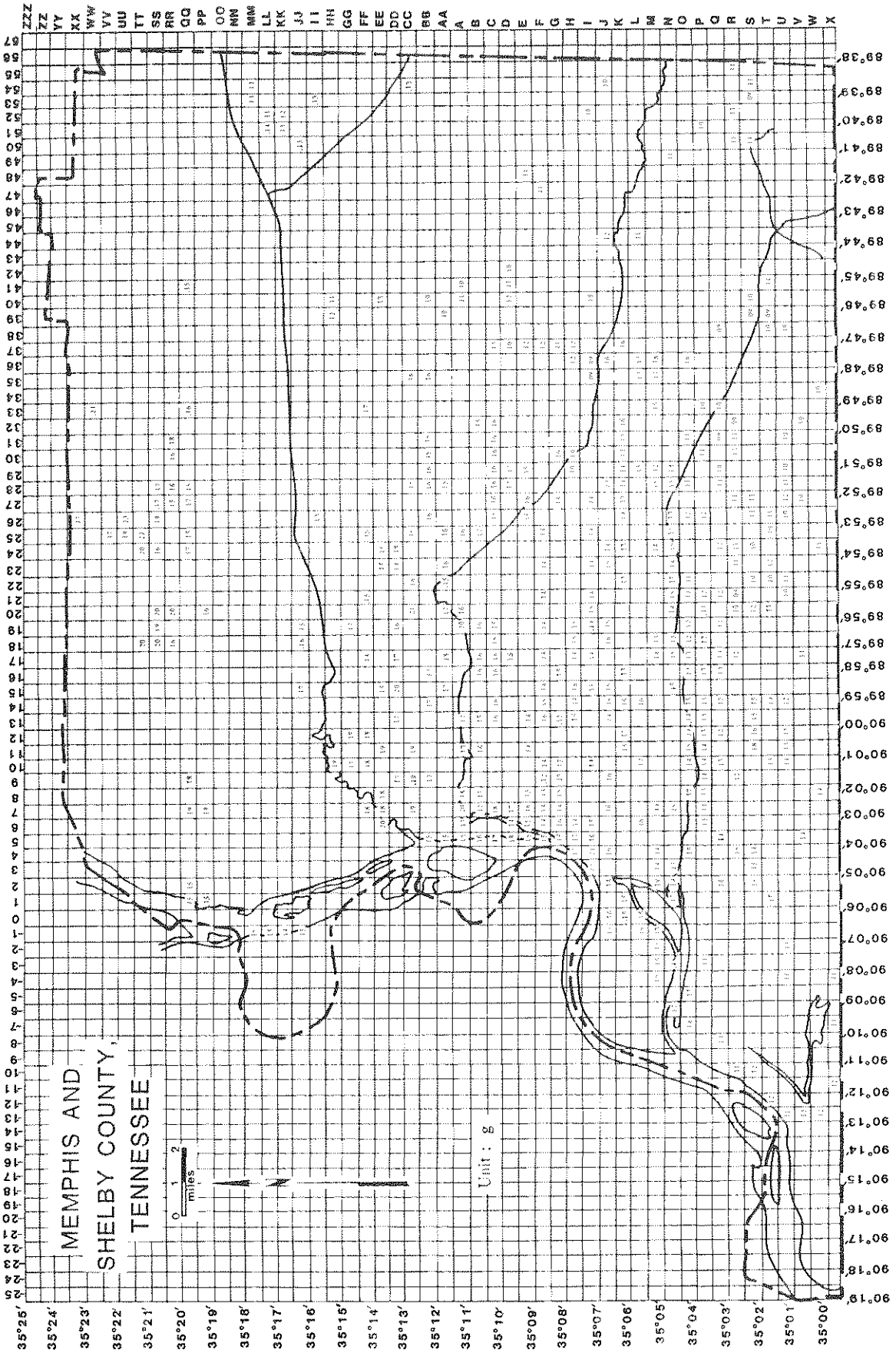

FIGURE 4-9 Map of Peak Ground Acceleration

4.4 Low-Strain and Dynamic Site Periods

The low-strain site periods T_S of all the soil deposits is computed using equation (4.2). The average shear wave velocity of a soil profile in equation (4.2) is computed from the shear wave velocity of individual layers. The average shear wave velocities of the upper 200 ft of soil profiles for all the sites are shown in a contour map (figure 4-10). The average shear wave velocity ranges from 950 to 1480 ft/sec. In general, the average shear wave velocity of the soil profiles along the Mississippi Alluvial Plain are at the lower range. Figure 4-11 shows the contour map of the low-strain site periods ranging from 0.56 to 0.84 second. The low-strain site period is an indicator of the soil conditions. For example, the low-strain site period of a site consisting of softer and looser material is usually larger. In general, the soil deposits with large low-strain site period (0.76 to 0.84 second) fall into the S_4 category along the Mississippi Alluvial Plain as shown in figure 4-11.

The dynamic site period corresponds to the period at which the spectral acceleration ratio has the largest value. The dynamic site period is usually larger than the low-strain site period. The larger value of the dynamic site period reflects the nonlinear behavior of soils. Figure 4-12 shows the contour map of the dynamic site periods for Memphis and Shelby County which range from 0.63 to 1.0 second.

4.5 Response Spectra

In model building codes, response spectra corresponding to different soil profile categories are specified for seismic-resistant design of building structures. In this study, 424 response spectra are obtained from the site response analyses. Each response spectrum is first normalized by the input peak bedrock acceleration. Next, the normalized response spectra are classified into three groups according to the soil profile categories listed in table 4-I. Then, the response spectra in the same group are statistically analyzed to determine the mean value and the standard deviation (SD). For S_2, S_3, and S_4 soil

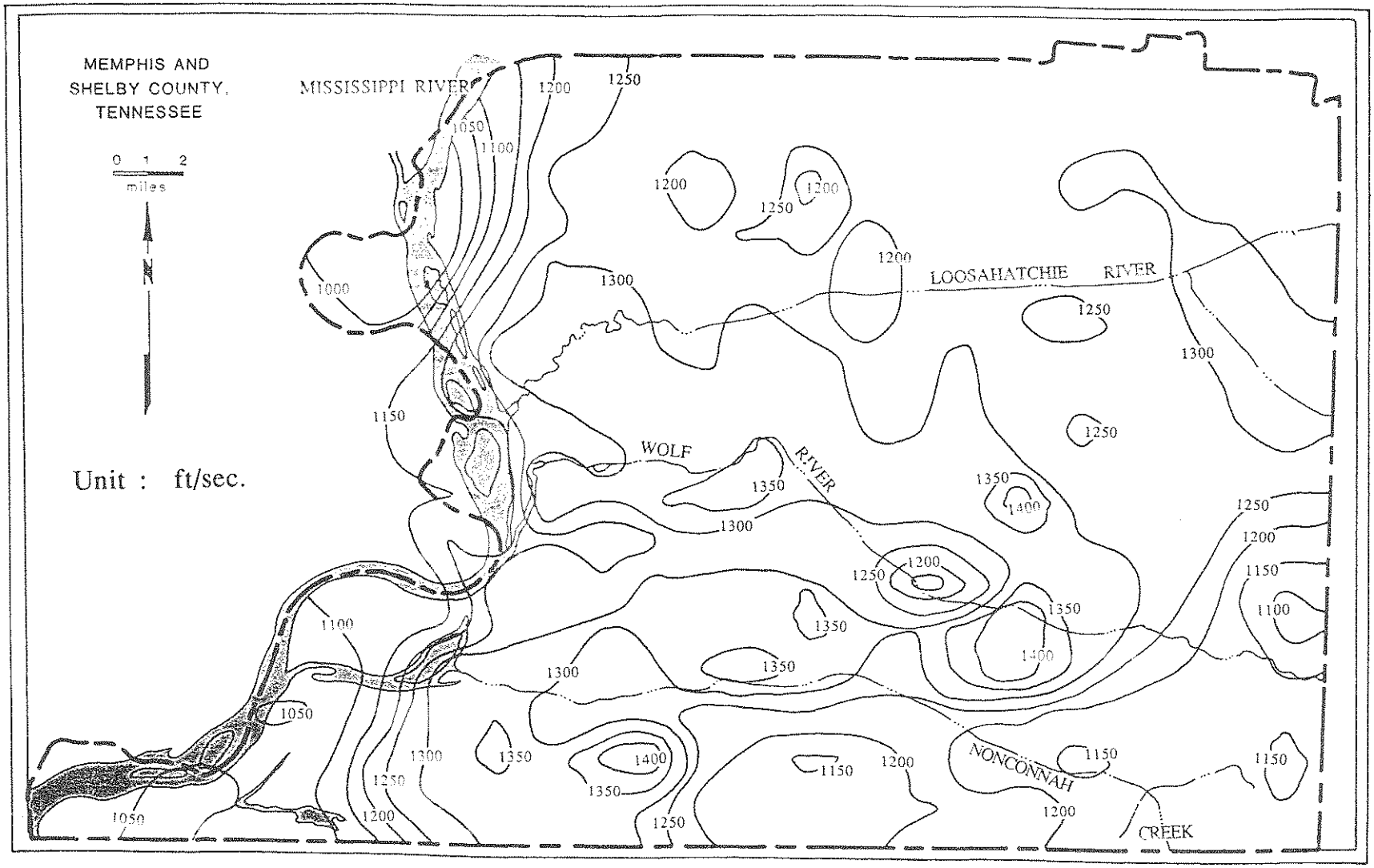

FIGURE 4-10 Contour Map of Average Shear Wave Velocity

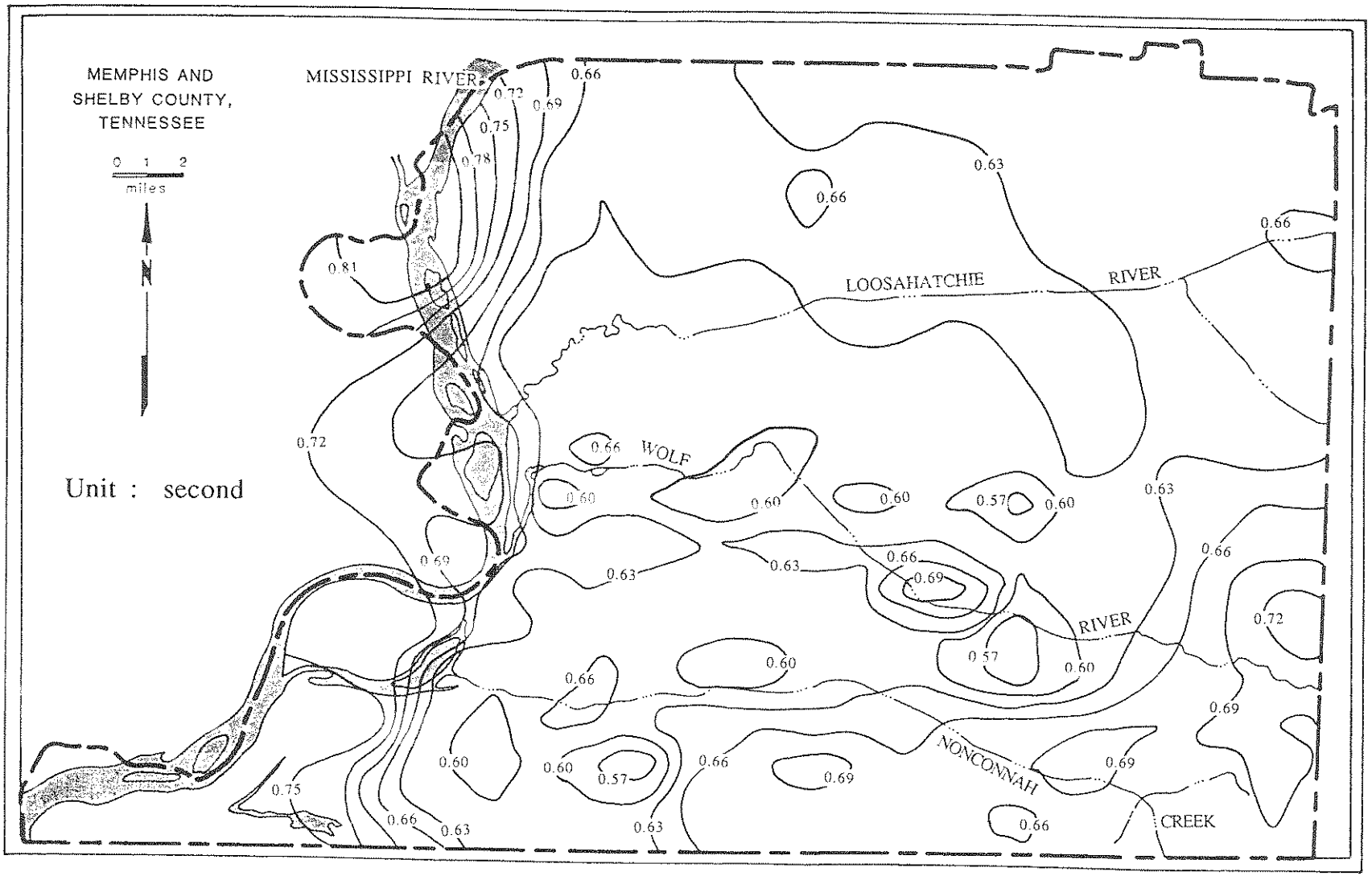

FIGURE 4-11 Contour Map of Low-Strain Site Period

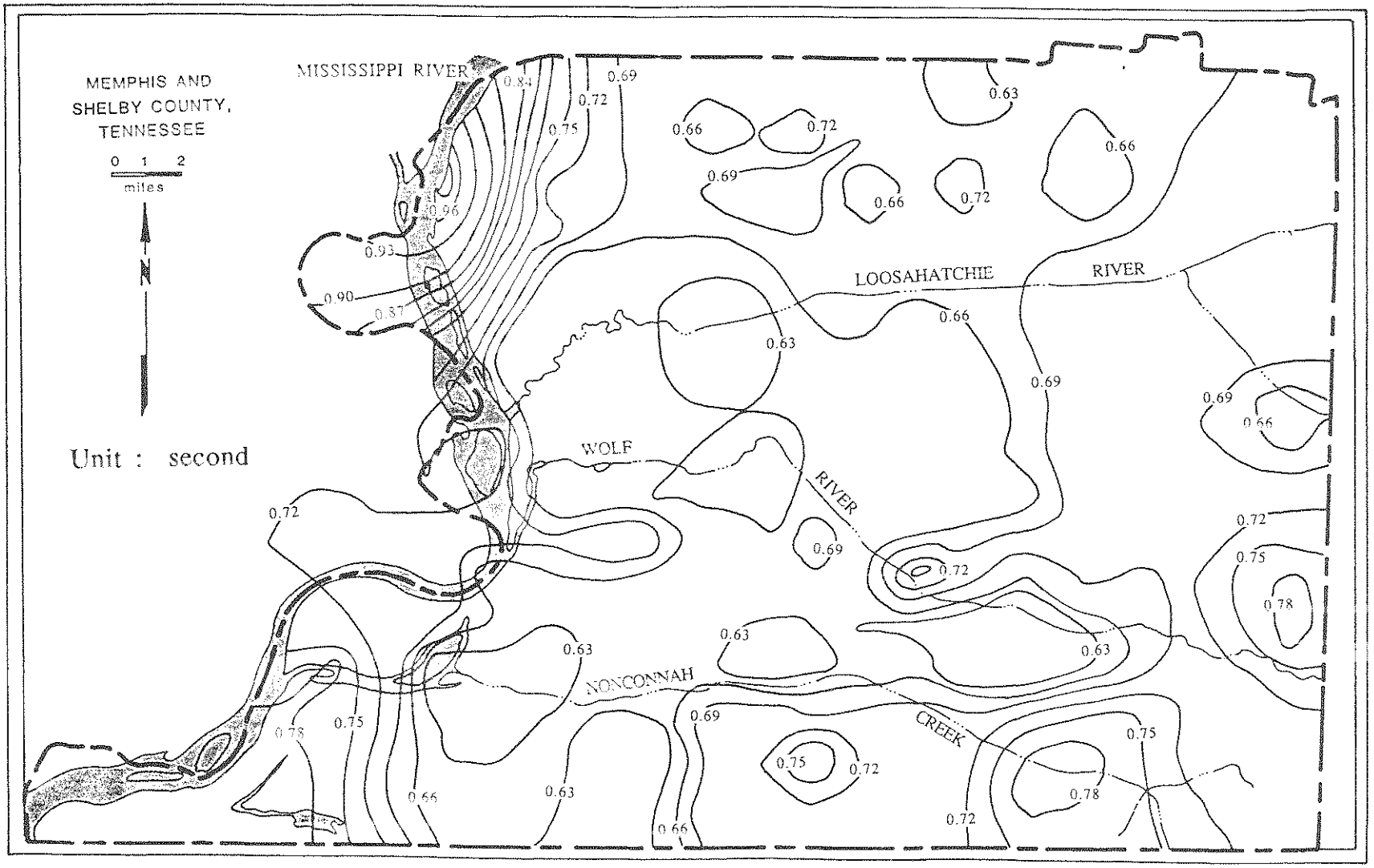

FIGURE 4-12 Contour Map of Dynamic Site Period

profile categories, the mean and mean $\pm$ one SD response spectra are shown in figures 4-13, 4-14, and 4-15, respectively. The mean response spectra of these three soil categories are also shown in figure 4-16. The peak spectral acceleration for S_4 category is slightly lower and is shifted to the right in comparisons to the S_2 and S_3 categories. The shifting is due to the larger low-strain site period associated with S_4 category. Furthermore, it is of interest to observe that the mean normalized response spectra for S_2 and S_3 categories are quite similar.

The same procedure without normalization is used to analyze the spectral acceleration ratios for all 424 sites. The mean spectral acceleration ratio spectrum for S_2, S_3, and S_4 categories are shown in figure 4-17. The spectral accelerations of the bedrock motions for all three soil categories are amplified significantly from 0.15 to about 1.4 seconds. F_{PSA} is the largest value of the spectral acceleration ratio. As shown in figure 4-18, the F_{PSA} value for Memphis and Shelby County ranges from 4.24 to 8.10.

4.6 Spectral Acceleration Maps

To indicate the approximate shape of the response spectrum at various locations in the Memphis area, the largest values of the spectral accelerations in three period intervals: $0 < T \leq 0.4$ second, $0.4 < T \leq 1.2$ seconds, and $1.2 < T \leq 3.0$ seconds are selected and shown in figures 4-19, 4-20, and 4-21, respectively. The periods corresponding to these largest values are classified according to the soil categories and then analyzed statistically to determine the mean value, standard deviation, and coefficient of variation (COV) as shown in table 4-II. On the basis of these statistics, the mean - SD value is used as the control period in the period interval of $0 < T \leq 0.4$ second, while the mean + SD values are used for the other two period intervals as shown in table 4-III. These control periods in table 4-III and the largest spectral accelerations for the three period intervals together with the PGA value (zero-period acceleration) can be used to construct an approximate response spectrum for a site. As an example, the approximate response spectrum

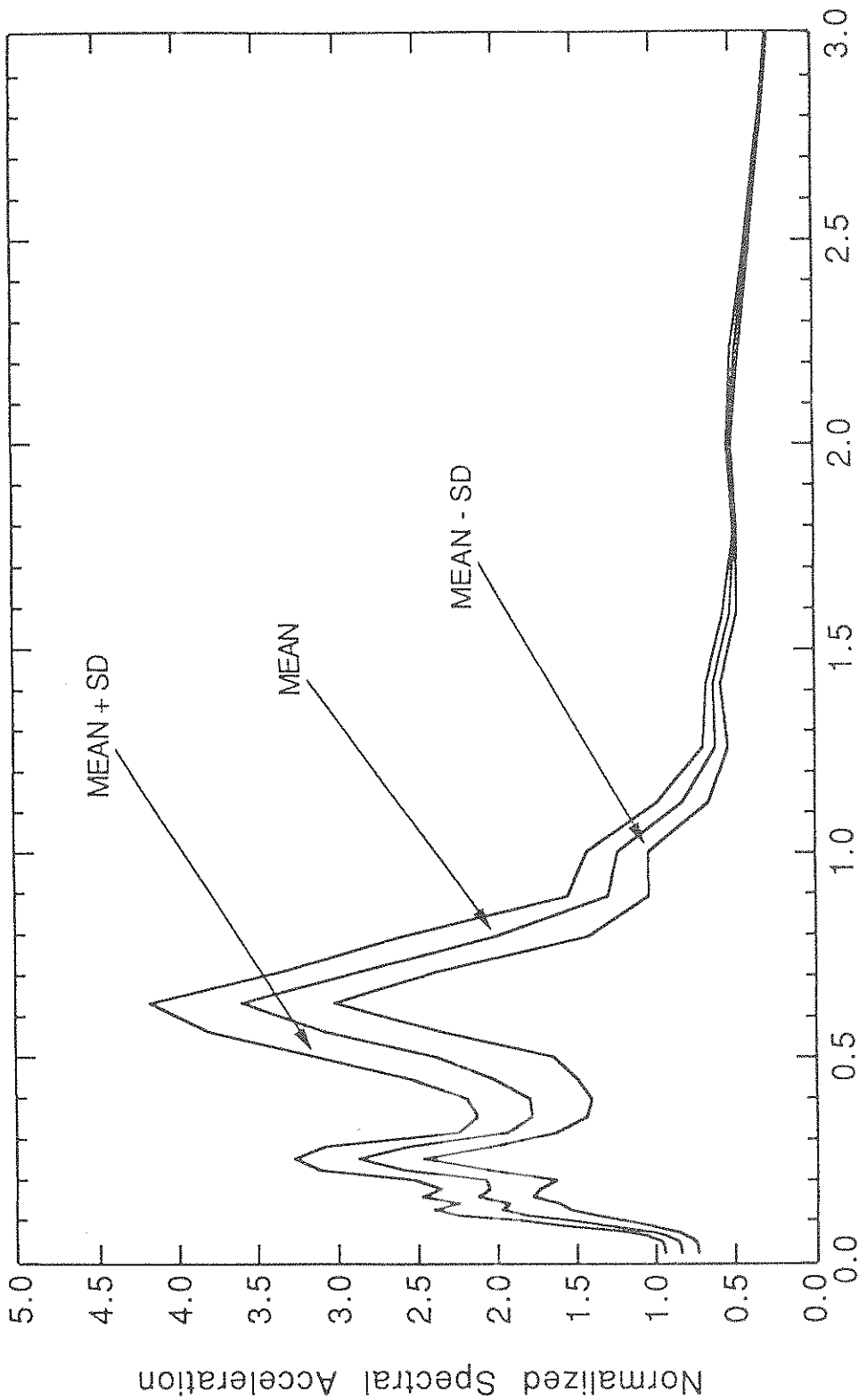

FIGURE 4-13 Response Spectra for S_2 Category

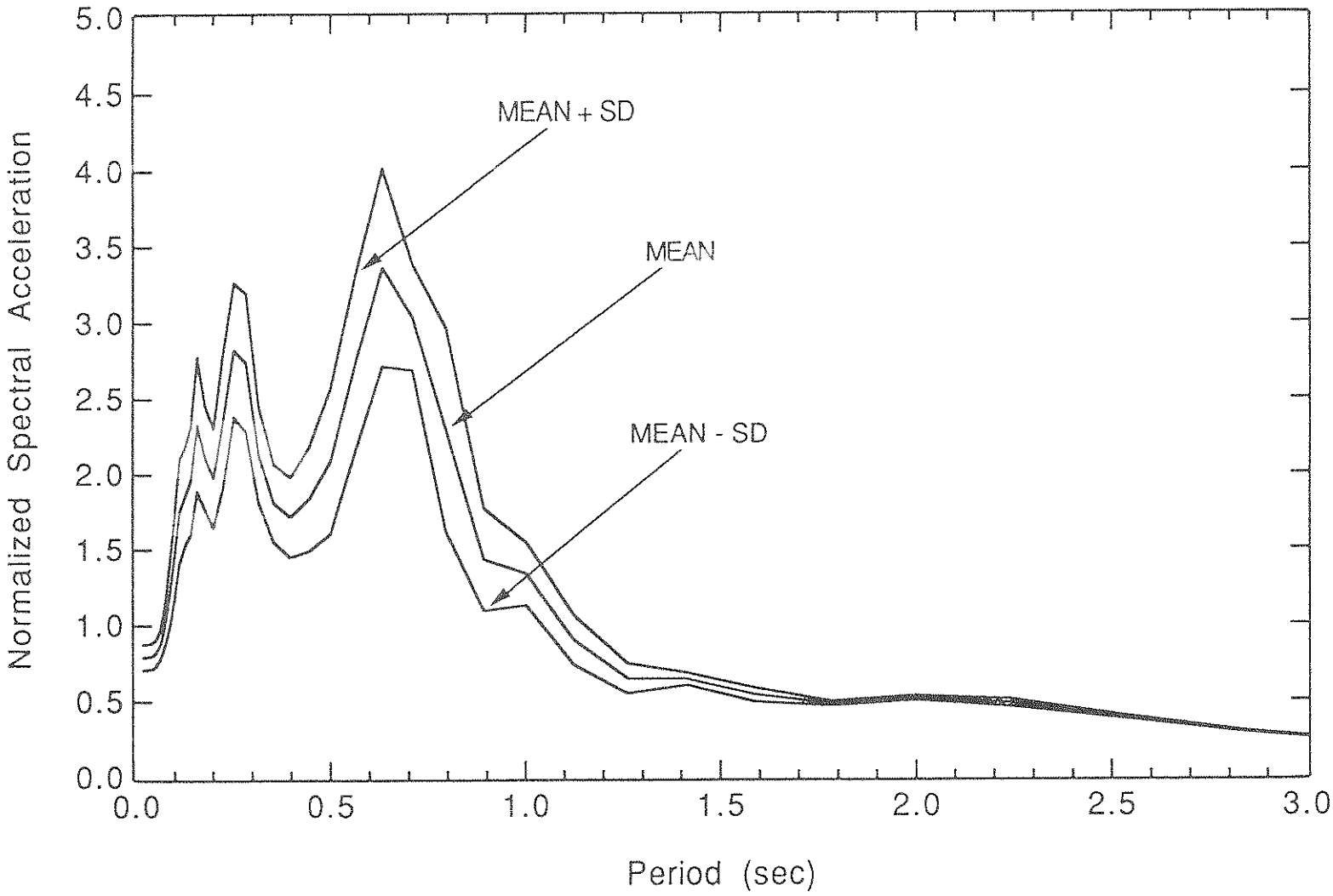

FIGURE 4-14 Response Spectra for S_3 Category

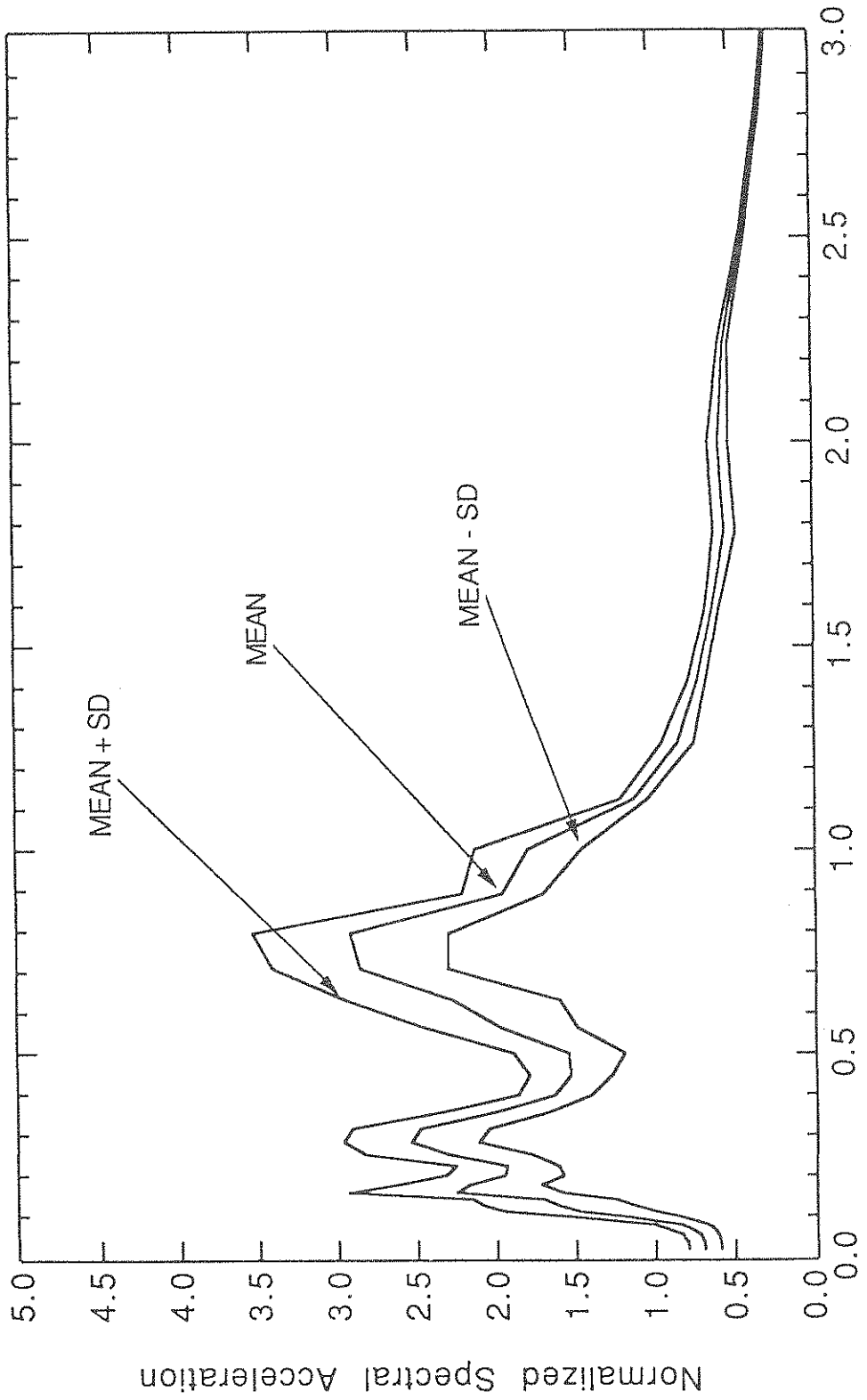

FIGURE 4-15 Response Spectra for S_4 Category

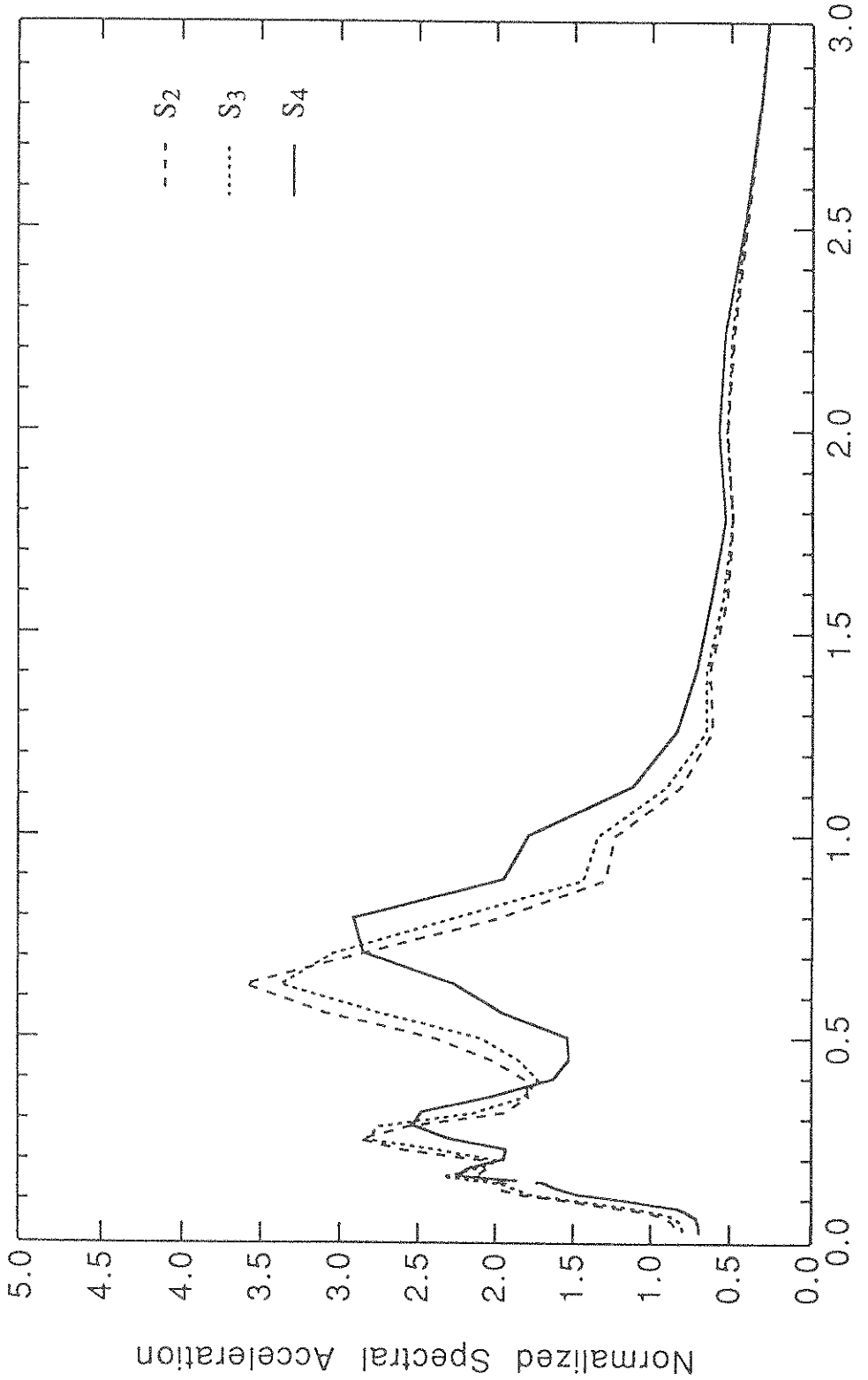

FIGURE 4-16 Mean Response Spectra

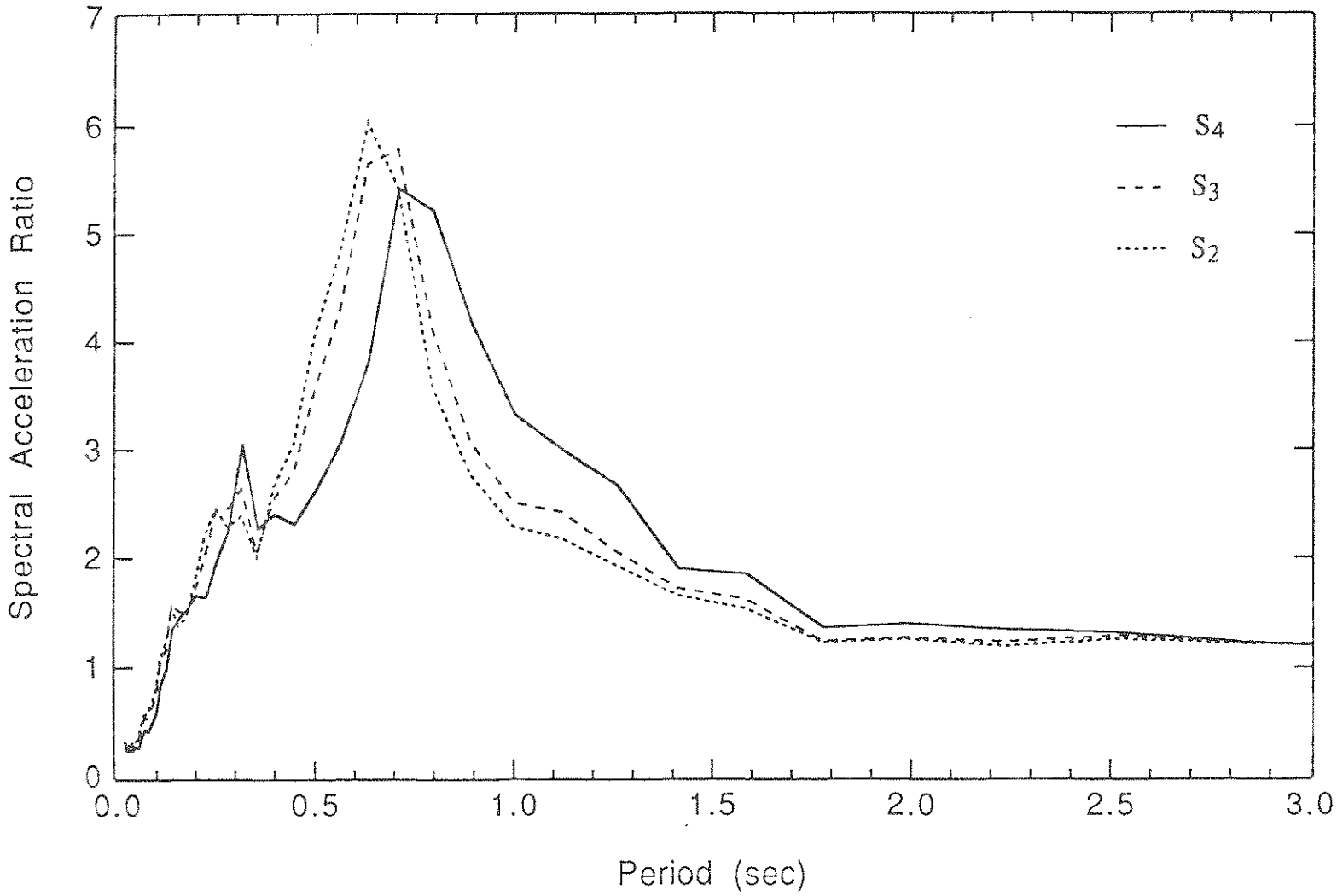

FIGURE 4-17 Mean Spectral Acceleration Ratio Spectra

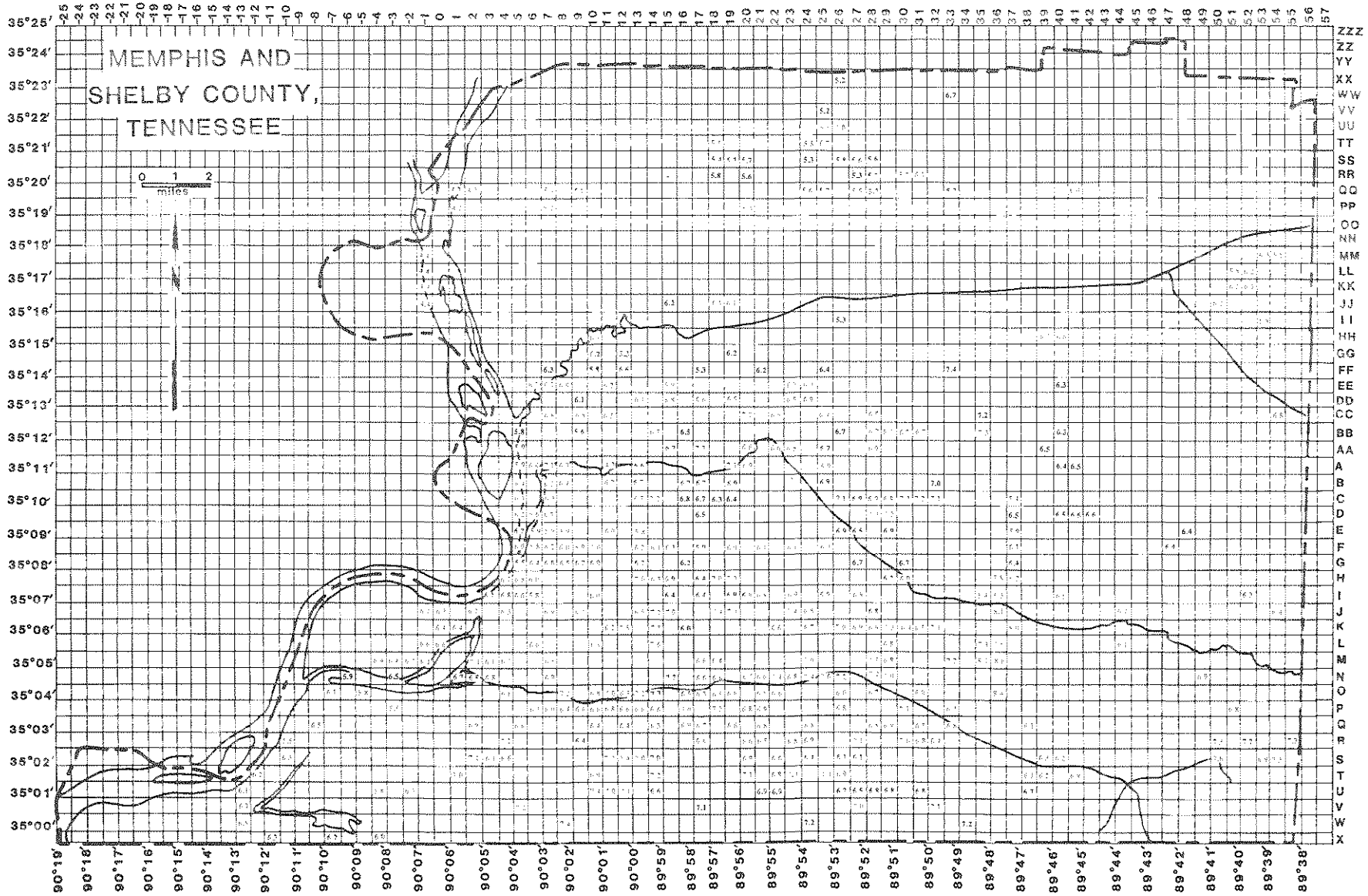

FIGURE 4-18 Map of F_{PSA} Factor

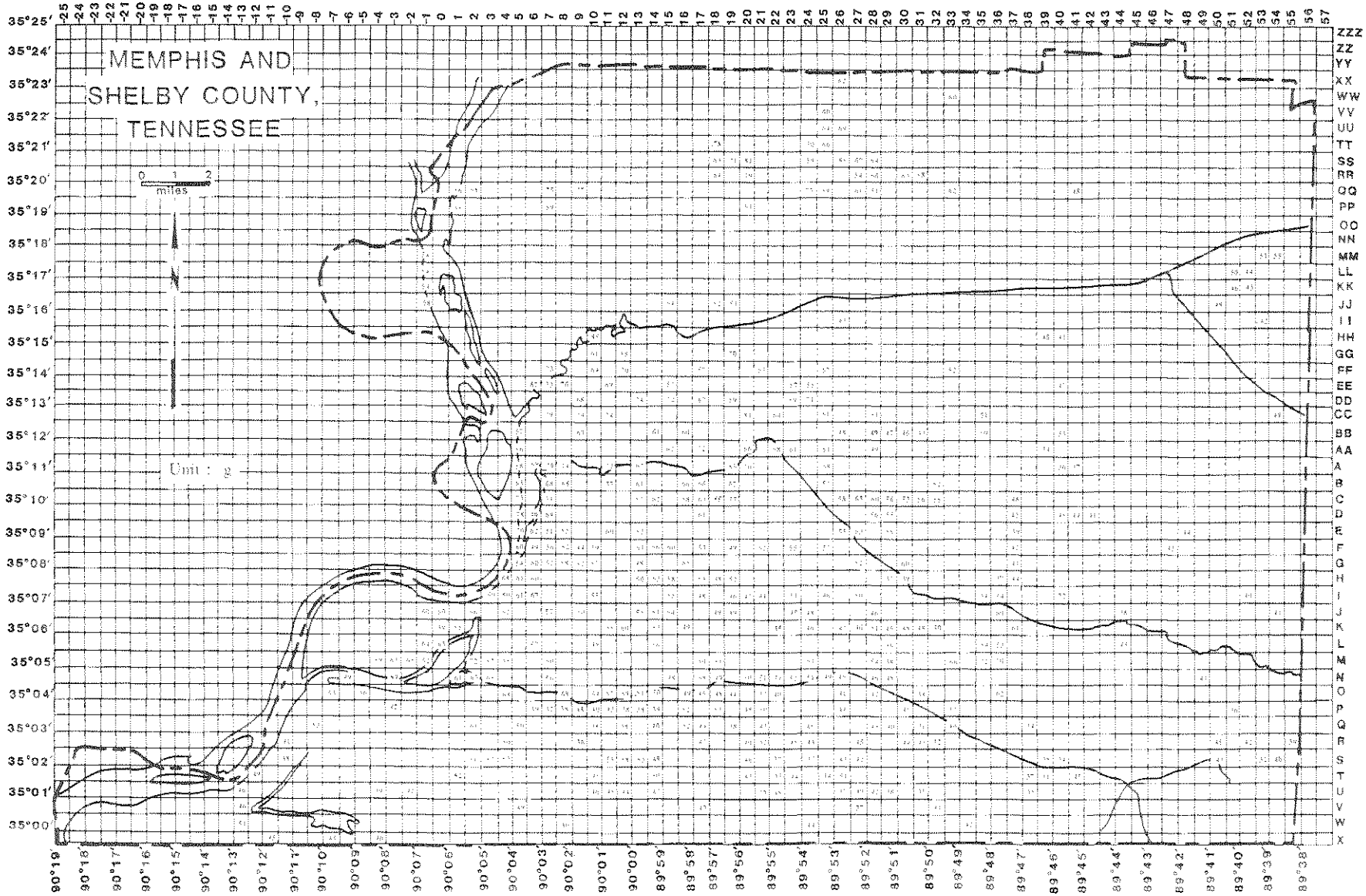

FIGURE 4-19 Map of Maximum Spectral Acceleration ($0 < T \leq 0.4$)

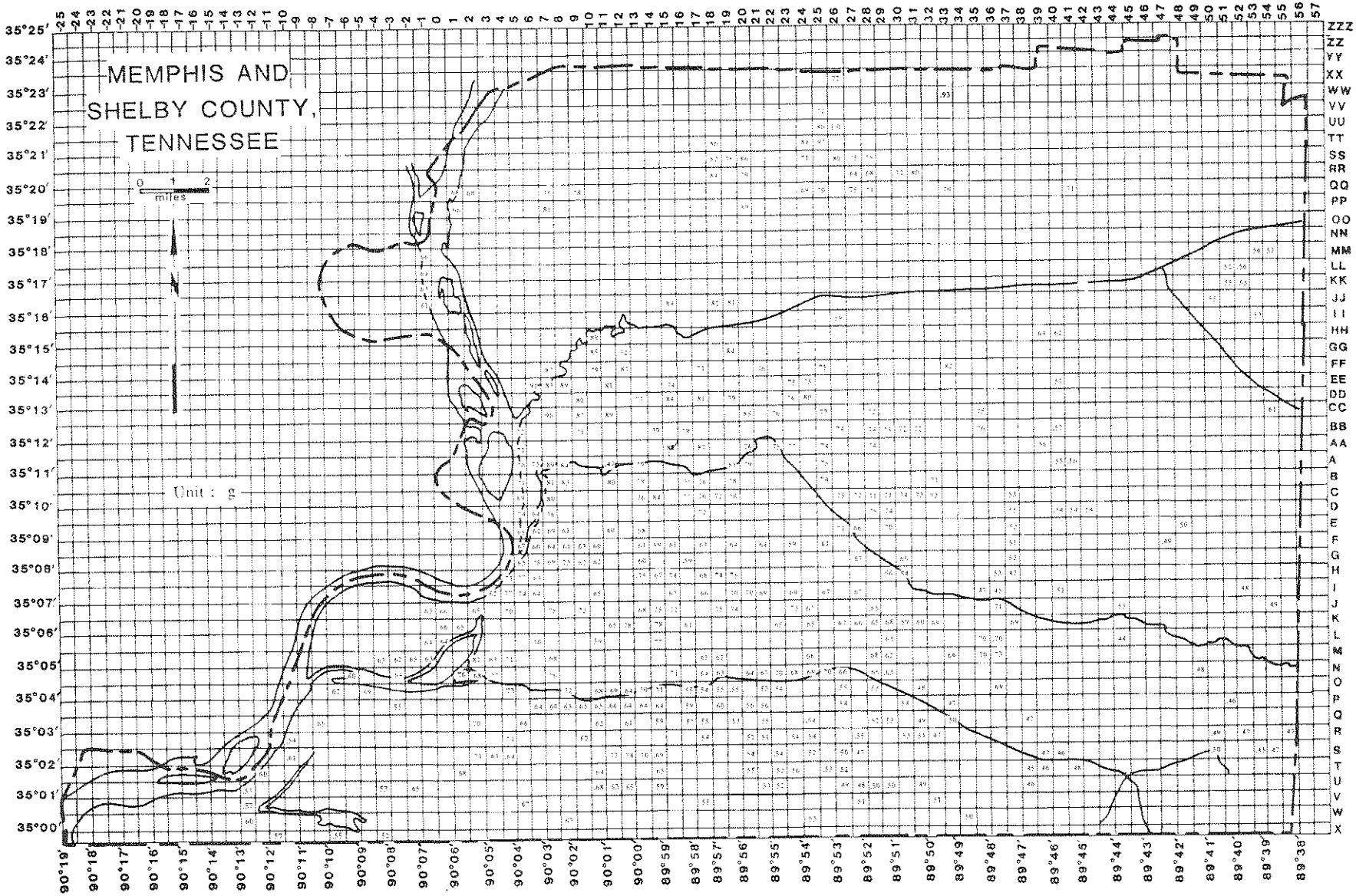

FIGURE 4-20 Map of Maximum Spectral Acceleration ($0.4 < T \leq 1.2$)

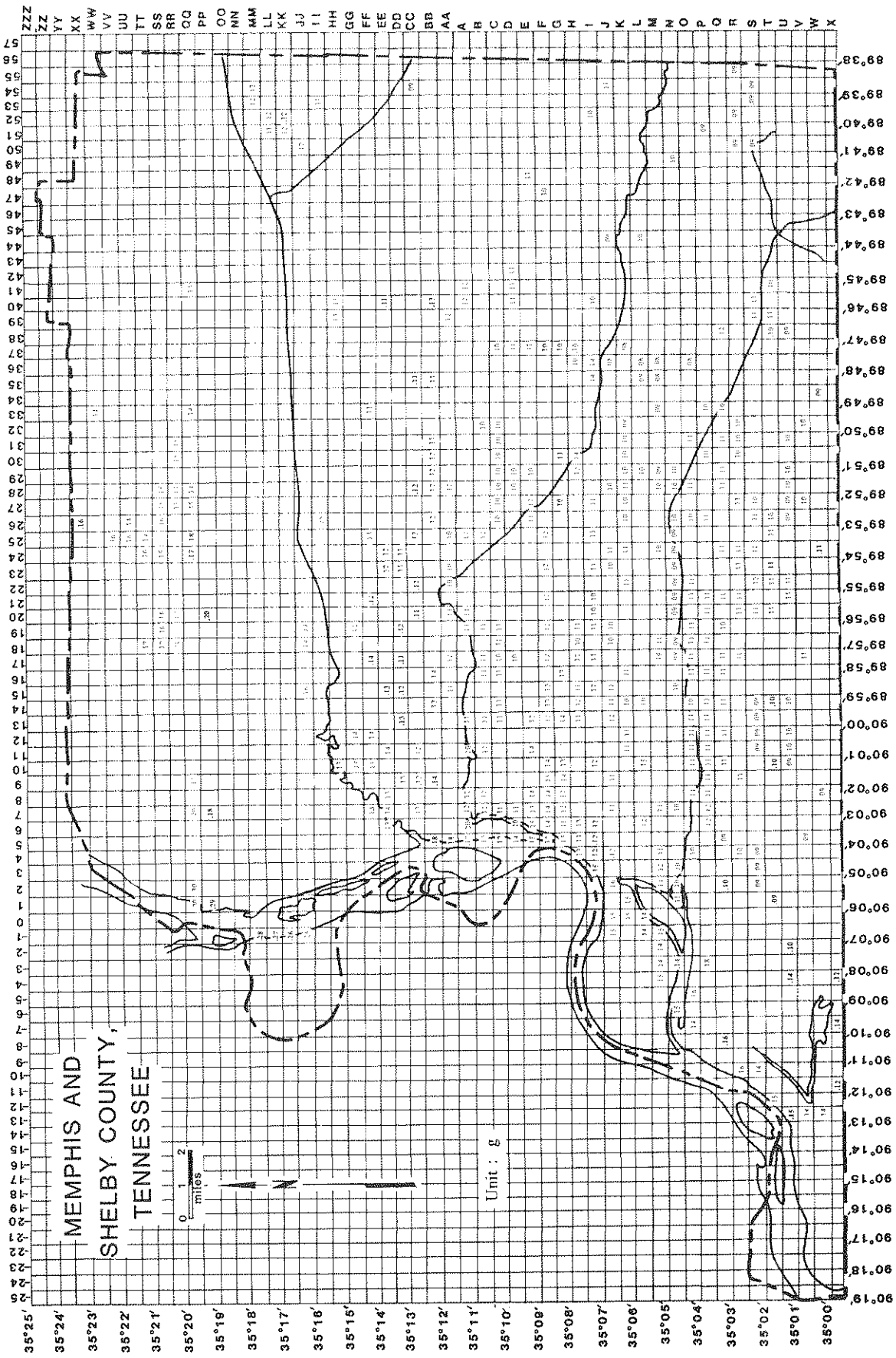

FIGURE 4-21 Map of Maximum Spectral Acceleration ($1.2 < T \leq 3.0$)

TABLE 4-II Statistics of Control Periods

Soil Profile Category	Period Interval (second)	Mean Value (second)	SD (second)	COV
S_2	$0.0 < T \leq 0.4$	0.25	0.0238	0.10
	$0.4 < T \leq 1.2$	0.65	0.0543	0.08
	$1.2 < T \leq 3.0$	1.36	0.0751	0.06
S_3	$0.0 < T \leq 0.4$	0.25	0.0384	0.15
	$0.4 < T \leq 1.2$	0.68	0.0625	0.09
	$1.2 < T \leq 3.0$	1.34	0.0769	0.06
S_4	$0.0 < T \leq 0.4$	0.28	0.0669	0.24
	$0.4 < T \leq 1.2$	0.81	0.1050	0.13
	$1.2 < T \leq 3.0$	1.27	0.0348	0.03

TABLE 4-III Recommended Control Periods for Approximate Response Spectra

Soil Profile Category	Period Interval (second)	Period (second)
S_2	$0.0 < T \leq 0.4$	0.23
	$0.4 < T \leq 1.2$	0.70
	$1.2 < T \leq 3.0$	1.44
S_3	$0.0 < T \leq 0.4$	0.21
	$0.4 < T \leq 1.2$	0.74
	$1.2 < T \leq 3.0$	1.42
S_4	$0.0 < T \leq 0.4$	0.21
	$0.4 < T \leq 1.2$	0.92
	$1.2 < T \leq 3.0$	1.30

and the original spectrum for the site J2 are shown in figure 4-22. It can be seen that the approximate response spectrum envelopes the original spectrum and is a good idealization for seismic-resistant design of structures.

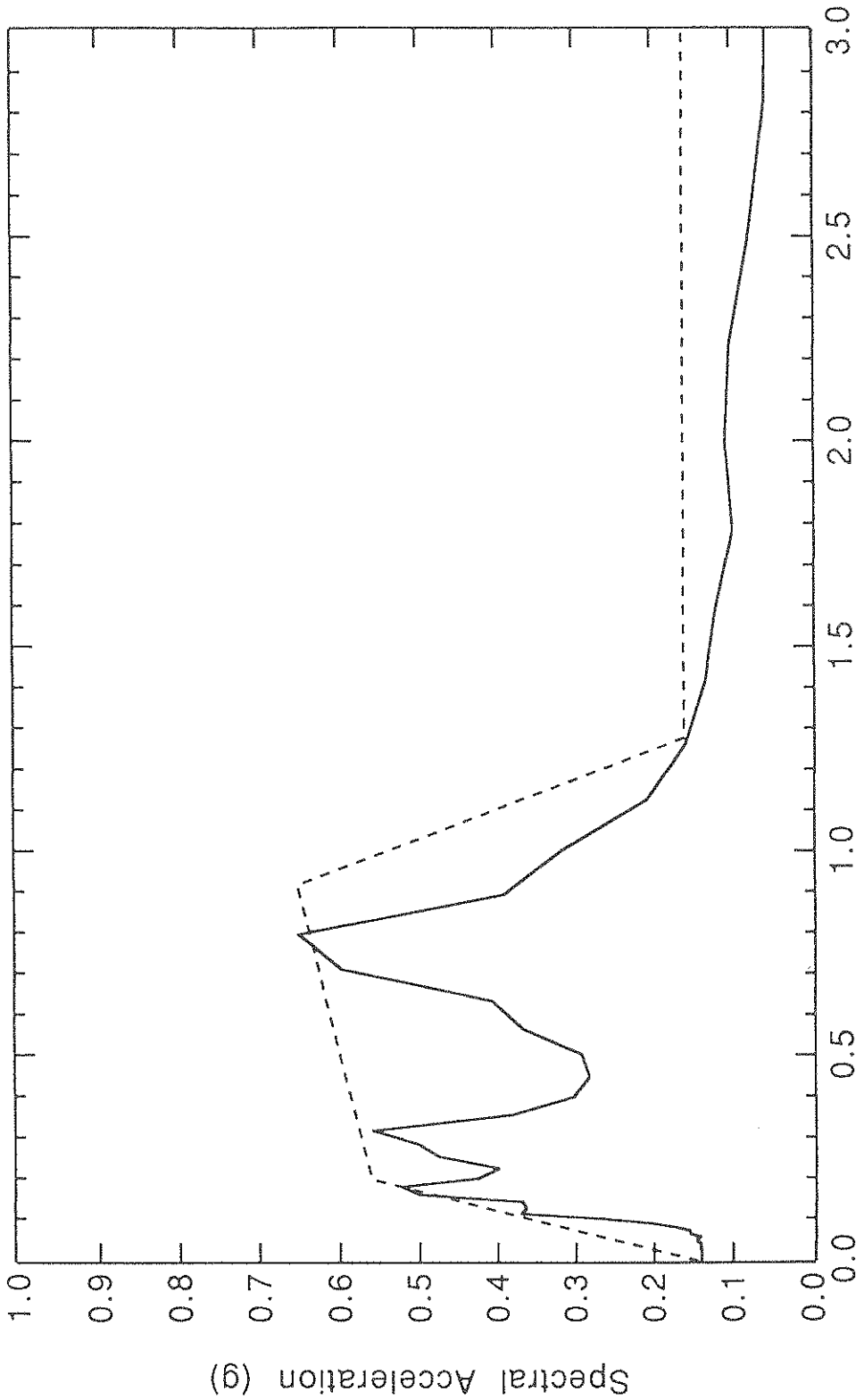

FIGURE 4-22 Approximate Response Spectrum for Site J2

SECTION 5

CONCLUSIONS

The site response study for Memphis and Shelby County has been carried out using the MASH computer program to evaluate the soil effects on earthquake ground motions. A total of 424 soil logs compiled by Ng et al. is used. A dynamic soil model is established for each boring log and then excited by an acceleration time history at the bedrock level resulting from a moment magnitude 7.5 New Madrid earthquake. The low-strain site period estimated from average shear wave velocity of a soil profile and the dynamic site period, at which the maximum spectral accelerations ratio occurs, are determined and shown in contour maps. The average shear wave velocity of the upper 200 ft soil profiles is also shown in a contour map. In addition, maps showing the peak ground acceleration and peak spectral acceleration ratio are also presented in this study.

The earthquake time histories and the corresponding response spectra at the ground surface are obtained from site response analyses. The response spectra are normalized by the peak bedrock accelerations and divided into groups according to soil profile categories specified in the 1988 Uniform Building Code. The normalized ground response spectra are then statistically analyzed to establish mean spectra corresponding to S_2, S_3, and S_4 categories. Furthermore, maps showing the largest spectral accelerations in three period intervals up to 3.0 seconds are also presented. From these values and the peak ground acceleration, the approximate response spectra at any location in the study area can be readily constructed without performing nonlinear site response analysis.

The results of the site response analysis indicate that the soil deposit acts as a filter when the bedrock earthquake motions are transmitted through it. The soil deposit filters out a significant portion of high frequency contents of the bedrock accelerations. On the other hand, it

strongly amplifies the bedrock spectral accelerations between 0.15 and 1.4 seconds. This amplification is important in engineering applications since most structures have fundamental period in this range.

The results of site response analysis are affected by the uncertainties associated with earthquake and site parameters. The uncertainties in earthquake motions resulting from the New Madrid seismic zone are large because strong motion data are scarce in this area. The uncertainties in the site parameters, in particular, the dynamic soil properties, could also significantly affect the site response. Thus, a sensitivity analysis needs to be carried out to ensure the results of the site response analysis. An example of such an analysis is shown in Reference 26. In addition, several soil properties used in this study are estimated on the basis of empirical correlations. It is, therefore, imperative that the geotechnical data and assumptions used in this study are evaluated before using the results from this study.

SECTION 6

REFERENCES

1. Dobry, R., and Vucetic, M., "Dynamic Properties and Seismic Response of Soft Clay Deposits," Proceedings of International Symposium on Geotechnical Engineering of Soft Soils, Vol. 2, Mexico City, Mexico, August, 1987, pp. 51-87.

2. Sharma, S., and Kovacs, W.D., "Microzonation of the Memphis, Tennessee Area, (phase 1)," School of Civil Engineering, Purdue University, May, 1980.

3. Seed, H.B., Whitman, R.V., Dezfulian, H., Dobry, R., and Idriss, I.M., "Soil Conditions and Building Damage in 1967 Caracas Earthquake," Journal of the Soil Mechanics and Foundations Division, ASCE, Vol. 98, No. SM8, August, 1972.

4. Seed, H.B., Romo, M.P., Sun, J., Jaime, A., and Lysmer, J., "Relationships Between Soil Conditions and Earthquake Ground Motions in Mexico City in the Earthquake of September 19, 1985," Report No. UCB/EERC-87/15, Earthquake Engineering Research Center, University of California, Berkeley, California, October, 1987.

5. "Loma Prieta Earthquake Reconnaissance Report", Earthquake Spectra, Supplement to Vol. 6, May, 1990.

6. Schnabel, P.B., Lysmer, J., and Seed, H.B., "SHAKE, A Computer Program for Earthquake Response Analysis of Horizontally Layered Sites," Report No. EERC 72-12, Earthquake Engineering Research Center, University of California, Berkeley, California, December, 1972.

7. Martin, P.P., and Seed, H.B., "MASH, A Computer Program for the Non-linear Analysis of Vertically Propagating Shear Waves in Horizontally Layered Deposits," Report No. UCB/EERC-78/23, Earthquake Engineering Research Center, University of California, Berkeley, California, October, 1978.

8. Hwang, H., Chen, C.H., and Yu, G., "Bedrock Accelerations in Memphis Area Due to Large New Madrid Earthquakes," Technical Report NCEER-89-0029, National Center for Earthquake Engineering Research, SUNY, Buffalo, NY, November, 1989.

9. Hunt, R.E., "Geotechnical Engineering Investigation Manual," McGraw-Hill Book Co., New York, 1984.

10. Ng, K.W., Chang, T.S., and Hwang, H., "Subsurface Conditions of Memphis and Shelby County," Technical Report NCEER-89-0021, National Center for Earthquake Engineering Research, SUNY, Buffalo, NY., July, 1989.

11. Bowles, J.E., "Physical and Geotechnical Properties of Soils," McGraw-Hill Book Co., Second Edition, New York, 1984.

12. Richart, F.E. Jr., Woods, R.D., and Hall, J.R., "Vibrations of Soils and Foundations," Prentice-Hall, Inc., Englewood Cliffs, New Jersey, 1970.

13. Hwang, H., and Lee, C.S., "Parametric Study of Site Response Analysis," Accepted for Publication in the International Journal of Soil Dynamics and Earthquake Engineering, 1990.

14. Seed, H.B., and Idriss, I.M., "Soil Moduli and Damping Factors for Dynamic Response Analysis," Report No. EERC 70-10, University of California, Berkeley, December, 1970.

15. Seed, H.B., Wong, R.T., Idriss, I.M., and Tokimatsu, K., "Moduli and Damping Factors for Dynamic Analyses of Cohesionless Soils," Journal of the Geotechnical Engineering Division, ASCE, Vol. 112, No.11, November, 1986, pp. 1016-1032.

16. Iwasaki, T., Tatsuoka, F., and Takagi, Y., "Dynamic Shear Deformation Properties of Sand for Wide Strain Range," Report of Civil Engineering Institution, No. 1085, Ministry of Construction, Tokyo, Japan, 1976.

17. Shibata, T., and Soelarno, D.S., "Stress-Strain Characteristics of Sands Under Cyclic Loading," Proceeding of Japanese Society of Civil Engineerings, No. 239, July, 1975, pp. 57-65.

18. Hardin, B.O., and Drnevich, V.P., "Shear Modulus and Damping in Soils: Design Equations and Curves," Journal of the Soil Mechanics and Foundations Division, ASCE, Vol. 98, No. SM7, July, 1972, pp. 667-692.

19. Richart, F.E. Jr., "Field and Laboratory Measurements of Dynamic Soil Properties," in Dynamic Response and Wave Propagation in Soils, Editor, Prange B., A. A. Balkema, Rotterdam, Netherlands, 1978, pp. 3-36.

20. Zen, K., Umehara, Y., and Hamada, K., "Laboratory Tests and In-Situ Seismic Survey on Vibratory Shear Modulus of Clayey Soils with Various Plasticities," Proceedings of Fifth Japan Earthquake Engineering Symposium, Tokyo, Japan, November, 1978, pp. 721-728.

21. Sun, J.I., Golesorkhi, R., and Seed, H.B., "Dynamic Moduli and Damping Ratios for Cohesive Soils," Report No. UCB/EERC-88/15, Earthquake Engineering Research Center, University of California, Berkeley, California, August, 1988.

22. Barkan, D.D., "Dynamics of Bases and Foundations," McGraw-Hill, New York, 1962.

23. Seed, H.B., Idriss, I.M., and Keifer, F.W., "Characteristics of Rock Motions during Earthquakes," Journal of the Soil Mechanics and Foundations Division, ASCE, Vol. 95, No. SM5, September, 1969, pp. 1199-1218.

24. Duke, C.M., and Leeds, D.J., "Site Characteristics of Southern California Strong Motion Earthquake Stations," Report No. 62-55, Department of Engineering, University of California, Los Angeles, 1962.

25. International Conference of Building Officials, "Uniform Building Code," 1988 Edition, Whittier, California, 1988.

26. Hwang, H., and Lee, C.S., "Site-Specific Response Spectra for Memphis Sheahan Pumping Station," Technical Report NCEER-90-0007, National Center for Earthquake Engineering Research, SUNY, Buffalo, NY., May 1990.

NATIONAL CENTER FOR EARTHQUAKE ENGINEERING RESEARCH
LIST OF TECHNICAL REPORTS

The National Center for Earthquake Engineering Research (NCEER) publishes technical reports on a variety of subjects related to earthquake engineering written by authors funded through NCEER. These reports are available from both NCEER's Publications Department and the National Technical Information Service (NTIS). Requests for reports should be directed to the Publications Department, National Center for Earthquake Engineering Research, State University of New York at Buffalo, Red Jacket Quadrangle, Buffalo, New York 14261. Reports can also be requested through NTIS, 5285 Port Royal Road, Springfield, Virginia 22161. NTIS accession numbers are shown in parenthesis, if available.

NCEER-87-0001 "First-Year Program in Research, Education and Technology Transfer," 3/5/87, (PB88-134275/AS).

NCEER-87-0002 "Experimental Evaluation of Instantaneous Optimal Algorithms for Structural Control," by R.C. Lin, T.T. Soong and A.M. Reinhorn, 4/20/87, (PB88-134341/AS).

NCEER-87-0003 "Experimentation Using the Earthquake Simulation Facilities at University at Buffalo," by A.M. Reinhorn and R.L. Ketter, to be published.

NCEER-87-0004 "The System Characteristics and Performance of a Shaking Table," by J.S. Hwang, K.C. Chang and G.C. Lee, 6/1/87, (PB88-134259/AS). This report is available only through NTIS (see address given above).

NCEER-87-0005 "A Finite Element Formulation for Nonlinear Viscoplastic Material Using a Q Model," by O. Gyebi and G. Dasgupta, 11/2/87, (PB88-213764/AS).

NCEER-87-0006 "Symbolic Manipulation Program (SMP) - Algebraic Codes for Two and Three Dimensional Finite Element Formulations," by X. Lee and G. Dasgupta, 11/9/87, (PB88-219522/AS).

NCEER-87-0007 "Instantaneous Optimal Control Laws for Tall Buildings Under Seismic Excitations," by J.N. Yang, A. Akbarpour and P. Ghaemmaghami, 6/10/87, (PB88-134333/AS).

NCEER-87-0008 "IDARC: Inelastic Damage Analysis of Reinforced Concrete Frame - Shear-Wall Structures," by Y.J. Park, A.M. Reinhorn and S.K. Kunnath, 7/20/87, (PB88-134325/AS).

NCEER-87-0009 "Liquefaction Potential for New York State: A Preliminary Report on Sites in Manhattan and Buffalo," by M. Budhu, V. Vijayakumar, R.F. Giese and L. Baumgras, 8/31/87, (PB88-163704/AS). This report is available only through NTIS (see address given above).

NCEER-87-0010 "Vertical and Torsional Vibration of Foundations in Inhomogeneous Media," by A.S. Veletsos and K.W. Dotson, 6/1/87, (PB88-134291/AS).

NCEER-87-0011 "Seismic Probabilistic Risk Assessment and Seismic Margins Studies for Nuclear Power Plants," by Howard H.M. Hwang, 6/15/87, (PB88-134267/AS).

NCEER-87-0012 "Parametric Studies of Frequency Response of Secondary Systems Under Ground-Acceleration Excitations," by Y. Yong and Y.K. Lin, 6/10/87, (PB88-134309/AS).

NCEER-87-0013 "Frequency Response of Secondary Systems Under Seismic Excitation," by J.A. HoLung, J. Cai and Y.K. Lin, 7/31/87, (PB88-134317/AS).

NCEER-87-0014 "Modelling Earthquake Ground Motions in Seismically Active Regions Using Parametric Time Series Methods," by G.W. Ellis and A.S. Cakmak, 8/25/87, (PB88-134283/AS).

NCEER-87-0015 "Detection and Assessment of Seismic Structural Damage," by E. DiPasquale and A.S. Cakmak, 8/25/87, (PB88-163712/AS).

NCEER-87-0016 "Pipeline Experiment at Parkfield, California," by J. Isenberg and E. Richardson, 9/15/87, (PB88-163720/AS). This report is available only through NTIS (see address given above).

NCEER-87-0017 "Digital Simulation of Seismic Ground Motion," by M. Shinozuka, G. Deodatis and T. Harada, 8/31/87, (PB88-155197/AS). This report is available only through NTIS (see address given above).

NCEER-87-0018 "Practical Considerations for Structural Control: System Uncertainty, System Time Delay and Truncation of Small Control Forces," J.N. Yang and A. Akbarpour, 8/10/87, (PB88-163738/AS).

NCEER-87-0019 "Modal Analysis of Nonclassically Damped Structural Systems Using Canonical Transformation," by J.N. Yang, S. Sarkani and F.X. Long, 9/27/87, (PB88-187851/AS).

NCEER-87-0020 "A Nonstationary Solution in Random Vibration Theory," by J.R. Red-Horse and P.D. Spanos, 11/3/87, (PB88-163746/AS).

NCEER-87-0021 "Horizontal Impedances for Radially Inhomogeneous Viscoelastic Soil Layers," by A.S. Veletsos and K.W. Dotson, 10/15/87, (PB88-150859/AS).

NCEER-87-0022 "Seismic Damage Assessment of Reinforced Concrete Members," by Y.S. Chung, C. Meyer and M. Shinozuka, 10/9/87, (PB88-150867/AS). This report is available only through NTIS (see address given above).

NCEER-87-0023 "Active Structural Control in Civil Engineering," by T.T. Soong, 11/11/87, (PB88-187778/AS).

NCEER-87-0024 Vertical and Torsional Impedances for Radially Inhomogeneous Viscoelastic Soil Layers," by K.W. Dotson and A.S. Veletsos, 12/87, (PB88-187786/AS).

NCEER-87-0025 "Proceedings from the Symposium on Seismic Hazards, Ground Motions, Soil-Liquefaction and Engineering Practice in Eastern North America," October 20-22, 1987, edited by K.H. Jacob, 12/87, (PB88-188115/AS).

NCEER-87-0026 "Report on the Whittier-Narrows, California, Earthquake of October 1, 1987," by J. Pantelic and A. Reinhorn, 11/87, (PB88-187752/AS). This report is available only through NTIS (see address given above).

NCEER-87-0027 "Design of a Modular Program for Transient Nonlinear Analysis of Large 3-D Building Structures," by S. Srivastav and J.F. Abel, 12/30/87, (PB88-187950/AS).

NCEER-87-0028 "Second-Year Program in Research, Education and Technology Transfer," 3/8/88, (PB88-219480/AS).

NCEER-88-0001 "Workshop on Seismic Computer Analysis and Design of Buildings With Interactive Graphics," by W. McGuire, J.F. Abel and C.H. Conley, 1/18/88, (PB88-187760/AS).

NCEER-88-0002 "Optimal Control of Nonlinear Flexible Structures," by J.N. Yang, F.X. Long and D. Wong, 1/22/88, (PB88-213772/AS).

NCEER-88-0003 "Substructuring Techniques in the Time Domain for Primary-Secondary Structural Systems," by G.D. Manolis and G. Juhn, 2/10/88, (PB88-213780/AS).

NCEER-88-0004 "Iterative Seismic Analysis of Primary-Secondary Systems," by A. Singhal, L.D. Lutes and P.D. Spanos, 2/23/88, (PB88-213798/AS).

NCEER-88-0005 "Stochastic Finite Element Expansion for Random Media," by P.D. Spanos and R. Ghanem, 3/14/88, (PB88-213806/AS).

NCEER-88-0006 "Combining Structural Optimization and Structural Control," by F.Y. Cheng and C.P. Pantelides, 1/10/88, (PB88-213814/AS).

NCEER-88-0007 "Seismic Performance Assessment of Code-Designed Structures," by H.H-M. Hwang, J-W. Jaw and H-J. Shau, 3/20/88, (PB88-219423/AS).

NCEER-88-0008 "Reliability Analysis of Code-Designed Structures Under Natural Hazards," by H.H-M. Hwang, H. Ushiba and M. Shinozuka, 2/29/88, (PB88-229471/AS).

NCEER-88-0009 "Seismic Fragility Analysis of Shear Wall Structures," by J-W Jaw and H.H-M. Hwang, 4/30/88, (PB89-102867/AS).

NCEER-88-0010 "Base Isolation of a Multi-Story Building Under a Harmonic Ground Motion - A Comparison of Performances of Various Systems," by F-G Fan, G. Ahmadi and I.G. Tadjbakhsh, 5/18/88, (PB89-122238/AS).

NCEER-88-0011 "Seismic Floor Response Spectra for a Combined System by Green's Functions," by F.M. Lavelle, L.A. Bergman and P.D. Spanos, 5/1/88, (PB89-102875/AS).

NCEER-88-0012 "A New Solution Technique for Randomly Excited Hysteretic Structures," by G.Q. Cai and Y.K. Lin, 5/16/88, (PB89-102883/AS).

NCEER-88-0013 "A Study of Radiation Damping and Soil-Structure Interaction Effects in the Centrifuge," by K. Weissman, supervised by J.H. Prevost, 5/24/88, (PB89-144703/AS).

NCEER-88-0014 "Parameter Identification and Implementation of a Kinematic Plasticity Model for Frictional Soils," by J.H. Prevost and D.V. Griffiths, to be published.

NCEER-88-0015 "Two- and Three- Dimensional Dynamic Finite Element Analyses of the Long Valley Dam," by D.V. Griffiths and J.H. Prevost, 6/17/88, (PB89-144711/AS).

NCEER-88-0016 "Damage Assessment of Reinforced Concrete Structures in Eastern United States," by A.M. Reinhorn, M.J. Seidel, S.K. Kunnath and Y.J. Park, 6/15/88, (PB89-122220/AS).

NCEER-88-0017 "Dynamic Compliance of Vertically Loaded Strip Foundations in Multilayered Viscoelastic Soils," by S. Ahmad and A.S.M. Israil, 6/17/88, (PB89-102891/AS).

NCEER-88-0018 "An Experimental Study of Seismic Structural Response With Added Viscoelastic Dampers," by R.C. Lin, Z. Liang, T.T. Soong and R.H. Zhang, 6/30/88, (PB89-122212/AS).

NCEER-88-0019 "Experimental Investigation of Primary - Secondary System Interaction," by G.D. Manolis, G. Juhn and A.M. Reinhorn, 5/27/88, (PB89-122204/AS).

NCEER-88-0020 "A Response Spectrum Approach For Analysis of Nonclassically Damped Structures," by J.N. Yang, S. Sarkani and F.X. Long, 4/22/88, (PB89-102909/AS).

NCEER-88-0021 "Seismic Interaction of Structures and Soils: Stochastic Approach," by A.S. Veletsos and A.M. Prasad, 7/21/88, (PB89-122196/AS).

NCEER-88-0022 "Identification of the Serviceability Limit State and Detection of Seismic Structural Damage," by E. DiPasquale and A.S. Cakmak, 6/15/88, (PB89-122188/AS).

NCEER-88-0023 "Multi-Hazard Risk Analysis: Case of a Simple Offshore Structure," by B.K. Bhartia and E.H. Vanmarcke, 7/21/88, (PB89-145213/AS).

NCEER-88-0024 "Automated Seismic Design of Reinforced Concrete Buildings," by Y.S. Chung, C. Meyer and M. Shinozuka, 7/5/88, (PB89-122170/AS).

NCEER-88-0025 "Experimental Study of Active Control of MDOF Structures Under Seismic Excitations," by L.L. Chung, R.C. Lin, T.T. Soong and A.M. Reinhorn, 7/10/88, (PB89-122600/AS).

NCEER-88-0026 "Earthquake Simulation Tests of a Low-Rise Metal Structure," by J.S. Hwang, K.C. Chang, G.C. Lee and R.L. Ketter, 8/1/88, (PB89-102917/AS).

NCEER-88-0027 "Systems Study of Urban Response and Reconstruction Due to Catastrophic Earthquakes," by F. Kozin and H.K. Zhou, 9/22/88, (PB90-162348/AS).

NCEER-88-0028 "Seismic Fragility Analysis of Plane Frame Structures," by H.H-M. Hwang and Y.K. Low, 7/31/88, (PB89-131445/AS).

NCEER-88-0029 "Response Analysis of Stochastic Structures," by A. Kardara, C. Bucher and M. Shinozuka, 9/22/88, (PB89-174429/AS).

NCEER-88-0030 "Nonnormal Accelerations Due to Yielding in a Primary Structure," by D.C.K. Chen and L.D. Lutes, 9/19/88, (PB89-131437/AS).

NCEER-88-0031 "Design Approaches for Soil-Structure Interaction," by A.S. Veletsos, A.M. Prasad and Y. Tang, 12/30/88, (PB89-174437/AS).

NCEER-88-0032 "A Re-evaluation of Design Spectra for Seismic Damage Control," by C.J. Turkstra and A.G. Tallin, 11/7/88, (PB89-145221/AS).

NCEER-88-0033 "The Behavior and Design of Noncontact Lap Splices Subjected to Repeated Inelastic Tensile Loading," by V.E. Sagan, P. Gergely and R.N. White, 12/8/88, (PB89-163737/AS).

NCEER-88-0034 "Seismic Response of Pile Foundations," by S.M. Mamoon, P.K. Banerjee and S. Ahmad, 11/1/88, (PB89-145239/AS).

NCEER-88-0035 "Modeling of R/C Building Structures With Flexible Floor Diaphragms (IDARC2)," by A.M. Reinhorn, S.K. Kunnath and N. Panahshahi, 9/7/88, (PB89-207153/AS).

NCEER-88-0036 "Solution of the Dam-Reservoir Interaction Problem Using a Combination of FEM, BEM with Particular Integrals, Modal Analysis, and Substructuring," by C-S. Tsai, G.C. Lee and R.L. Ketter, 12/31/88, (PB89-207146/AS).

NCEER-88-0037 "Optimal Placement of Actuators for Structural Control," by F.Y. Cheng and C.P. Pantelides, 8/15/88, (PB89-162846/AS).

NCEER-88-0038 "Teflon Bearings in Aseismic Base Isolation: Experimental Studies and Mathematical Modeling," by A. Mokha, M.C. Constantinou and A.M. Reinhorn, 12/5/88, (PB89-218457/AS).

NCEER-88-0039 "Seismic Behavior of Flat Slab High-Rise Buildings in the New York City Area," by P. Weidlinger and M. Ettouney, 10/15/88, (PB90-145681/AS).

NCEER-88-0040 "Evaluation of the Earthquake Resistance of Existing Buildings in New York City," by P. Weidlinger and M. Ettouney, 10/15/88, to be published.

NCEER-88-0041 "Small-Scale Modeling Techniques for Reinforced Concrete Structures Subjected to Seismic Loads," by W. Kim, A. El-Attar and R.N. White, 11/22/88, (PB89-189625/AS).

NCEER-88-0042 "Modeling Strong Ground Motion from Multiple Event Earthquakes," by G.W. Ellis and A.S. Cakmak, 10/15/88, (PB89-174445/AS).

NCEER-88-0043 "Nonstationary Models of Seismic Ground Acceleration," by M. Grigoriu, S.E. Ruiz and E. Rosenblueth, 7/15/88, (PB89-189617/AS).

NCEER-88-0044 "SARCF User's Guide: Seismic Analysis of Reinforced Concrete Frames," by Y.S. Chung, C. Meyer and M. Shinozuka, 11/9/88, (PB89-174452/AS).

NCEER-88-0045 "First Expert Panel Meeting on Disaster Research and Planning," edited by J. Pantelic and J. Stoyle, 9/15/88, (PB89-174460/AS).

NCEER-88-0046 "Preliminary Studies of the Effect of Degrading Infill Walls on the Nonlinear Seismic Response of Steel Frames," by C.Z. Chrysostomou, P. Gergely and J.F. Abel, 12/19/88, (PB89-208383/AS).

NCEER-88-0047 "Reinforced Concrete Frame Component Testing Facility - Design, Construction, Instrumentation and Operation," by S.P. Pessiki, C. Conley, T. Bond, P. Gergely and R.N. White, 12/16/88, (PB89-174478/AS).

NCEER-89-0001 "Effects of Protective Cushion and Soil Compliancy on the Response of Equipment Within a Seismically Excited Building," by J.A. HoLung, 2/16/89, (PB89-207179/AS).

NCEER-89-0002 "Statistical Evaluation of Response Modification Factors for Reinforced Concrete Structures," by H.H-M. Hwang and J-W. Jaw, 2/17/89, (PB89-207187/AS).

NCEER-89-0003 "Hysteretic Columns Under Random Excitation," by G-Q. Cai and Y.K. Lin, 1/9/89, (PB89-196513/AS).

NCEER-89-0004 "Experimental Study of 'Elephant Foot Bulge' Instability of Thin-Walled Metal Tanks," by Z-H. Jia and R.L. Ketter, 2/22/89, (PB89-207195/AS).

NCEER-89-0005 "Experiment on Performance of Buried Pipelines Across San Andreas Fault," by J. Isenberg, E. Richardson and T.D. O'Rourke, 3/10/89, (PB89-218440/AS).

NCEER-89-0006 "A Knowledge-Based Approach to Structural Design of Earthquake-Resistant Buildings," by M. Subramani, P. Gergely, C.H. Conley, J.F. Abel and A.H. Zaghw, 1/15/89, (PB89-218465/AS).

NCEER-89-0007 "Liquefaction Hazards and Their Effects on Buried Pipelines," by T.D. O'Rourke and P.A. Lane, 2/1/89, (PB89-218481).

NCEER-89-0008 "Fundamentals of System Identification in Structural Dynamics," by H. Imai, C-B. Yun, O. Maruyama and M. Shinozuka, 1/26/89, (PB89-207211/AS).

NCEER-89-0009 "Effects of the 1985 Michoacan Earthquake on Water Systems and Other Buried Lifelines in Mexico," by A.G. Ayala and M.J. O'Rourke, 3/8/89, (PB89-207229/AS).

NCEER-89-R010 "NCEER Bibliography of Earthquake Education Materials," by K.E.K. Ross, Second Revision, 9/1/89, (PB90-125352/AS).

NCEER-89-0011 "Inelastic Three-Dimensional Response Analysis of Reinforced Concrete Building Structures (IDARC-3D), Part I - Modeling," by S.K. Kunnath and A.M. Reinhorn, 4/17/89, (PB90-114612/AS).

NCEER-89-0012 "Recommended Modifications to ATC-14," by C.D. Poland and J.O. Malley, 4/12/89, (PB90-108648/AS).

NCEER-89-0013 "Repair and Strengthening of Beam-to-Column Connections Subjected to Earthquake Loading," by M. Corazao and A.J. Durrani, 2/28/89, (PB90-109885/AS).

NCEER-89-0014 "Program EXKAL2 for Identification of Structural Dynamic Systems," by O. Maruyama, C-B. Yun, M. Hoshiya and M. Shinozuka, 5/19/89, (PB90-109877/AS).

NCEER-89-0015 "Response of Frames With Bolted Semi-Rigid Connections, Part I - Experimental Study and Analytical Predictions," by P.J. DiCorso, A.M. Reinhorn, J.R. Dickerson, J.B. Radziminski and W.L. Harper, 6/1/89, to be published.

NCEER-89-0016 "ARMA Monte Carlo Simulation in Probabilistic Structural Analysis," by P.D. Spanos and M.P. Mignolet, 7/10/89, (PB90-109893/AS).

NCEER-89-P017 "Preliminary Proceedings from the Conference on Disaster Preparedness - The Place of Earthquake Education in Our Schools," Edited by K.E.K. Ross, 6/23/89.

NCEER-89-0017 "Proceedings from the Conference on Disaster Preparedness - The Place of Earthquake Education in Our Schools," Edited by K.E.K. Ross, 12/31/89, (PB90-207895).

NCEER-89-0018 "Multidimensional Models of Hysteretic Material Behavior for Vibration Analysis of Shape Memory Energy Absorbing Devices, by E.J. Graesser and F.A. Cozzarelli, 6/7/89, (PB90-164146/AS).

NCEER-89-0019 "Nonlinear Dynamic Analysis of Three-Dimensional Base Isolated Structures (3D-BASIS)," by S. Nagarajaiah, A.M. Reinhorn and M.C. Constantinou, 8/3/89, (PB90-161936/AS).

NCEER-89-0020 "Structural Control Considering Time-Rate of Control Forces and Control Rate Constraints," by F.Y. Cheng and C.P. Pantelides, 8/3/89, (PB90-120445/AS).

NCEER-89-0021 "Subsurface Conditions of Memphis and Shelby County," by K.W. Ng, T-S. Chang and H-H.M. Hwang, 7/26/89, (PB90-120437/AS).

NCEER-89-0022 "Seismic Wave Propagation Effects on Straight Jointed Buried Pipelines," by K. Elhmadi and M.J. O'Rourke, 8/24/89, (PB90-162322/AS).

NCEER-89-0023 "Workshop on Serviceability Analysis of Water Delivery Systems," edited by M. Grigoriu, 3/6/89, (PB90-127424/AS).

NCEER-89-0024 "Shaking Table Study of a 1/5 Scale Steel Frame Composed of Tapered Members," by K.C. Chang, J.S. Hwang and G.C. Lee, 9/18/89, (PB90-160169/AS).

NCEER-89-0025 "DYNA1D: A Computer Program for Nonlinear Seismic Site Response Analysis - Technical Documentation," by Jean H. Prevost, 9/14/89, (PB90-161944/AS).

NCEER-89-0026 "1:4 Scale Model Studies of Active Tendon Systems and Active Mass Dampers for Aseismic Protection," by A.M. Reinhorn, T.T. Soong, R.C. Lin, Y.P. Yang, Y. Fukao, H. Abe and M. Nakai, 9/15/89, (PB90-173246/AS).

NCEER-89-0027 "Scattering of Waves by Inclusions in a Nonhomogeneous Elastic Half Space Solved by Boundary Element Methods," by P.K. Hadley, A. Askar and A.S. Cakmak, 6/15/89, (PB90-145699/AS).

NCEER-89-0028 "Statistical Evaluation of Deflection Amplification Factors for Reinforced Concrete Structures," by H.H.M. Hwang, J-W. Jaw and A.L. Ch'ng, 8/31/89, (PB90-164633/AS).

NCEER-89-0029 "Bedrock Accelerations in Memphis Area Due to Large New Madrid Earthquakes," by H.H.M. Hwang, C.H.S. Chen and G. Yu, 11/7/89, (PB90-162330/AS).

NCEER-89-0030 "Seismic Behavior and Response Sensitivity of Secondary Structural Systems," by Y.Q. Chen and T.T. Soong, 10/23/89, (PB90-164658/AS).

NCEER-89-0031 "Random Vibration and Reliability Analysis of Primary-Secondary Structural Systems," by Y. Ibrahim, M. Grigoriu and T.T. Soong, 11/10/89, (PB90-161951/AS).

NCEER-89-0032 "Proceedings from the Second U.S. - Japan Workshop on Liquefaction, Large Ground Deformation and Their Effects on Lifelines, September 26-29, 1989," Edited by T.D. O'Rourke and M. Hamada, 12/1/89, (PB90-209388/AS).

NCEER-89-0033 "Deterministic Model for Seismic Damage Evaluation of Reinforced Concrete Structures," by J.M. Bracci, A.M. Reinhorn, J.B. Mander and S.K. Kunnath, 9/27/89.

NCEER-89-0034 "On the Relation Between Local and Global Damage Indices," by E. DiPasquale and A.S. Cakmak, 8/15/89, (PB90-173865).

NCEER-89-0035 "Cyclic Undrained Behavior of Nonplastic and Low Plasticity Silts," by A.J. Walker and H.E. Stewart, 7/26/89, (PB90-183518/AS).

NCEER-89-0036 "Liquefaction Potential of Surficial Deposits in the City of Buffalo, New York," by M. Budhu, R. Giese and L. Baumgrass, 1/17/89, (PB90-208455/AS).

NCEER-89-0037 "A Determinstic Assessment of Effects of Ground Motion Incoherence," by A.S. Veletsos and Y. Tang, 7/15/89, (PB90-164294/AS).

NCEER-89-0038 "Workshop on Ground Motion Parameters for Seismic Hazard Mapping," July 17-18, 1989, edited by R.V. Whitman, 12/1/89, (PB90-173923/AS).

NCEER-89-0039 "Seismic Effects on Elevated Transit Lines of the New York City Transit Authority," by C.J. Costantino, C.A. Miller and E. Heymsfield, 12/26/89, (PB90-207887/AS).

NCEER-89-0040 "Centrifugal Modeling of Dynamic Soil-Structure Interaction," by K. Weissman, Supervised by J.H. Prevost, 5/10/89, (PB90-207879/AS).

NCEER-89-0041 "Linearized Identification of Buildings With Cores for Seismic Vulnerability Assessment," by I-K. Ho and A.E. Aktan, 11/1/89.

NCEER-90-0001 "Geotechnical and Lifeline Aspects of the October 17, 1989 Loma Prieta Earthquake in San Francisco," by T.D. O'Rourke, H.E. Stewart, F.T. Blackburn and T.S. Dickerman, 1/90, (PB90-208596/AS).

NCEER-90-0002 "Nonnormal Secondary Response Due to Yielding in a Primary Structure," by D.C.K. Chen and L.D. Lutes, 2/28/90.

NCEER-90-0003 "Earthquake Education Materials for Grades K-12," by K.E.K. Ross, 4/16/90.

NCEER-90-0004 "Catalog of Strong Motion Stations in Eastern North America," by R.W. Busby, 4/3/90.

NCEER-90-0005 "NCEER Strong-Motion Data Base: A User Manuel for the GeoBase Release (Version 1.0 for the Sun3)," by P. Friberg and K. Jacob, 3/31/90.

NCEER-90-0006 "Seismic Hazard Along a Crude Oil Pipeline in the Event of an 1811-1812 Type New Madrid Earthquake," by H.H.M. Hwang and C-H.S. Chen, 4/16/90.

NCEER-90-0007 "Site-Specific Response Spectra for Memphis Sheahan Pumping Station," by H.H.M. Hwang and C.S. Lee, 5/15/90.

NCEER-90-0008 "Pilot Study on Seismic Vulnerability of Crude Oil Transmission Systems," by T. Ariman, R. Dobry, M. Grigoriu, F. Kozin, M. O'Rourke, T. O'Rourke and M. Shinozuka, 5/25/90.

NCEER-90-0009 "A Program to Generate Site Dependent Time Histories: EQGEN," by G.W. Ellis, M. Srinivasan and A.S. Cakmak, 1/30/90.

NCEER-90-0010 "Active Isolation for Seismic Protection of Operating Rooms," by M.E. Talbott, Supervised by M. Shinozuka, 6/8/9.

NCEER-90-0011 "Program LINEARID for Identification of Linear Structural Dynamic Systems," by C-B. Yun and M. Shinozuka, 6/25/90.

NCEER-90-0012 "Two-Dimensional Two-Phase Elasto-Plastic Seismic Response of Earth Dams," by A.N. Yiagos, Supervised by J.H. Prevost, 6/20/90.

NCEER-90-0013 "Secondary Systems in Base-Isolated Structures: Experimental Investigation, Stochastic Response and Stochastic Sensitivity," by G.D. Manolis, G. Juhn, M.C. Constantinou and A.M. Reinhorn, 7/1/90.

NCEER-90-0014 "Seismic Behavior of Lightly-Reinforced Concrete Column and Beam-Column Joint Details," by S.P. Pessiki, C.H. Conley, P. Gergely and R.N. White, 8/22/90.

NCEER-90-0015 "Two Hybrid Control Systems for Building Structures Under Strong Earthquakes," by J.N. Yang and A. Danielians, 6/29/90.

NCEER-90-0016 "Instantaneous Optimal Control with Acceleration and Velocity Feedback," by J.N. Yang and Z. Li, 6/29/90.

NCEER-90-0017 "Reconnaissance Report on the Northern Iran Earthquake of June 21, 1990," by M. Mehrain, 10/4/90.

NCEER-90-0018 "Evaluation of Liquefaction Potential in Memphis and Shelby County," by T.S. Chang, P.S. Tang, C.S. Lee and H. Hwang, 8/10/90.

NCEER-90-0019 "Experimental and Analytical Study of a Combined Sliding Disc Bearing and Helical Steel Spring Isolation System," by M.C. Constantinou, A.S. Mokha and A.M. Reinhorn, 10/4/90.

NCEER-90-0020 "Experimental Study and Analytical Prediction of Earthquake Response of a Sliding Isolation System with a Spherical Surface," by A.S. Mokha, M.C. Constantinou and A.M. Reinhorn, 10/11/90.

NCEER-90-0021 "Dynamic Interaction Factors for Floating Pile Groups," by G. Gazetas, K. Fan, A. Kaynia and E. Kausel, 9/10/90.

NCEER-90-0022 "Evaluation of Seismic Damage Indices for Reinforced Concrete Structures," by S. Rodríguez-Gómez and A.S. Cakmak, 9/30/90.

NCEER-90-0023 "Study of Site Response at a Selected Memphis Site," by H. Desai, S. Ahmad, G. Gazetas and M.R. Oh, 10/11/90.

NCEER-90-0024 "A User's Guide to Strongmo: Version 1.0 of NCEER's Strong-Motion Data Access Tool for PCs and Terminals," by P.A. Friberg and C.A.T. Susch, 11/15/90.

NCEER-90-0025 "A Three-Dimensional Analytical Study of Spatial Variability of Seismic Ground Motions," by L-L. Hong and A.H.-S. Ang, 10/30/90.

NCEER-90-0026 "MUMOID User's Guide - A Program for the Identification of Modal Parameters," by S. Rodríguez-Gómez and E. DiPasquale, 9/30/90.

NCEER-90-0027 "SARCF-II User's Guide - Seismic Analysis of Reinforced Concrete Frames," by S. Rodríguez-Gómez, Y.S. Chung and C. Meyer, 9/30/90.

NCEER-90-0028 "Viscous Dampers: Testing, Modeling and Application in Vibration and Seismic Isolation," by N. Makris and M.C. Constantinou, 12/20/90.

NCEER-90-0029 "Soil Effects on Earthquake Ground Motions in the Memphis Area," by H. Hwang, C.S. Lee, K.W. Ng and T.S. Chang, 8/2/90.